Metastable Ion Studies: The Formation of $C_5H_7O^+$ and $C_2H_3O^+$ from the Molecular Ion of 5-Hexene-2-one

Giorgio G. Attardo

A Thesis

in

the Department

of

Chemistry

Presented in Partial Fulfillment of the Requirements
for the degree of Master of Science at
Concordia University
Montréal, Québec, Canada

December 1983

ABSTRACT

METASTABLE ION STUDIES: THE FORMATION OF $C_5H_7O^+$ AND $C_2H_3O^+$ FROM THE MOLECULAR ION OF 5-HEXENE-2-ONE

Giorgio G. Attardo

The electron impact induced fragmentations of 5-hexene-2-one leading to the formation of $C_5H_7O^+$ and $C_2H_3O^+$ are investigated for the ion source and the second field-free region of the reversed Nier-Johnson geometry mass spectrometer. By employing some of the contemporary mass spectrometric techniques (such as metastable peak shape analysis, Mass Analyzed Ion Kinetic Energy spectrometry and Collisional Activation spectrometry) in conjunction with site specific isotopically labelled analogs the postulation of plausible mechanisms is made possible.

In the ion source, $C_2H_3O^+$ originates from 5-hexene-2-one$^{+\cdot}$ exclusively via α-cleavage. This is also the predominant process in the second field-free region but, in this time frame, a rearrangement mechanism is proposed as a minor pathway.

Formation of $C_5H_7O^+$ in the ion source is shown to occur primarily via α-cleavage, with δ-cleavage identified as a possible minor reaction pathway. Interpretation of methyl loss processes occurring in the metastable time frame is

difficult because of the operation of at least two independent H/D scrambling processes; the occurrence of keto-enol tautomerism involving C-1 and C-3, and the randomization of hydrogen atoms from C-3, C-4 and C-6 are postulated on the basis of experimental results.

Three reaction channels for methyl radical loss from the molecular ion of 5-hexene-2-one are proposed. Loss of C-1 and C-6 as methyl proceeds via α-cleavage and δ-cleavage, respectively. A mechanism involving rearrangement to a cyclic reacting configuration followed by competitive losses of C-1 and C-6 is also proposed, consistent with experimental observations. On the basis of collisional activation spectrometry, a structure is assigned for the $C_5H_7O^+$ ion formed via α-cleavage.

IN MEMORY OF MY FATHER

ACKNOWLEDGEMENT

I wish to express my sincere gratitude to Dr. R.T.B. Rye for his constructive guidance and criticism during the course of my graduate studies. He is also thanked for supporting me financially during one semester.

Special thanks are given to Professor J.L. Holmes and his staff for allowing the use of the research facilities at the Ottawa/Carleton Mass Spectrometric Studies Center. In particular, I am grateful to Dr. C. Kazakoff for running the GC-MS spectra and to Dr. F.P. Lossing for obtaining the thermochemical measurements.

The National Science and Engineering Research Council of Canada is acknowledged for their financial support during my graduate studies.

Finally, I thank Ms. D. Gordon for her patience in typing this Thesis.

TABLE OF CONTENTS

List of Tables

List of Figures

List of Figures

List of Figures

CHAPTER 1 INTRODUCTION AND STATEMENT OF OBJECTIVE

With the advent of modern instrumentation, and the development of new ionization methods, the characterization of gas phase ion structures has become an important aspect of mass spectrometry. Indeed, the contemporary mass spectrometer has been described as the complete chemical laboratory for the production, purification and analysis of gas phase ions[1]. The use of metastable peaks characteristics as a probe of ion structure [2] and the introduction by McLafferty and co-workers of collisional activation techniques[3] have played significant roles in this development. Numerous examples of the application of these mass spectrometric techniques to ion structure elucidation are to be found in the recent literature; the series of papers by McAdoo et al[4] on $[C_3H_5O]^+$, and the work by Holmes and co-workers[5] on $[C_2H_3O]^+$ can be cited as good examples of current activity in this field.

1.1 Previous work on isomeric $C_6H_{10}O$ compounds

A number of recent studies have examined the structure of the $[C_5H_7O]^+$ ions generated from isomeric $C_6H_{10}O$ precursors. Particular interest has been focussed on the ion generated by ε-fission in α,β-unsaturated aldehydes and ketones. Van de Sande and co-workers[6] determined from the collisional activation (CA) spectra of

suitable precursors that the m/z 83 ion generated from 2-hexenal does not have the dihydropyrillium structure proposed by McLafferty[7], but is acyclic as predicted by Meyerson[8] (structure 1). Methyl loss from the cyclohexenols has been studied by a number of groups[9,10,11]; Buchs et al[10] proposed structure (2) for source generated $[C_5H_7O]^+$ ions from 2-cyclohexenol, on the basis of extensive labelling studies; Lignac and Tabet[11] have recently suggested that isomerization of the molecular ion to [methyl-2-cyclopentenol]$^+$ occurs prior to methyl loss, with (3) as the postulated structure for m/z 83. Structure (3) has also been proposed for the product ion arising by methyl loss from the molecular ion of 3-cyclohexenol[12]. A number of studies on the fragmentation of substituted pyrans have been reported[6,13,14], but definitive conclusions were not reached as to the structure of the fragment ions.

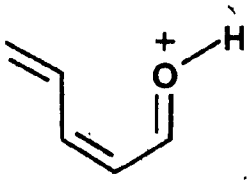

(1)

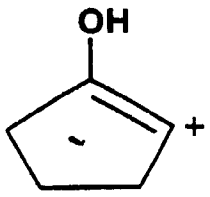

(2)

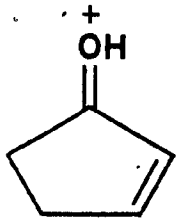

(3)

1.1.1 Previous work on 5-hexene-2-one

An extensive review of the literature turned up only two previously published studies of the mass spectral behaviour of 5-hexene-2-one. In a 1972 report, Djerassi et al. concluded that ion peaks at m/z 83 and m/z 43 were due to α-cleavage of the molecular ion, and were unaffected by the presence of the double bond[15]. Quite recently, Lignac and Tabet reported[11] that the metastable peak generated by methyl loss from the molecular ion of 5-hexene-2-one has a composite shape; thus the Djerassi postulate of only simple cleavage cannot be correct for generation of m/z 83 in the metastable time frame.

1.2 Objectives of this work

The electron impact induced fragmentation of 5-hexene-2-one is of interest because of the presence of two separated, but potentially competitive, functionalities in the molecule. The work reported in this Thesis was undertaken with two goals in mind:

a) To determine the fragmentation mechanism(s) leading to generation of m/z 83 and m/z 43.

b) To assign structure(s) to the m/z 83 fragment ion, based on the results of thermochemical measurement, metastable peak characteristics and collisional activation studies.

CHAPTER 2 FUNDAMENTAL ASPECTS OF MASS SPECTROMETRY

Mass spectrometry is one of the oldest spectroscopic methods used for chemical analysis. While major instrumental developments over the past 50 years have led to the design of different types of mass spectrometers for various specialized applications, all mass spectrometers perform the same basic functions. Neutral compounds are ionized to give gaseous molecular ions which may then fragment to give additional ions. The ions are then separated according to their mass to charge ratio (m/z) and their relative abundances recorded to give a conventional mass spectrum. The methods employed for ionization, separation and collection are characteristic of the particular type of mass spectrometer used. In organic mass spectrometry much of the work is done using electron impact (EI) ionization followed by magnetic separation of the ions; in this chapter a brief discussion of this type of mass spectrometer is presented.

2.1 The Mass Spectrometer

A double focussing instrument with Nier-Johnson geometry (Fig. 2.1) is a widely used type of mass spectrometer in the area of organic mass spectrometry. The basic components of such an instrument are an EI ion source, an electrostatic analyser (ESA) and a magnetic analyser. Ion detection is usually by means of an electron multiplier, which converts

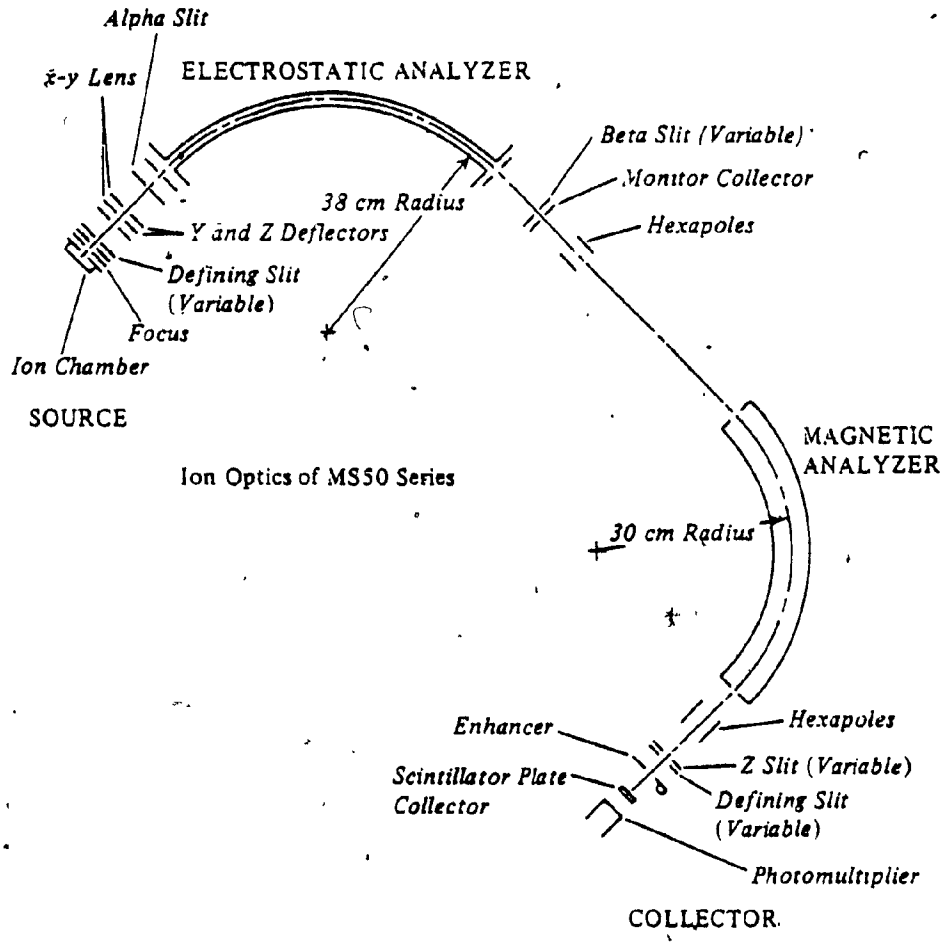

FIGURE 2.1 Schematic diagram of a conventional Nier-Johnson geometry mass spectrometer of modern design (17)

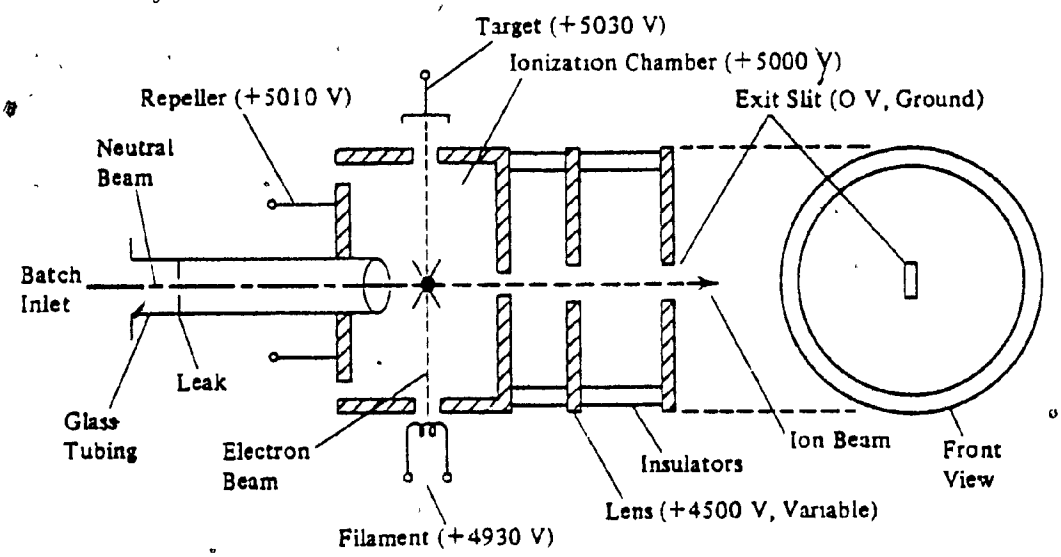

FIGURE 2.2 A typical EI ion source arrangement (17)

ion flux into current. In this section, some of the physical aspects of ion production, separation and detection are presented.

2.1.1 Electron Impact Source

Figure 2.2 shows a typical electron-impact source. The vapourized sample is admitted via a molecular leak into the ionization chamber, where it is crossed by a high energy (70 eV) electron beam. If an electron passes close enough to dislodge one of the electrons from a molecule, ionization occurs and a positive ion is produced:

$$M + e \longrightarrow M^{+\cdot} + 2e$$

It is important to note that the ionized molecule is an odd-electron ion and is therefore represented at $M^{+\cdot}$. Ionization occurs about 100 times faster than a molecular vibration[16]; thus the ion will conserve the vibrational energy level occupied by the neutral molecule prior to electron impact. This is known as 'vertical' ionization.

The ionization process produces $M^{+\cdot}$ in a variety of electronically excited states. Molecular ions with very large internal energies will fragment in the source (residence time ca. 1 usec.) to give ions of lower mass:

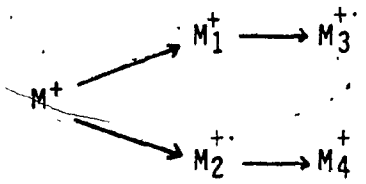

etc

Those molecular ions with somewhat lower internal energies may fragment during their flight from the source of the collector, if they possess enough excess energy above the threshold for decomposition (see discussion of QET, p 13).

Ions formed in the ionization chamber (Figure 2.2) will be repelled into the accelerating region of the source, and will then be accelerated across a potential drop of several kilovolts. For a potential drop V, an ion of mass m and charge e will acquire a kinetic energy of eV, and therefore:

$$\frac{m v^2}{2} = eV, \ (z=1) \quad \ldots\ldots\ldots\ldots\ldots\ldots\ldots\ldots (2.1)$$

or

$$v = \left(\frac{2\ eV}{m}\right)^{1/2} \quad \ldots\ldots\ldots\ldots\ldots\ldots\ldots\ldots (2.2)$$

From Eqn. 2.2 and the flight distance, the lifetime of a particular ion may be computed for different regions of the mass spectrometer.

2.1.2 The Magnetic Analyser

After the ion beam leaves the source, the magnetic analyser will separate the ions according to their mass-to-charge ratio by dispersing the ions into curved trajectories.

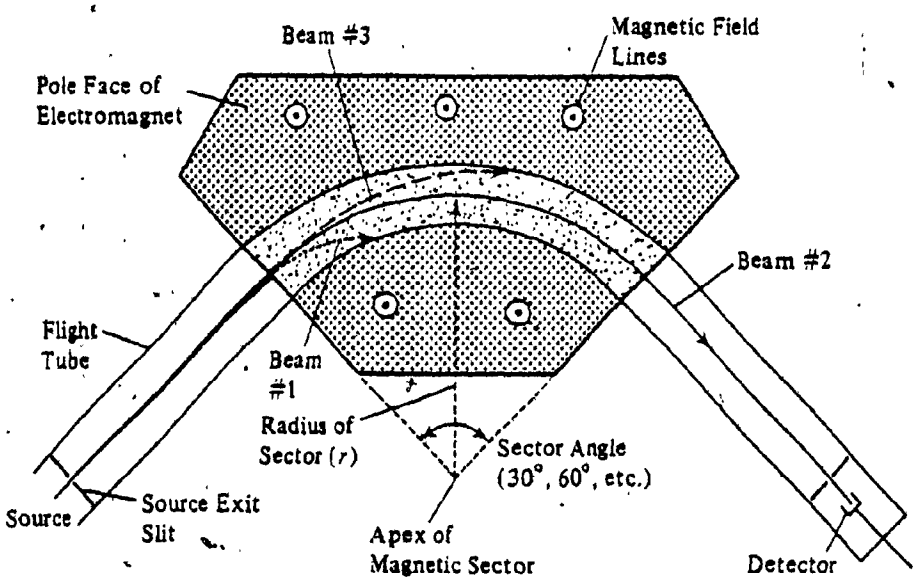

FIGURE 2.3 Schematic diagram of a typical magnetic sector (17)

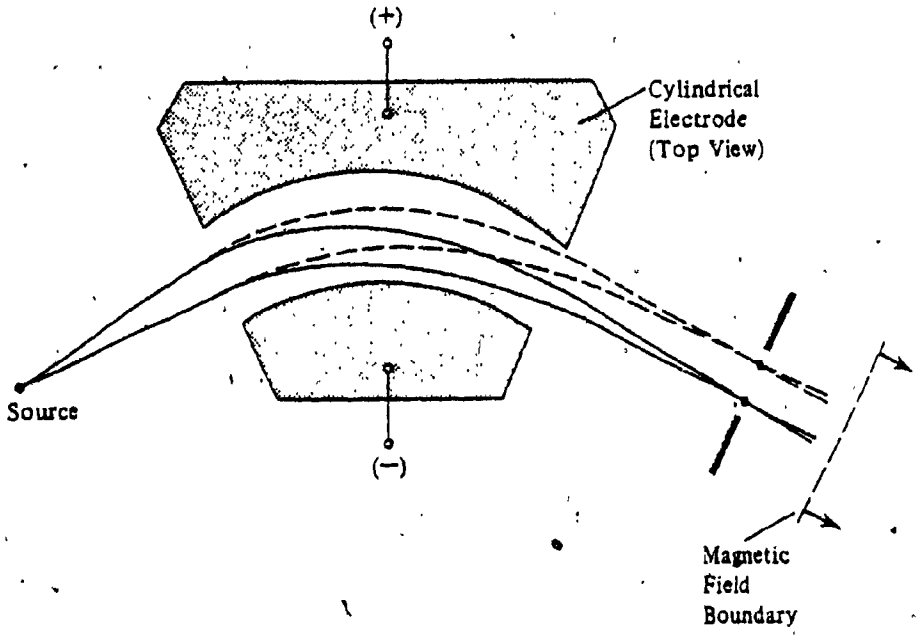

FIGURE 2.4 Schematic diagram of an Electrostatic Analyser (17)

A typical magnetic sector is shown in Figure 2.3. Ions of low m/z will be deflected the most (beam 1), and those of high m/z will deflect the least (beam 3). Ions will pass through the sector along a central trajectory only if the magnetic centripetal force of BeV, where B is the magnetic field strength, is balanced by their own centrifugal force mv/R, where R is the radius of curvature. Hence:

$$\frac{m\,v^2}{R} = BeV \qquad \text{.....(2.3)}$$

and by combining Eqns. 2.1 and 2.3 we obtain:

$$\frac{m}{e} = \frac{B^2R^2}{2V} \qquad \text{.....(2.4)}$$

From this relationship, it becomes apparent that the ion beam can be separated into its component ions by varying either the magnetic field strength or the accelerating voltage. Most modern instruments are equipped with electromagnets and therefore magnetic field scanning is commonly used.

Instruments employing only a magnetic sector for ion separation are referred to as single focussing mass spectrometers. The main disadvantage of such instruments is limited resolution, ca. 5000. Resolution is defined as:

$$R = \frac{m}{\Delta m} \qquad \text{.....(2.5)}$$

where Δm is the mass difference between two resolved peaks and m is the nominal mass. Limited resolution occurs because the ions leave the source with a spread of translational kinetic energies. This energy spread can be greatly reduced by using an electrostatic analyser to provide kinetic energy focussing.

2.1.3 The Electrostatic Analyser

In an instrument of conventional Nier-Johnson geometry the electrostatic analyser (ESA) is placed between the source and the magnetic sector. The ESA consists of two cylindrical electrodes (Figure 2.4) with a voltage of equal magnitude but of opposite polarity applied to each electrode. Ions will pass through the ESA when the electrostatic force acting on them is just balanced by the centrifugal force. Therefore:

$$\frac{m v^2}{R_e} = z e F \qquad \ldots\ldots(2.6)$$

where z is the number of charges on the ion, F is the field strength and R_e is the radius of curvature of the electrostatic analyser. By combining equations 2.1 and 2.6 we obtain:

$$R_e = \frac{2V}{F} \qquad \ldots\ldots(2.7)$$

The ions will follow the radius R_e providing they were accelerated through the same predetermined accelerating voltage. Since the ions in the source experience a small range of accelerating voltages, different radii of curvature will be followed. Hence, ions with different kinetic energies will be focussed at different points by the ESA. Thus by varying the width of the ESA exit slit an ion beam with a very small spread of kinetic energy can be obtained.

In normal operation the ESA voltage is set to give the maximum signal intensity and the exit slit width optimized to give the desired spread of ion kinetic energy. By combining the focussing action of the ESA with that of the magnetic sector resolution of ca. 150 000 has been achieved[17].

2.2 Ion Nomenclature

A discussion of the different kinds of positive ions produced in the mass spectrometer is presented in this section. A brief description of the terminology used to describe the various types of ions and ion structures is given.

2.2.1 The Molecular Ion

The molecular ion is a positively charged ion formed in the initial ionization process by removal of an electron from a neutral molecule. It is convenient to identify two types of molecular ion structure: the ionization threshold structure

(IT) and the reacting configuration (RC). The IT structure refers to the configuration of the molecular ion at the threshold energy required for its formation; such a structure may not have sufficient energy, or the required geometry, to undergo fragmentation. The RC structure refers to ions with appropriate energy and geometry for decomposition.

After the molecular ion is formed, structural rearrangement may occur prior to fragmentation. If the rearranged ion possesses sufficient internal energy for decomposition it would be classified as having a reacting configuration. It is often the case that fragmentations in the source occur from IT structures. However, in the first field-free region (between the source and the ESA) and in the second field-free region (between the ESA and the magnetic analyser) fragmenting ion structures are always referred to as reacting configurations.

2.2.2 Fragment Ions

A fragmentation process will lead to a fragment (daughter) ion and a neutral fragment:

$$M^{+\cdot} \longrightarrow F_1^+ + N_1^{\cdot}$$

or

$$M^{+\cdot} \longrightarrow F_2^+ + N_2^{\cdot}$$

The fragmenting, or parent, ion can yield an even-electron fragment ion F_1^+ and a neutral radical $N_1^{\cdot}$, or an odd-electron fragment ion $F_2^{+\cdot}$ and a neutral molecule N_2.

2.2.3 Metastable Ions

A full treatment of the quasi-equilibrium theory (QET) is beyond the scope of this thesis; a full treatment is given in a number of excellent reviews[2,16,18]. The key feature of the theory as it applies to mass spectrometry is that ions, formed in the source with a wide range of internal energies, will exhibit a range of fragmentation rates. An approximate relationship between internal energy, E, and rate constant for fragmentation, k, is:

$$K = V\left(\frac{E - E_0}{E}\right)^{s-1} \qquad \text{.....(2.8)}$$

where E_0 is the activation energy for the fragmentation, v is the frequency factor and s is the effective number of oscillators. For ions containing a very large internal energy the rate constant will be approximately equal to the frequency factor; hence for a simple cleavage process the fragmentation will occur in the period of one vibration when the internal energy is large. If E is somewhat greater than, but of the same order of magnitude as, E_0 fragmentation will occur only after several vibrations. This will decrease

the rate constant, and hence increase the reaction time. Therefore, fragmentations may occur anywhere between the source and the collector, depending on the internal energy of the fragmenting ion.

Metastable ions are those which do not fragment in the source but which possess sufficient internal energy to have a k such that they decompose before reaching the collector. Most ions decomposing in the ESA or magnetic sectors will collide with the walls and be lost. Those that do pass will be recorded over a wide m/z range, and will be difficult to identify. Metastable fragmentations occurring in the field-free regions between the sectors may be recorded and identified quite easily. For a mass spectrometer of conventional geometry, fragment ions formed in the first field-free region will not pass through the ESA because they do not have the correct kinetic energy. They could be recorded by making appropriate changes in the ESA and accelerating voltages. This technique will be considered in a later section of the thesis. Ions formed in the second field-free region will be transmitted through the magnetic sector with an apparent mass m* given[2] by:

$$m^* = \frac{m_2^2}{m_1} \qquad \text{.....(2.9)}$$

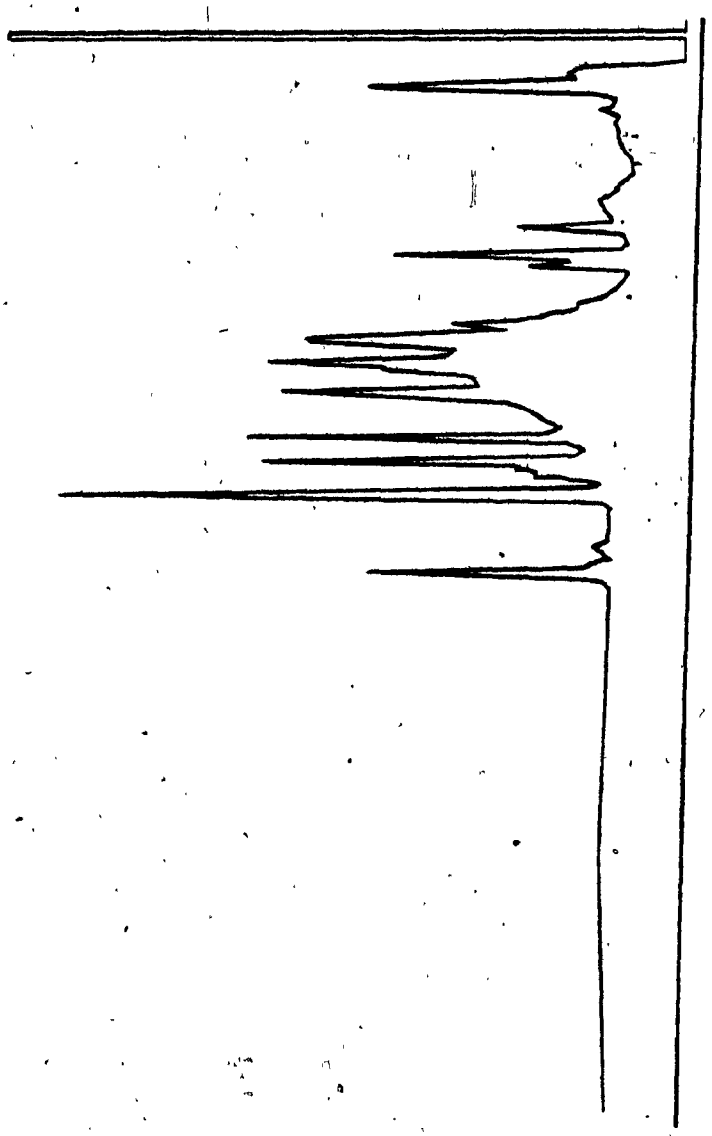

FIGURE 2.5 IKE spectrum of n-decane (19)

where m_2 is the mass of the fragment ion and m_1 is the mass of the parent. From the apparent mass, metastable transitions may be identified in a conventional mass spectrum.

2.3 Instruments of Reversed Nier-Johnson Geometry

In a double focussing mass spectrometer of conventional Nier-Johnson geometry, metastable decompositions occurring in the first field-free region remain undetected under normal operating conditions because the accelerating and ESA voltages are constant. A fragment ion, M_2, resulting from a metastable transition $M_1^{+\cdot} \longrightarrow M_2^+ + M_3^{\cdot}$ will have a fraction of the kinetic energy of the precursor ion. Thus if V_0e is the kinetic energy of M_1, the daughter ion will have a kinetic energy M_2V_0e/M_1 ($z_1 = z_2 = 1$). In order to detect the metastable transition, the ratio of accelerating voltage of ESA voltage must be raised by a factor of M_1/M_2. This can be achieved by appropriate changes in either accelerating voltage or ESA voltage. The metastable transition would then be recorded by an ion detector positioned after the electrostatic analyser. If the ESA voltage is scanned (with constant accelerating voltage) the resulting spectrum is an Ion Kinetic Energy (IKE) spectrum (Figure 2.5).

There are several problems associated with the above

scanning techniques. Any change in the accelerating voltage will alter the focussing conditions in the ion source. If the ESA voltage is lowered to E_2 from the initial value E_0 such that E_2/E_0 equals M_2/M_1, it is obvious that any other fragment ion, M_F, formed by the metastable decomposition of a precursor ion Mp, will also be transmitted if the ratio M_F/Mp equals M_2/M_1. Hence, several metastable peaks may overlap, causing difficulties in the interpretation of the IKE spectrum, and making the study of a single metastable transition difficult.

Geometry reversal is a solution to the problems outlined above. The term 'reverse geometry' as applied to a Nier-Johnson instrument means that the ESA is placed <u>after</u> the magnetic analyser. In such an instrument the first field-free region is between the magnetic analyser and the ion source, and the second field-free region is between the magnet and the ESA. Study of metastable decompositions occurring in the second field-free region of such an instrument is greatly simplified. The magnet is tuned to pass precursor ions of the desired m/z ratio, and the ESA voltage is scanned downwards from its normal setting E_0. All metastable transitions of the chosen precursor are thus recorded at appropriate ESA voltages, as previously discussed. The accelerating voltage remains constant. This technique is advantageous because only the metastable ions

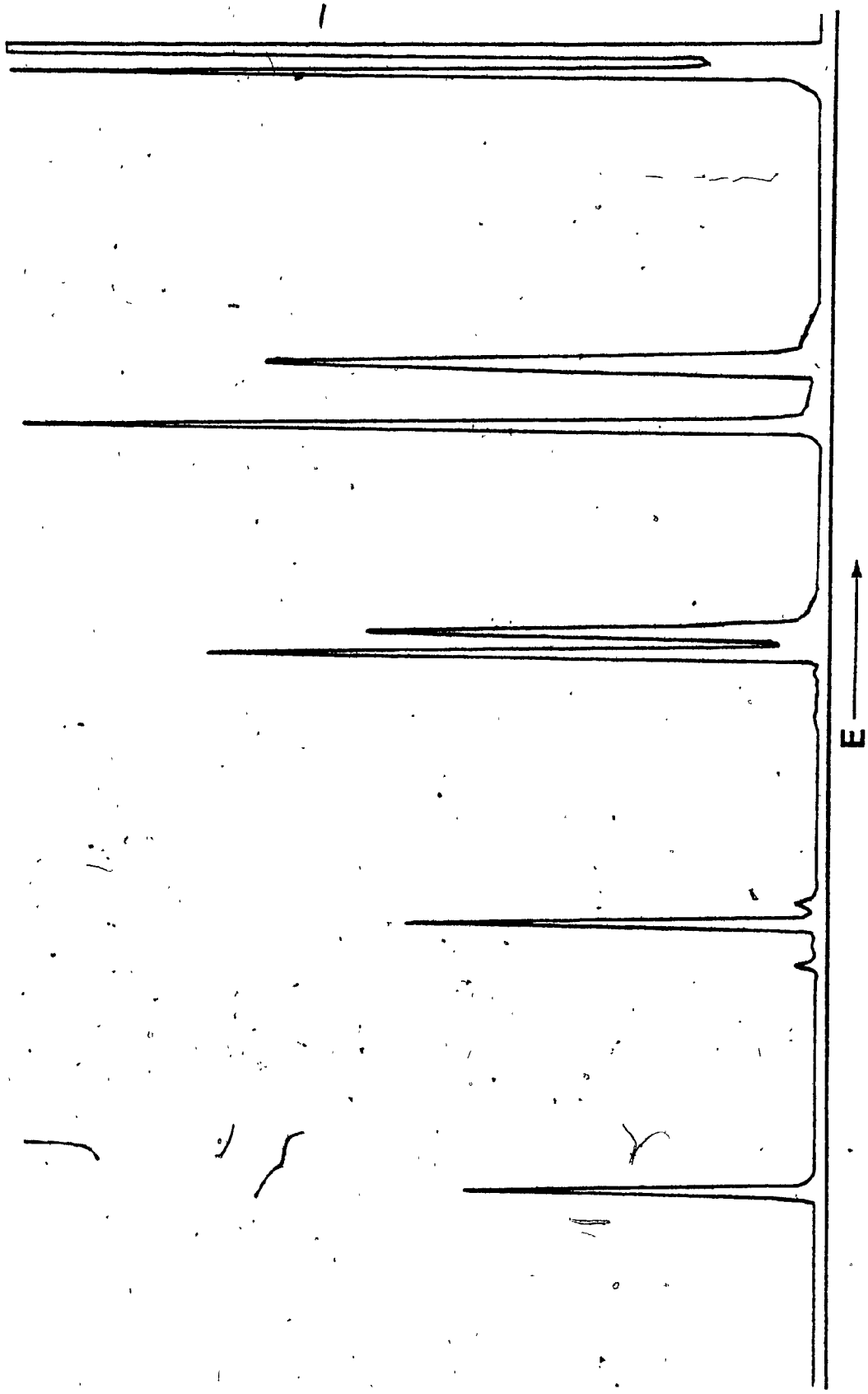

FIGURE 2.6 MIKE spectrum of trans-2-hexenal

of the chosen precursor ion are recorded. The spectrum obtained by such a scan is termed a Mass Analysed Ion Kinetic Energy (MIKE) spectrum; a typical example is shown in Figure 2.6. The usefullness of MIKE spectra for characterization of gas phase ion structures will be considered in the next Chapter.

A feature of the MIKE spectrum that is worth noting is that the peaks, commonly referred to as metastable peaks, are much broader than the peaks observed in a conventional mass spectrum. This peak broadening is a well known characteristic of metastable peaks, and arises because part of the excess energy of the fragmenting ion is released as kinetic energy, T. The fragment ions acquire a range of translational energies, leading to peak broadening. This feature will be considered in greater detail in the next Chapter.

2.4 Collisional Activation

It is possible to induce fragmentation of ions, which have insufficient internal energy to undergo metastable decomposition, by colliding them with neutral gas molecules. The collision of a neutral molecule with ions having a large translational kinetic energy will be inelastic, resulting in the conversion of part of the ion kinetic energy into excitation energy. This may lead to fragmentation if the

resulting internal energy is greater than the activation energy of the fragmentation process. It is important to note that fragmentation is induced in ions which may have a non-reacting configuration, and which therefore may have a different structure than that of ions undergoing metastable decomposition.

To obtain a collisional activation spectrum, it is necessary to fit the mass spectrometer with a collision cell or chamber, which is mounted in a field-free region of the ion path. For instruments of reverse geometry it is convenient to mount the collision cell in the second field-free region, a short distance from the entrance to the ESA. This is advantageous because fragmentation can be induced in ions generated in the source or produced, by metastable decomposition, in the first field-free region. As the collision cell is operated at a gas pressure significantly higher than that in the source or ion flight path, differential pumping of moderately high capacity is required.

Since collisional activation occurs in a field-free region, the induced fragmentations can be detected as described earlier for metastable decompositions; indeed the resulting spectrum is very similar in appearance to a MIKE spectrum. It should be noted, in fact, that metastable decompositions of the selected precursor ion will be recorded

along with the collision induced fragmentations in the collisional activation (CA) spectrum.

There are two ways of differentiating collision induced fragmentation (CIF) peaks from metastable peaks. In the first method, the pressure of collision gas in systematically reduced, and the peak height is plotted as a function of pressure. A linear plot with a zero intercept is indicative of a collision induced process with no metastable (unimolecular) component. If the intercept is not zero, an overlap of a metastable peak and a CIF peak is indicated. The second method involves applying a potential (1 to 5 kV) to the collision cell. Separation of metastable and CIF peaks will occur because fragment ions formed in the cell will have a different translational energy than those formed by metastable decomposition outside the cell.

There has been extensive application of CA spectra to problems of gas phase ion structure determination. Collisional activation spectra are more informative than MIKE spectra because there are many more collision induced fragmentations than there are metastable decompositions. The application of CA mass spectrometry to structure determination of gas phase ions will be considered in the following Chapter.

CHAPTER 3 SOME MASS SPECTROMETRIC METHODS FOR THE CHARACTERIZATION OF GAS PHASE ION STRUCTURES

The formulation of an accurate fragmentation mechanism requires that the reaction pathway be completely identified; i.e. the initial reactant ion and final products must be known, as well as the identity of all intermediate reacting species. It is obvious that, in order to specify initial and final species completely, the structure of these species must be known. Isotopic labelling has long been used to aid in the identification of reactant and product species in mass spectrometric fragmentations. Over the past 30 years an increasing variety of techniques have been developed to tackle the problem of ion structure determination. Most of the modern techniques assign a structure to an ion on the basis of comparison with isomeric ions of known structure; a satisfactory structure assignment is achieved when the use of several different methods leads to the same conclusion. This Chapter illustrates the application of some of these methods.

3.1 Ion Thermochemistry

The thermochemical method is based on the principle that the heat of formation (ΔH_F) of an ion is characteristic of its composition and structure. Generation of a particular fragment ion from a neutral molecule requires a minimum amount of energy, the appearance energy (AE). Reference to a

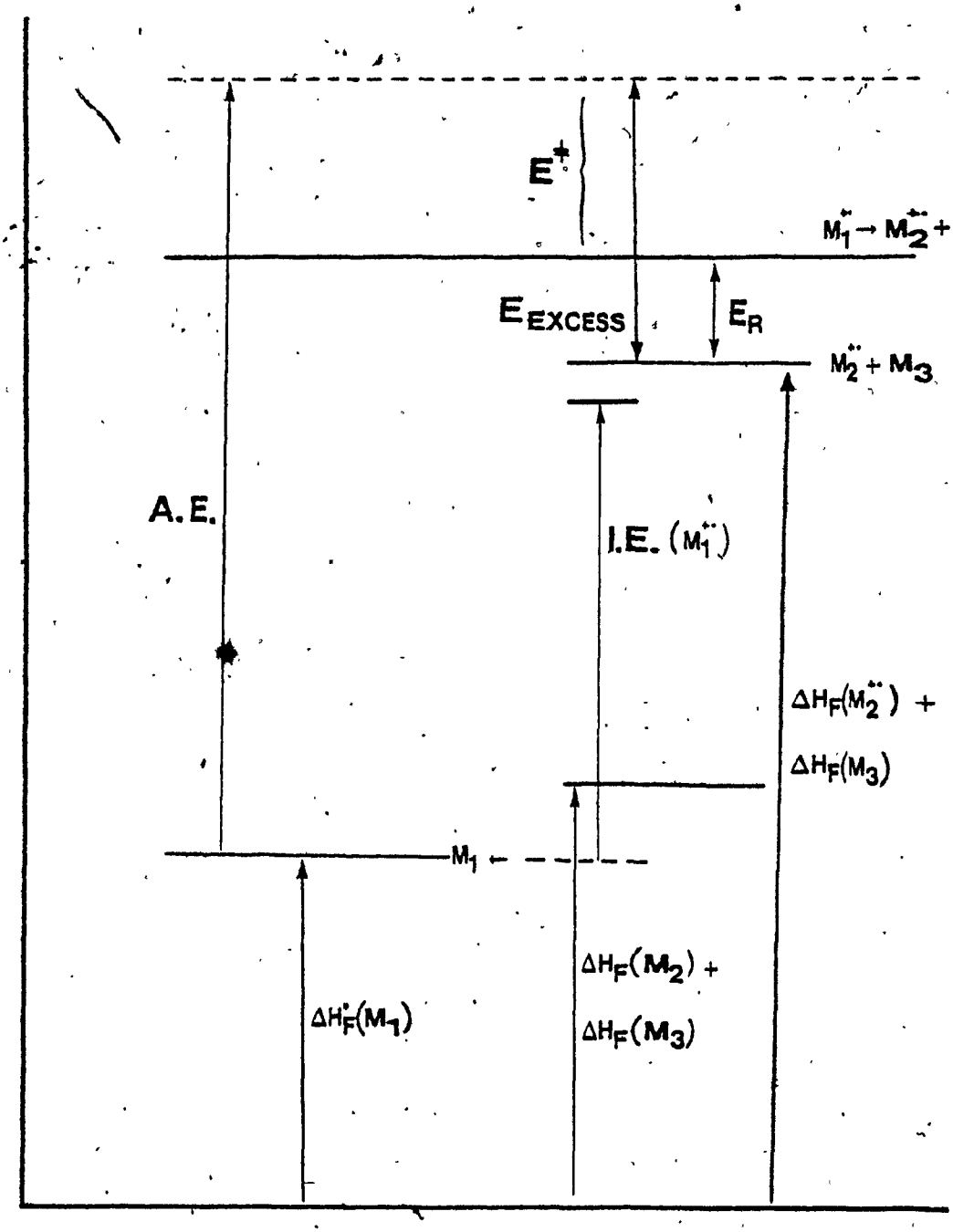

FIGURE 3.1 Thermochemical quantities related to the fragmentation of an ion ($M_1^{+\cdot}$)

typical fragmentation process (Figure 3.1) illustrates the relationship between the AE of a fragment ion and the heats of formation of the species involved:

$$A.E. + \Delta H^{\circ}(M_1) = \Delta H_F(M_2^{+\cdot}) + \Delta H_F(M_3) + E \text{ excess} \quad (3.1)$$

and therefore:

$$\Delta H_F(M_2^{+\cdot}) = A.E. + \Delta H_F(M_1) - H_F(M_3) - E \text{ excess} \quad (3.2)$$

The excess energy term is made up of two components, the reverse activation energy, E_R, and the energy content of the fragmenting species above the thermochemical threshold, $E^{\neq}$. For a fragmentation occurring at the thermochemical threshold with a negligible reverse activation energy, we may write:

$$\Delta H_F(M_2^{+\cdot}) = A.E. + \Delta H_F(M_1) - \Delta H_F(M_3) \quad (3.3)$$

The characterization of the fragment ion structure is then attempted by comparison of the measured heat of formation with the ΔH_F values for other isomeric ions of known structure.

As an example of this technique, consider the attempt to identify the C_5H_8 fragment ion generated by loss of water from the molecular ion of cyclopentanol[20]. The AE of $C_5H_8^{+\cdot}$ was found to be 9.66 ± 0.06 eV; this value,

taken with the heats of formation of cyclopentanol(g) and water (g) of -239 kJ mol^{-1} and -242 kJ mol^{-1}, respectively, gave 920 ± 7 kJ mol^{-1} as the heat of formation of $C_5H_8^{+\cdot}$. The IE of cyclopentanol was found to be 9.58 ± 0.06 eV, thus the fragmentation occurs close to the thermochemical threshold. A minimum estimate of E_R, based on kinetic energy release (T) values, is 12.6 kJ mol^{-1} Three isomeric $C_5H_8^{+\cdot}$ ions are possible candidates for the fragment ion under study; cyclopentene (ΔH_F = 904 kJ mol^{-1}), penta-1,3- diene (ΔH_F = 904 kJ mol^{-1}) and isoprene (ΔH_F = 929 kJ mol^{-1}). In this case the thermochemical approach was able to narrow down the list of possible structures, but other techniques were required to determine the correct structure.

There are several problems associated with the use of ion thermochemistry to determine ion structure. The acurate measurement of ionization and appearance energies is difficult, and requires the use of monoenergetic electrons(21). The excess energy term is often not negligible, and can be difficult to evaluate. For fragmentations having a small excess energy term, the method is quite valuable.

3.2 MIKE Spectrometry

The use of MIKE spectra to characterize ion structures is based on the assumption that the internal energy of the

the fragmenting ion does not affect the relative abundances of metastable peaks. Thus if two isomeric ions give identical MIKE spectra they are assumed to have the same structure. A significant drawback of this comparison is that only a few metastable peaks may be present in the MIKE spectrum, and it is therefore possible that ions of different structure may give somewhat similar MIKE spectra.

Several studies[22,23,24] have shown that differences in the internal energy of ions with identical structures may lead to variations in the relative abundance ratios observed in the MIKE spectra. Hence the presence of different MIKE spectra should not be attributed to different ion structure if only small variations occur in the relative abundance ratios.

The technique does have several advantages. The metastable time window is well defined; fragmentation of ions with lifetimes between 10^{-6} and 10^{-5} seconds, and having internal energies of 0 - 1 eV above the lowest threshold will be observed. MIKE spectrometry becomes very useful when isotopically labelled compounds are used in the study of fragmentation processes. The elucidation of mechanistic details such as hydrogen transfers, ring closure and site of fragmentation is possible from the MIKE spectra of appropriately labelled precursors.

The utility of the method is illustrated by the following example. The $C_2H_4O_2^{+\cdot}$ ion formed from

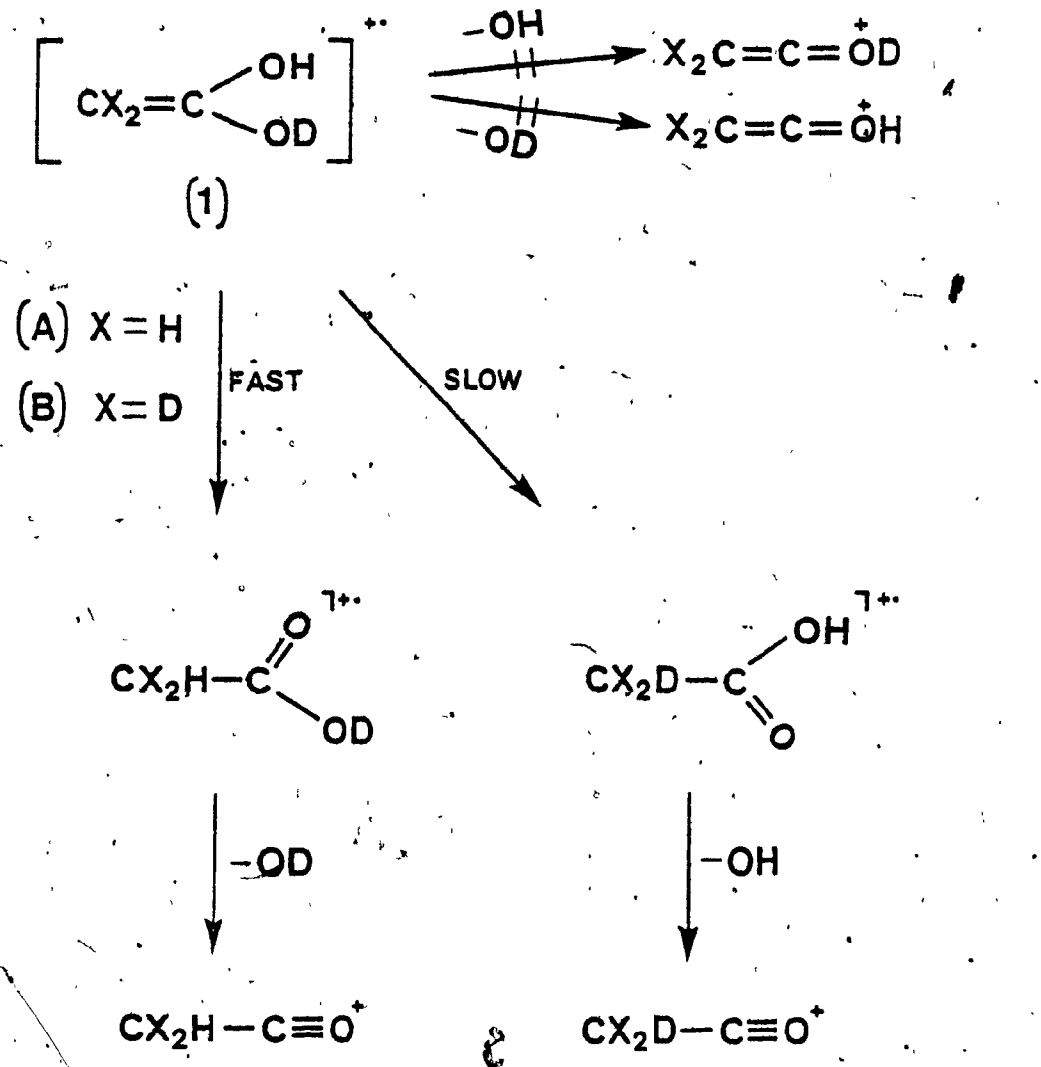

FIGURE 3.2 Competitive loss of hydroxyl from $C_2H_4O_2^{+\cdot}$ (1)

aliphatic acids was found to have the enolic structure[25] (1) shown in Figure 3.2. Loss of hydroxyl from (1) did not occur by simple cleavage. This was shown from the MIKE spectra of deuterium labelled $C_2H_4O_2^{+\cdot}$ ions. A simple cleavage pathway (Figure 3.2) would lead to OH and OD loss in a ratio of 1:1. For both labelled compounds (A and B) the observed ratio was 1:2.6. This value could not arise by complete H/D randomization, and the rearrangement mechanism shown in Figure 3.2 was proposed. In this case the transfer of a hydrogen is favoured over the transfer of a deuterium.

The utility of isotopically labelled compounds in MIKE spectrometry may be limited when complete randomization occurs. The interpretation of MIKE spectra can become quite difficult when one or more isotopic exchange processes occur prior to metastable fragmentations. Isotopic exchange pathways can be identified by comparison of the normalized abundance ratios for a fragmentation process with calculated exchange probabilities.

3.3 Metastable Peak Characteristics

The shape of a metastable peak measured under conditions of good energy resolution can be used to characterize a fragmentation process. During a metastable fragmentation, part of the internal energy of the fragmenting

ion will be converted into translational energy of the products. The width of the metastable peak will depend on the magnitude of this kinetic energy release, T. The kinetic energy released in the decomposition has two origins: the excess energy, $E^{\neq}$, and the reverse activation energy, E_R. Therefore T can be defined as:

$$T = T^{\neq} + T_R \quad \ldots\ldots\ldots\ldots\ldots\ldots\ldots\ldots\ldots\ldots (3.4)$$

where $T^{\neq}$ and T_R are the contributions from the reverse activation energy and the excess energy above threshold, respectively. The separate evaluation of $T^{\neq}$ and T_R is not easy, and the total T is used for the characterization of gas phase ion structures and fragmentation mechanisms.

Beynon et al[2] have shown that T is related to the metastable peak width by:

$$T = \frac{y^2 m_1^2 eV}{16 \times m_2 m_3} \left(\frac{\Delta E}{E}\right)^2 \quad \ldots\ldots\ldots\ldots\ldots\ldots\ldots\ldots\ldots\ldots (3.5)$$

where m_1, m_2, m_3 are the masses of the precursor ion, fragment ion and second fragment product, respectively. The charge numbers of the precursor and fragment ion are X and Y, and ΔE and E are ESA voltages corresponding to the metastable peak width and main beam, respectively. The kinetic energy release at half height, $T_{0.5}$, is usually

determined, irrespective of peak shape. The comparison of the $T_{0.5}$ value for a particular metastable transition with $T_{0.5}$ values for known transitions may lead to structural inference. The limitation on this approach is that it assumes that the transitions being compared have similar shape; comparison of T values determined at several (normalized) heights is often more satisfactory. A better method for comparison involves obtaining the distribution of kinetic energy release corresponding to the metastable peak shape. The n(T) distribution obtained for a particular metastable fragmentation can then be compared with the distributions obtained from known metastable transitions. If two metastable processes generate identical n(T) distributions it is assumed that the same fragmentation pathways are involved.

Metastable peak shapes can be of two general types. For relatively small kinetic energy releases, the metastable peak will have a Gaussian-like shape (although true Gaussian peaks are rare). Flat-topped or dished metastable peaks are observed when the kinetic energy release is large; it should be noted that the peak shape in such cases is influenced by instrumental factors. The presence of flat-topped or dished metastable peaks is often indicative of a rearrangement process having a significant reverse activation energy[26]. Composite peak shapes, combining the two general types just

described, are also observed. Such composite metastable peaks may arise if a precursor ion loses two different fragments of the same mass, or when two isomeric ions fragment to give one or two daughter ions. In general, composite metastable peaks occur when more than one process is involved in a metastable fragmentation. Analysis of composite peaks is complicated. In favourable cases, the components of the composite peaks may be resolved by deconvolution (Appendix C details such a procedure, developed by the author), or by suitable isotopic labelling.

3.4 Collisional Activation (CA) Spectrometry

CA spectrometry is another comparative technique which may lead to the identification of a gas phase ion structure. This method has the advantage of providing several peaks for comparison. If the CA spectra of two ions, generated from different precursors, are the same within experimental error then it is inferred that the two ions have identical structures. Thus an unknown ion structure may be determined by comparison with reference ions of known structure.

The technique is illustrated in the following example. An investigation[27] of $C_2H_5O^+$ ions generated from a variety of precursors showed that three ion structures were involved. From a comparison of the CA spectra (Table 3.1) it is apparent that the $C_2H_5O^+$ ion structure is the same

for precursors 1 and 2. Precursors 3, 4, and 5 gave very similar CA spectra and therefore common $C_2H_5O^+$ structures are assumed. Precursors 3 and 6 were used to generate reference structures by chemical ionization with H_2O.

TABLE 3.1

Partial CA Spectra of $C_2H_5O^+$

	Relative Abundance (m/z)						
Precursor	24	25	26	28	30	31	Ion Structure
$CH_3OCH_2CH_2OCH_3$(1)	1	1	4	41	43	12	$CH_3O{=}CH_2^+$
$CH_3OCH_2CH_2CN$(2)	1	2	4	39	43	12	$CH_3O{=}CH_2^+$
CH_3CHO(3)	4	16	45	18	14	3	$CH_3CH{=}OH^+$
$(CH_3)_2CHOH$(4)	4	14	49	15	14	4	$CH_3CH{=}OH^+$
$CH_3CH_2(CH_3)CHOH$(5)	5	16	47	17	12	3	$CH_3CH{=}OH^+$
CH_2CH_2O(6)	4	15	42	13	11	16	$CH_2CH_2OH^+$

A major drawback of CA spectrometry is apparent when the threshold for isomerization is lower than that for decomposition. If two structurally different stable ions have a low threshold for rearrangement to a common structure their CA spectra will be identical. This effect can be detected if the CA spectra of two or more ions of known, different structure match with the CA spectrum of the ion under investigation.

CHAPTER 4 EXPERIMENTAL

This chapter presents the instrumental and synthetic procedures employed for this research project. In order to study the fragmentation mechanism for methyl loss from the molecular ion of 5-hexene-2-one, we have synthesized a series of isotopically labelled analogs. These included 5-hexene-2-one-1-^{13}C; 5-hexene-2-one-1,1,1-d_3; 5-hexene-2-one-1,1,1,3,3-d_5; 5-hexene-2-one-4,4-d_2; 5-hexene-2-one-6,6-d_2; and 5-hexene-2-one-1,1,1,3,3,6,6-d_7. Synthetic procedures have been previously reported[28,29] only for the d_5 and 6,6-d_2 analogs; other compounds are novel. Unlabelled compounds used for mass spectroscopic studies were purchased from Aldrich Chemical Co., 4-pentenoic acid was obtained from ICN pharmaceuticals. Synthesis of isotopically labelled analogs of trans-2-hexenal was unsuccessful. A report on the attempted procedures is given.

The original mass spectroscopic data have been summarized in Appendix A. Only specific examples of some spectra have been included in this chapter. Mathematical methods employed for treatment of mass spectroscopic data are described in Appendix B and C. Appendix D includes NMR spectra of final, synthetic products. They have been compiled in the same order as discussed in the synthesis sections.

4.1 INSTRUMENTATION

Instrumentation and experimental techniques are reported in three parts. First, instrumental procedures employed for mass spectroscopic studies are discussed. The second part is involved with the characterization of synthetic intermediates. Finally, purification via preparative gas chromatography is described.

4.1.1 MASS SPECTROMETRY

Preliminary research work was done with a Hitachi Perkin-Elmer RMU-7 mass spectrometer in the reversed Nier-Johnson geometry.(30) The ESA power supply was composed of a Kepco OPS 500B operational power supply with an output of 0-500V. The OPS 500B was driven by a Kepco FG-100A function generator supplying a linear ramp voltage of 0-20V. Voltage was read on a HP 3440A digital volt meter and was converted into ESA sector volts by multiplying it by 24.43. The instrument was operated with sample pressures ca. 3.5×10^{-6} mm Hg and at -2.8KV accelerating voltage. Spectra were recorded with a Watanabe servocorder.

When instrumental limitations were present, further experimentation was done at the University of Ottawa with a VG Analytical ZAB 2-F mass spectrometer in the reversed

Nier-Johnson geometry. This instrument was equipped with a collision cell located prior to the ESA. Accelerating voltages of 8kV and sample pressures ca. 3×10^{-7}m bar were the usual operating conditions. Conventional mass spectra were obtained on UV sensitive paper with a Visicorder. A pen recorder was used for other spectra.

Conventional Mass Spectra

Conventional mass spectra were obtained with the RMU-7 mass spectrometer in the following way. Samples were admitted to the electron impact source via a Granville-Phillips variable leak valve (series 203). The ion beam was deflected to an electron multiplier located in the second field-free region and the magnet was manually tuned on an arbitrary m/z value for maximum signal intensity. The beam was then directed through the ESA and the sector's voltage was varied until maximum signal strength was reached. The optimum signal was obtained by focusing the ion beam with two electrostatic lenses located in the source. Conventional spectra were then recorded by scanning the magnet's current from 25mA to 110mA at a speed of 5mA/min. The electron multiplier voltage was usually set at 1.5kV.

The procedure for running conventional mass spectra with the ZAB 2-F mass spectrometer was the same as described for

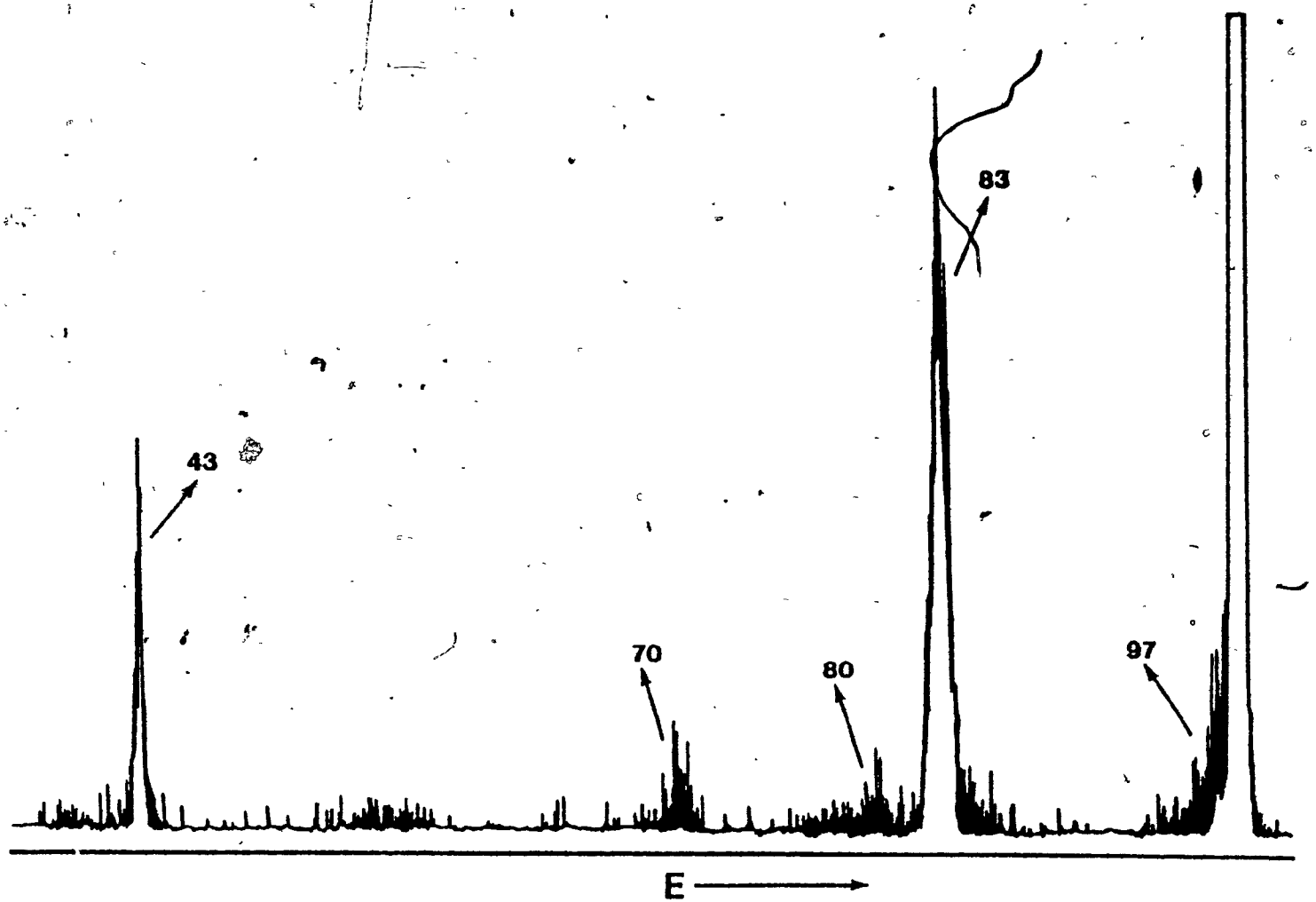

FIGURE 4.1 MIKE spectrum of 5-hexene-2-one$^{+\cdot}$ obtained from the RMU-7 mass spectrometer

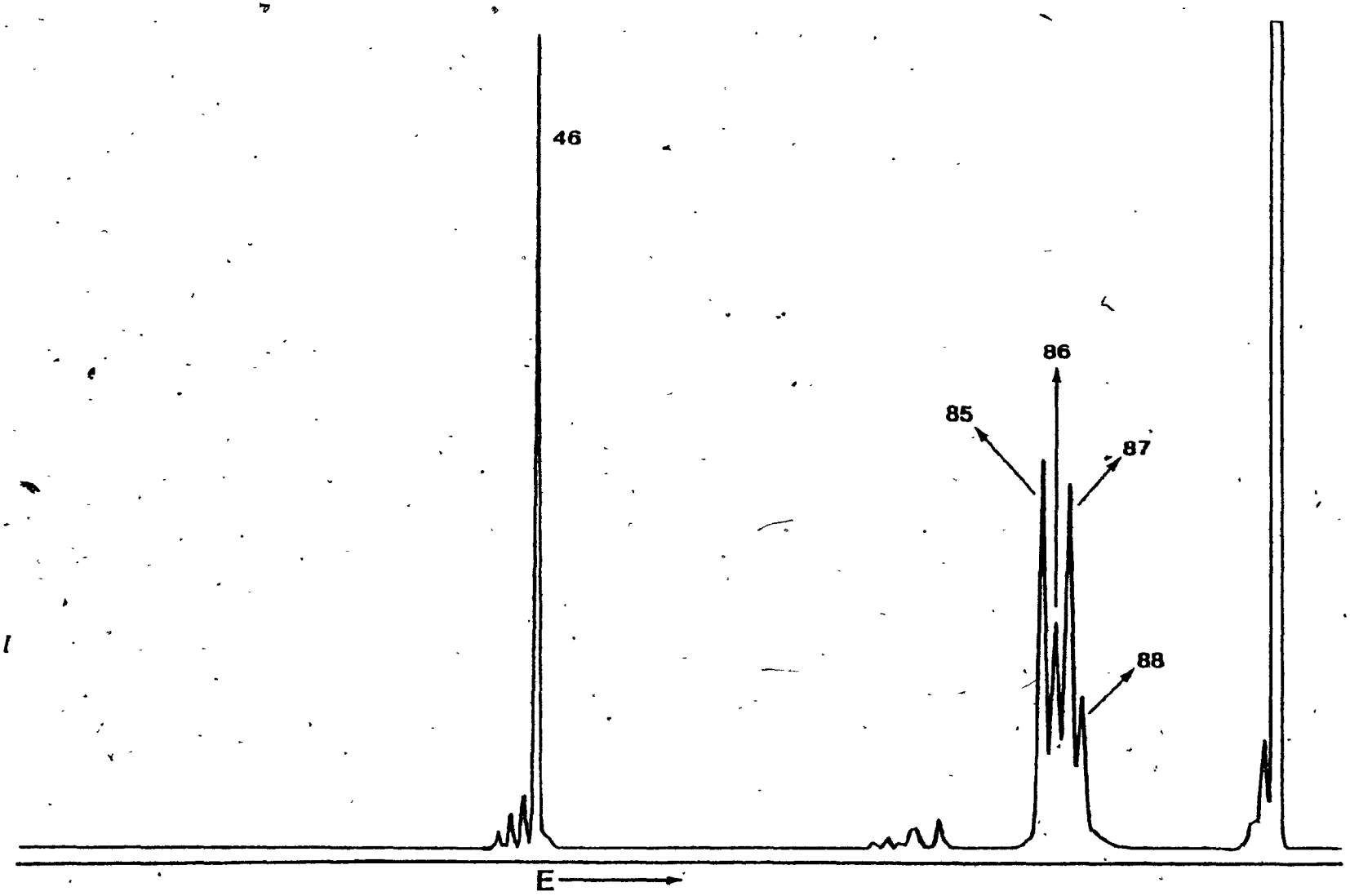

FIGURE 4.2 MIKE spectrum of 5-hexene-2-one-1,1,1,3,3-d_5 $^{+\cdot}$ obtained from the ZAB2-F mass spectrometer

the RMU-7 with minor exceptions. In addition to the variable leak valve, samples (ca. 3µl) could be introduced via a heated injection port.

MIKE Spectra

The procedure for running MIKE spectra was the same for both mass spectrometers. In general, two MIKE spectra were run for each compound: one for the molecular ion (ie; m/z 98 for 5-hexene-2-one) and another for $M^{+\cdot}$-methyl. A typical procedure involved initial tuning of the magnet to the desired ion, m/z 98 for example, followed by a ESA voltage scan. For the RMU-7, the voltage was varied from ca. 3.00V to ca. 11.10V at a speed of 0.01V/sec. When desired, metastable peaks were expanded (ie: $98^{+\cdot} \longrightarrow 83^{+} + {}^{\cdot}CH_3$) by scanning at a slower rate (0.001V/sec). Expanded metastable peaks were obtained for methyl loss from the molecular ion of 5-hexene-2-one, its labelled analogs, and trans-2-hexenal. Original MIKE spectra obtained from the RMU-7 and ZAB 2-F mass spectrometers are shown in figures 4.1 and 4.2.

In order to optimize metastable peak shapes, good energy resolution was necessary. This was done by narrowing the source and ESA exit slits until the width at the base of the molecular ion peak reached a minimum. Typical widths were

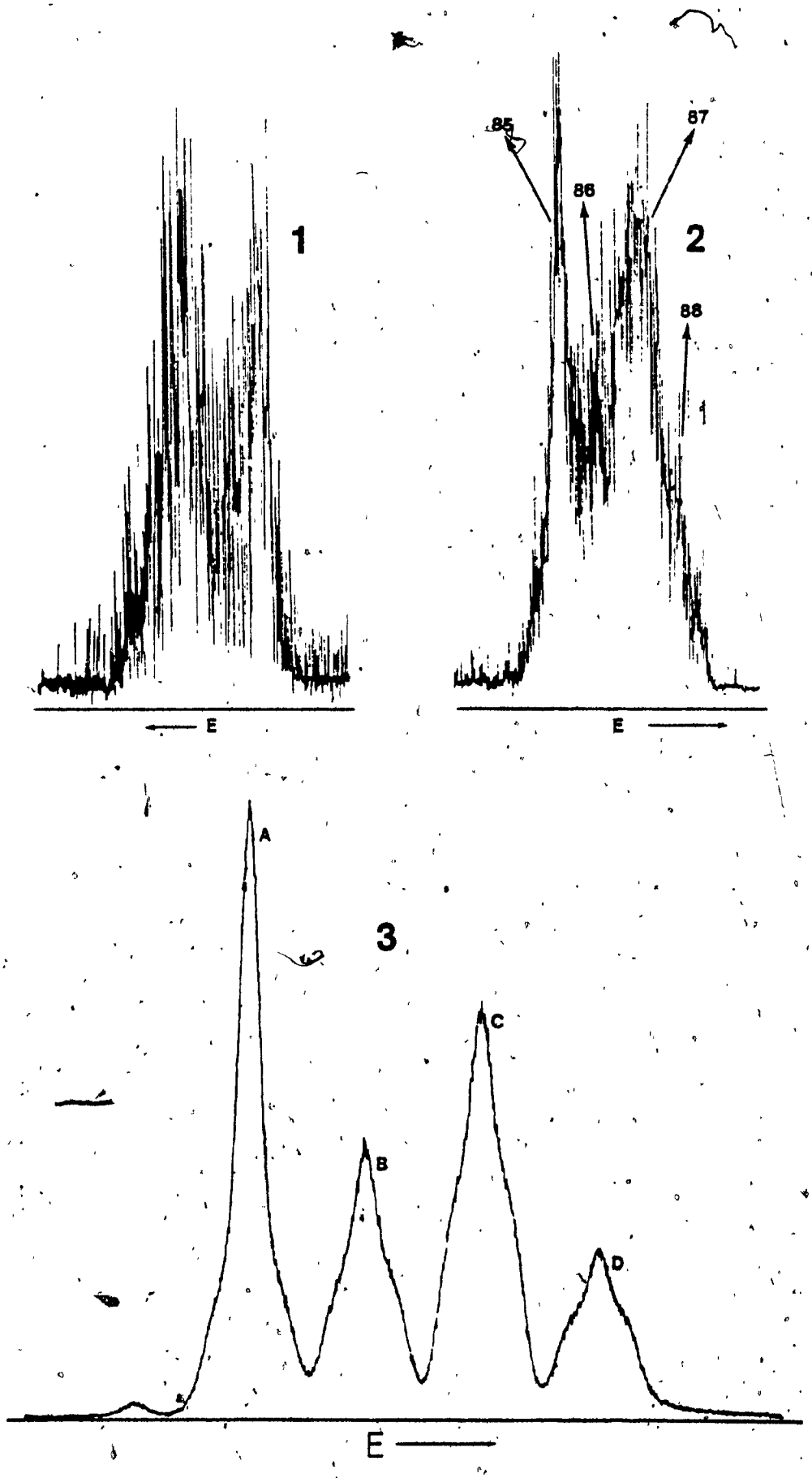

FIGURE 4.3 Methyl loss region in the MIKE spectrum of 5-hexene-2-one-1,1,1,3,3-d_5: 1-from RMU-7; 2-after signal averaging of 1; 3-from ZAB 2-F (A to D = 85 to 88)

11V from the RMU-7 and 4V for the ZAB 2-F; they corresponded to energy resolutions of 255 and 2000, respectively. The problem with the RMU-7 was loss of sensitivity as the slits were narrowed. Signal intensity was improved by increasing the gain but poor signal to noise ratios resulted. A preliminary attempt to signal average a metastable peak was done with an Apple II microcomputer by collecting 2000 data points from each scan, summing ten scans and averaging them. This was applied for the expanded methyl loss region from the MIKE spectrum of 5-hexene-2-one-1,1,1,3,3-d_5 (Fig. 4.3). Although the signal to noise ratio was upgraded, signal averaging was not totally effective for separating the individual methyl loss processes. In contrast, the ZAB 2-F mass spectrometer provided good sensitivity with adequate signal to noise ratios and high energy resolution. Since the ZAB 2-F was necessary for CA spectra, we have also used it to obtain well resolved metastable peak scans. Thus the idea of signal averaging was not pursued at this time. All spectra were taken using ca. 70eV ionizing electrons but, in the case of 5-hexene-2-one expanded metastable peak scans for loss of methyl from the molecular ion were also run at different electron energies. This was done by reducing the repeller voltage and then decreasing the electron energy to the desired value. The scanning procedure was identical as described for MIKE spectra.

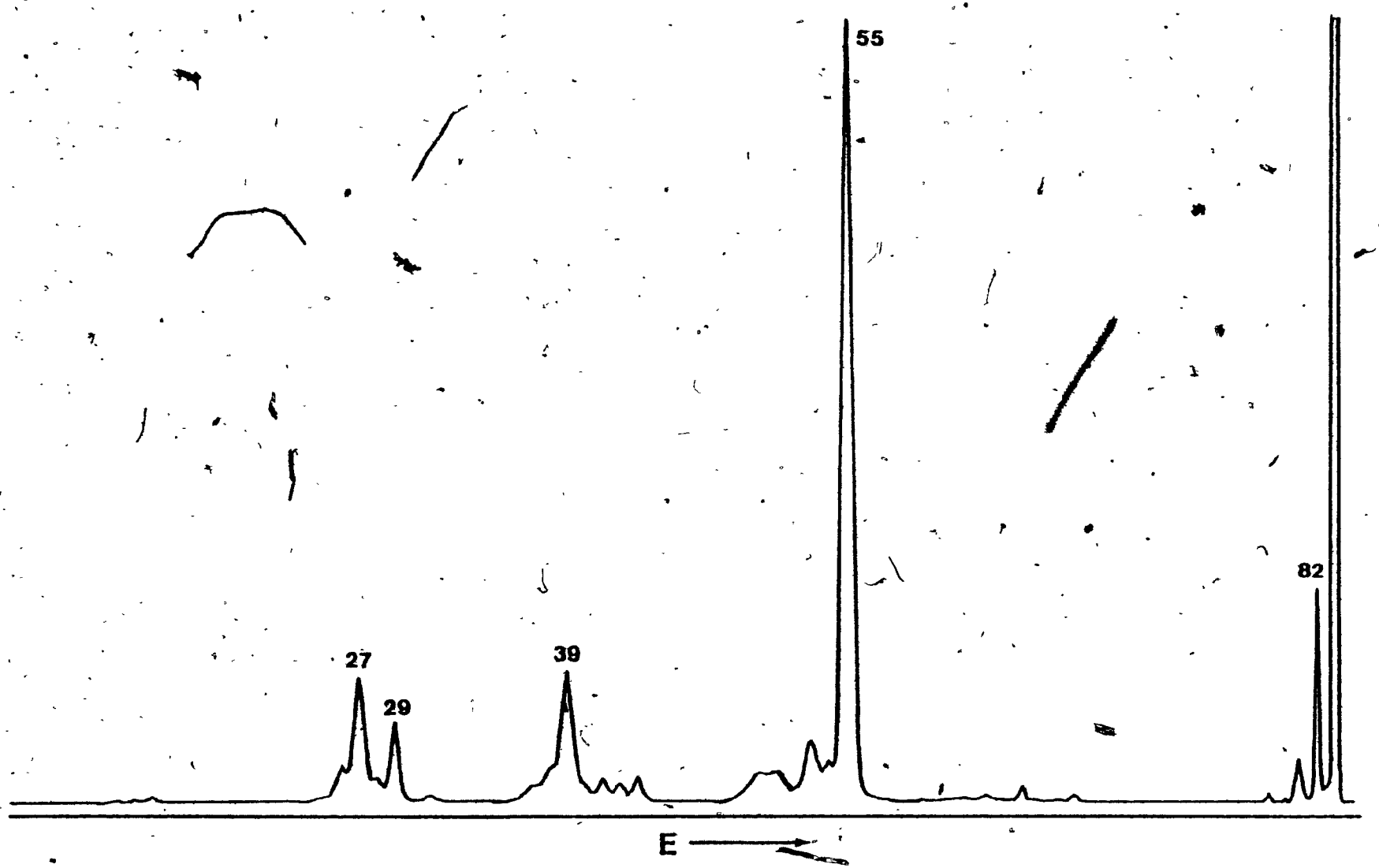

FIGURE 4.4 CA spectrum of M/Z 83 originating from 5-hexene-2-one-1-^{13}C

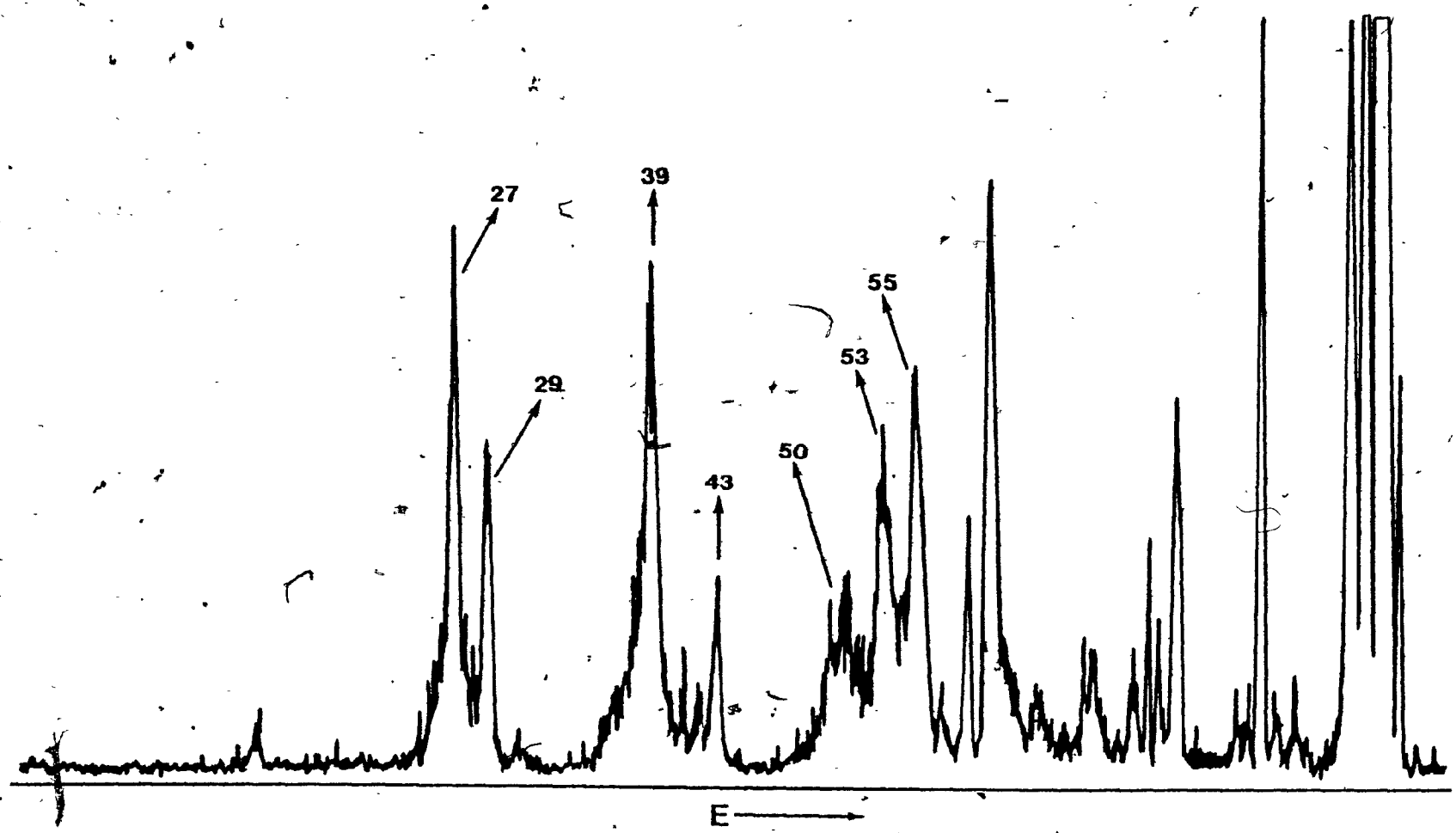

FIGURE 4.5 CA spectrum of m^* 83 originating in the first field free region from 5-hexene-2-one-1-^{13}C

CA Spectra

The actual procedure for obtaining CA spectra is identical to the one described for MIKE spectra except that a collision chamber located in the second field-free region, just prior to the ESA, is required. Since the RMU-7 mass spectrometer was not equipped with such a chamber, all CA spectra were run with the ZAB 2-F.

During the scanning procedure, the ions entering the collision chamber were continuously collided with helium gas. This resulted in an increased amount of fragmentations. Collision induced and metastable fragmentations were recorded simultaneously. An example of a CA spectrum is shown in Fig. 4.4.

Figure 4.5 shows a CA spectrum of a metastably generated ion. This was obtained using a method similar to that described previously. In this case, the magnet is tuned to pass the fragment ion produced by metastable decomposition in the first field free region (ie: m/z = 70.30 for m/z 83 from m/z 98).

4.1.2 Characterization of Synthetic Intermediates

In general, synthetic intermediates were identified by NMR using a Varian T-60 NMR spectrometer. Operating conditions were: sweep time = 250 sec, filter = 1 or 2, RF power level = 0.032, sweep width = 500Hz and spinning rate ca. 40RPS. In most cases, an external TMS reference standard was used. Infrared spectra were obtained from a Perkin-Elmer 599B spectrophotometer. Solids were run as KBr pellets and liquids as smears.

In addition to NMR spectroscopy, final products were characterized by mass spectrometry and gas chromatography. When they were relatively pure, conventional mass spectra were obtained from the Hitachi RMU-7 mass spectrometer. Gas chromatography-mass spectrometry (GC-MS) was required for product mixtures. At the University of Ottawa, a VG Analytical 7070E mass spectrometer interfaced with a Dani 2800 gas chromatograph was employed in this case. Data was processed with VG software on a PDP-11 mini computer system.

Gas chromatography was useful for showing the presence of a desired product in mixtures. Chromatograms were obtained from a GOW MAC series 750 gas chromatograph equipped with a 6 feet x 0.125 inch OV-17 column and a flame ionization detector. Running conditions involved column temperatures between 70°C to 90°C and ca. 35 ml/min nitrogen

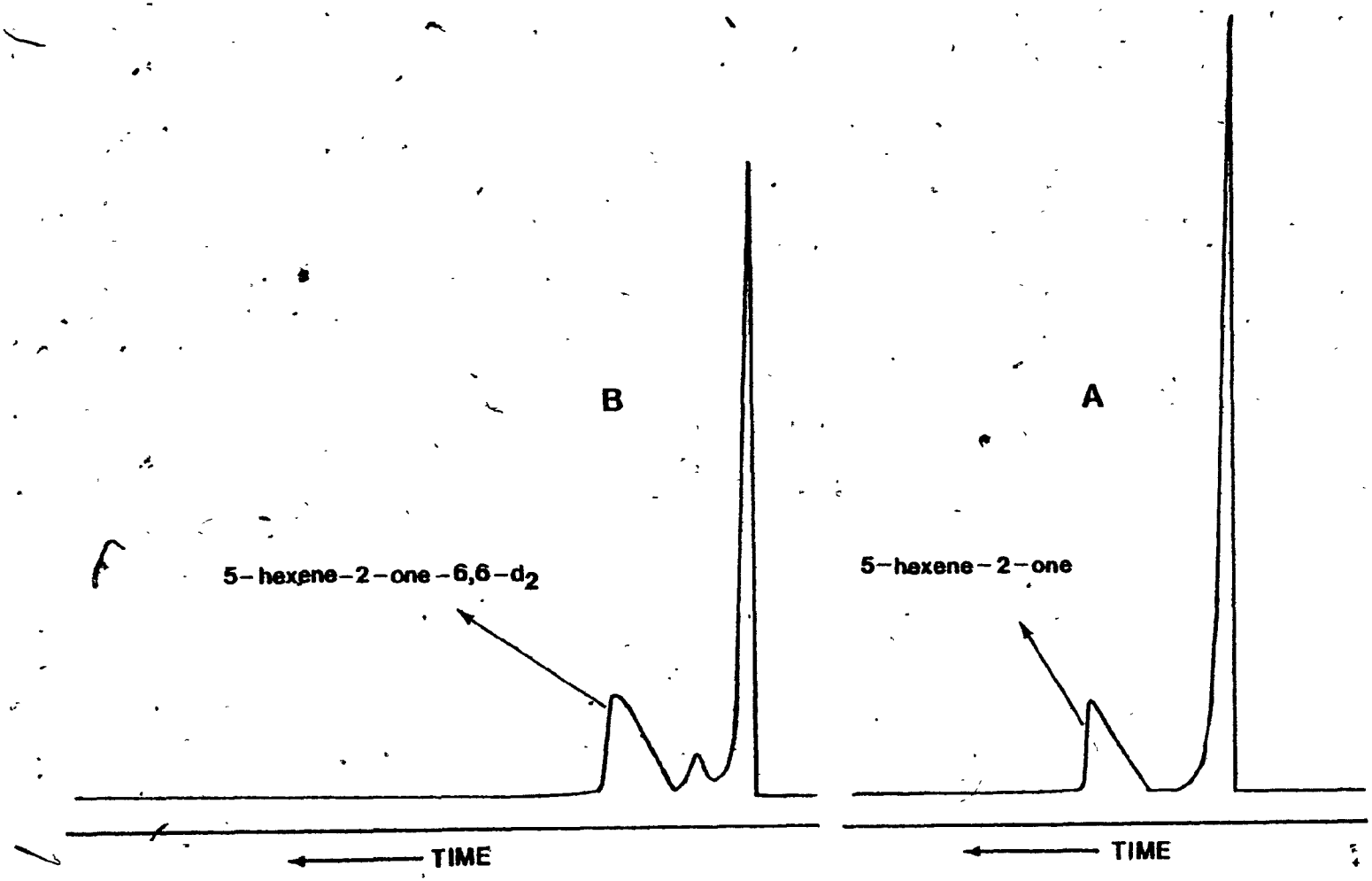

FIGURE 4.6 Gas chromatograms: (A) 5-hexene-2-one in ether (B) 5-hexene-2-one-6,6-d_2 in product mixture

flow rate. Analysis of product mixture was done in the following way. First a chromatogram was obtained from a standard solution containing 5-hexene-2-one, for example, in a pure solvent identical to the product's solution. By comparing the GC retention time corresponding to the peak for 5-hexene-2-one with retention times from the mixture, one was able to determine the presence of the labelled analog (Fig. 4.6). Gas chromatography was also useful for providing an estimate of product concentrations. This was done by dividing the area under the peak corresponding to a product by the sum of areas from all peaks.

4.1.3 Purification via Preparative Gas Chromatography

After preliminary analysis of product mixtures by gas chromatography, synthetic labelled analogs of 5-hexene-2-one were purified by preparative gas chromatography. A Pye series 105 automatic preparative gas chromatograph equipped with a 99:1 splitter, a 6 feet x 0.25 inch OV-17 column and a flame ionization detector was used. Column temperatures were usually set at 60°C with a nitrogen flow rate ca. 35 ml/min.

After injecting a 10 µl sample in the chromatograph the effluent was collected when the peak corresponding to the product began to appear. Products were trapped in capillary tubes cooled in liquid nitrogen. Depending on the solution's concentration, between 10 to 20 injections were required for an adequate sample volume.

4.2 Synthesis of Isotopically Labelled Analogs of 5-Hexene-2-one and Trans-2-hexenal

Procedures employed for the synthesis of labelled compounds are compiled in this section. All synthetic routes were tried twice with unlabelled reagents and when a satisfactory result was obtained, synthesis of the labelled analog was then carried out.

Most reagents were purchased from Aldrich Chemical Co.; isotopically labelled reagents were obtained from Merck Sharpe and Dohme Isotopes. Vinyl lithium was custom prepared by Lachat Chemical Co.

4.2.1 Synthesis of 5-hexene-2-one-1,1,1,3,3-d_5

Synthetic Scheme:

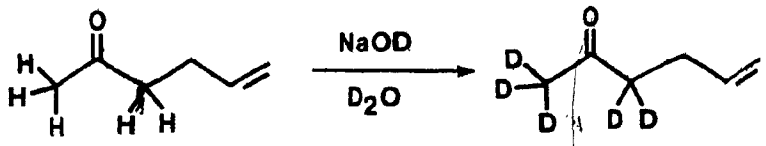

Procedure:

Following a modification of the procedure described by Simeral and Maciel,[28] 0.168 g of freshly cut sodium was added slowly to 15 ml of D_2O at 0° C in a 50 ml round bottom flask. To this basic solution was added 4 ml of 5-hexene-2-one and the resulting two phase system was stirred for 36 hours at 4° C. The mixture was then extracted four times with 20 ml portions of ether, the ethereal layers were combined, and dried over anhydrous $MgSO_4$. The ether was removed under reduced pressure and the residue was subjected to a second deuterium exchange as described above. This time the two phase system was separated. The top layer was found to be greater than 85% d_5 labelled 5-hexene-2-one. Work up of the aqueous layer afforded more product.

MS, m/z(% RA): 27(14.8); 28(11.9); 39(19.3); 41(13.3); 46(100.0); 57(50.6); 85(17.6); 103(42.8).

^{1}H-NMR(CCl_4,60MHz); δ = 2.33(d,2H); 4.85(m,2H); 5.75(m,1H).

Authentic 5-hexene-2-one (Aldrich Chemical Co.):

^{1}H-NMR(CCl_4,60MHz); δ = 1.90(s,3H); 2.25(m,4H); 4.80(m,2H); 5.65(m,1H).

4.2.2 Synthesis of 5-Hexene-2-one-4,4-d_2

A synthetic method for 5-hexene-2-one-4,4-d_2 has never been previously reported. This compound was prepared from a modified model synthesis devised according to the procedure used for 6-heptene-2-one-5,5-d_2[31]. An alternative route is discussed in section 4.2.3.

Synthetic Scheme

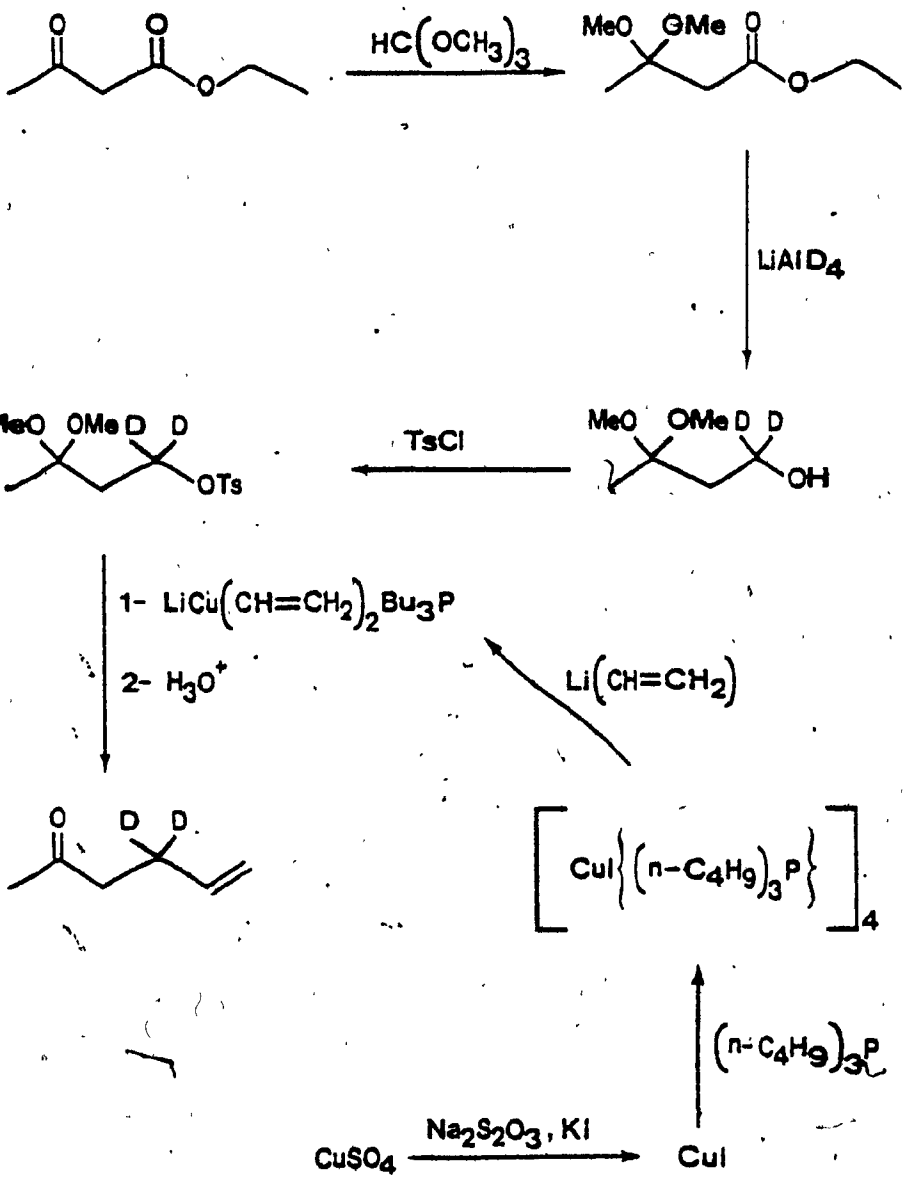

Procedure:

Under a nitrogen atmosphere, 12 ml of acetyl chloride was added to a solution of 30 g of ethyl acetoacetate in 60 ml of dry methanol and 120 ml of methyl orthoformate. The mixture was allowed to stand over molecular sieves for 72 hours at room temperature. The solution was then poured into pentane containing excess anhydrous sodium carbonate and allowed to stand overnight. After filtration and removal of the pentane under reduced pressure, the residue was fractionated to give 3,3-dimethoxy ethyl butyrate in 77% yield (B.P. 56°C at 24 mm Hg). ^{1}H-NMR (Pure, 60MHz); δ = 1.11(t,3H); 1.28(s,3H); 2.48(s,2H); 3.03(s,6H); 3.99(q,2H).

A solution of 2.2 g of the ketal butyrate in 50 ml of anhydrous ether was added dropwise under nitrogen to a stirred mixture of 2.6 g $LiAlD_4$ in 75 ml of ether. The mixture was stirred for one hour at room temperature and then refluxed for 1.5 hours. After cooling, workup was done with 15% aqueous NaOH(32) by first adding 2.6 ml of water followed by 2.6 ml of 15% NaOH and finally 8 ml of water. The mixture was stirred for 1.5 hours, the salts filtered off, and the ether removed under reduced pressure. Fractionation of the residue yielded 13.2 g of 3,3-dimethoxy butanol-1,1-d_2 (B.P. 58°C at 22 mmHg).

^{1}H-NMR(Pure, 60MHz); δ = 1.07(s,3H); 1.62(s,2H); 2.95(s, 6H); 3.67(s,1H).

To an ice cooled solution containing 30 g of tosyl chloride in 15 ml of dry pyridine was added dropwise 10 g of ketal alcohol in 10 ml of pyridine. During the addition, a considerable amount of heat was evolved. It was important to maintain the temperature below 5°C otherwise yields decreased drastically (We have found that no tosylate was obtainable if the temperature reached about 30°C). The mixture was allowed to stand overnight at 0°C and then poured into 100 ml of ice-cold water. The aqueous solution was extracted five times with 50 ml portions of ether and the combined ethereal layers were successively washed with saturated sodium bicarbonate and 10% aqueous HCl. After drying over $MgSO_4$, the ether was removed under reduced pressure to yield a crude oil containing 3,3-dimethoxybutyl tosylate-1,1-d_2 (40% W/W) and pyridine (60% W/W). Since any attempt to purify the tosylate resulted in rapid decomposition, the mixture was used for the next step. Only a pure unlabelled sample for immediate identification by NMR spectroscopy was obtained.
^{1}H-NMR(CCl_4, 60MHz); δ = 0.89(s,3H); 1.65(s,2H); 1.98(s,3H); 2.70(s,6H); 7.23(d of d,4H).

Prior to the next step, 0.045 moles of lithium divinyl cuprate tri-n-butylphosphine complex[33] was prepared by slowly adding a solution of 0.090 mole of vinyl lithium in

THF to a cooled (-78°C), stirred, THF solution of 0.045 mole tetrakis [iodo(tri-n-butylphosphine).copper (1)][34] (procedure described later). The formation of a blue black mixture indicated a positive reaction.

Following the procedure of Johnson,[35] a solution containing 0.022 mole of the ketal tosylate in 10 ml of dry THF was added dropwise to the stirred solution of the complex. The mixture was allowed to reach 0°C, stirred for 2 hours, and then poured into saturated aqueous ammonium chloride. The aqueous solution was filtered and extracted five times with 50 ml aliquots of ether. After drying over anhydrous $MgSO_4$, the ether was removed using a 61 cm Vigreux Column. The residue was distilled to remove any solid solutes and the distillate was separated in two fractions. Residual THF was fractionated out of one portion and the residue was combined with 1 ml of ether. The ethereal solution was then washed three times with 10% HCl, 10% sodium bicarbonate, and saturated NaCl. Presence of 5-hexene-2-one-4,4-d_2 was confirmed by NMR spectroscopy, GC and GC-MS. A sample was isolated by preparative GC. ^{1}H-NMR(crude, 60MHz); δ = 1.85(s,3H); 2.15(s,2H); 5.0(ABX system, 3H).

Preparation of tetrakis iodo(tri-n-butylphosphine) copper(1)

Copper(I) iodide[36] was prepared by adding dropwise a solution containing 73.0 g of potassium iodide and 56.0 g of sodium thiosulfate penta-hydrate in 200 ml of water to a stirred solution containing 50 g of copper(II) sulfate penta-hydrate in 150 ml of water. The addition was continued until a pale flesh colored endpoint was reached. The greyish precipitate was allowed to settle for one hour and the aqueous supernatant was decanted slowly without disturbing the solid. The slush was then filtered under suction through a medium porosity sintered glass funnel. The residue was then washed several times with water, ethanol, ether and then air dried. The product was dried for three days in a vacuum desiccator containing silica gel and concentrated H_2SO_4.

The copper(I) iodide was purified by dissolving 13.2 g of crude material in a solution containing 130 g of potassium iodide in 100 ml of water and then adding 3 g of activated charcoal. The mixture was stirred until colorless; then filtered. To the filtrate was added 12.5 ml of tri-n-butylphosphine. The solution was shaken for 10 min. This resulted in the formation of a gel which did not crystallize upon mixing or scratching. The gel was isolated, dissolved in a minimal amount of hot 1.5:1 ethanol/isopropyl alcohol solvent mixture and allowed to cool in an ice bath.

This procedure resulted in the formation of a white crystalline precipitate which was filtered and washed with distilled water, 95% ethanol, and then air dried. Two subsequent recrystallizations were sufficient to yield pure tetrakis [iodo(tri-n-butylphosphine) copper(I)] (M.P. 74°C; lit.[34]: M.P. 75°C).

4.2.3 An Alternative Synthetic Route for 5-Hexene-2-one-4,4-d_2

A second synthetic route was considered for the preparation of 5-hexene-2-one-4,4-d_2. It was similar to the one described in 4.2.2 except that a different tosylate was made. Instead of the dimethoxy group, the carbonyl was protected with a dioxolane. The problem associated with this route was the instability of the tosylate. A full report of the procedure employed is given here.

Synthetic Scheme

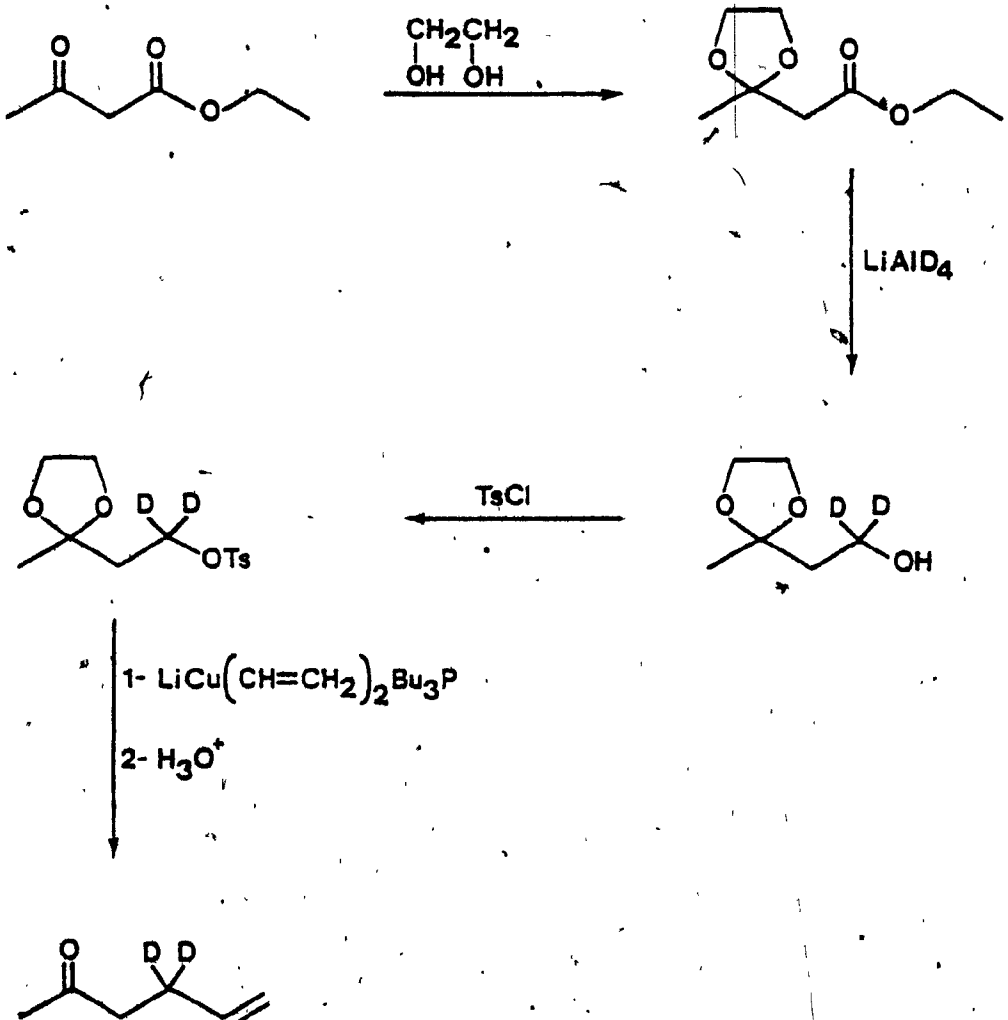

Procedure:

Ethylene glycol ketal of ethyl acetoacetate:

Using Johnson's procedure,[35] in a 250 ml round bottom flask, equipped with a Dean-Stark water separator and a condenser, was introduced 35 g of ethyl acetoacetate, 0.10 g of p-toluene sulfonic acid, 80 g of ethylene glycol and 100 ml of benzene. The two phase mixture was stirred and refluxed for 18 hours. After cooling, the benzene layer was separated, washed successively with water, saturated sodium bicarbonate, water and then saturated sodium chloride. The benzene layer was dried over anhydrous magnesium sulfate and the solvent was then removed under reduced pressure. Fractional distillation of the residue, using a 61 cm long Vigreux column, yielded 35.5 g of 3-dioxolane ethyl butyrate (76% yield; B.P. 62°C at 19 mmHg).

^{1}H-NMR(Pure, 60 MHz); δ = 0.90(t,3H); 1.05(s,3H); 2.20(s 2H); 3.55(s,4H); 3.70(masked q,2H).

3-dioxolane-n-butanol:

The ketal ester was reduced to the ketal alcohol using the same procedure as discussed in 4.2.2 for 3,3-dimethoxy ethyl butyrate. A good yield of 3-dioxolane-n-butanol was obtained.

^{1}H-NMR(Pure, 60MHz); δ = 1.10(s,3H); 1.65(t,2H); 3.45(q, 2H); 3.70(s,4H); 4.00(t,1H).

3-dioxolane-n-butyl tosylate:

Using a modification of Johnson's procedure,[35] 2.6 g of 3-dioxolane-n-butanol and 4.0 g of tosyl chloride were dissolved in 50 ml of ether. To the cooled (-20°C) and stirred solution was then added 3.0 g of freshly powdered sodium hydroxide over a 30 minute period. The mixture was stirred for one hour and then added to an ice-water slush. The ether layer was separated, washed with ice cold water and dried over anhydrous magnesium sulfate. The ethereal layer was concentrated, and an NMR spectrum was obtained to confirm the presence of the tosylate compound.
^{1}H-NMR(CCl_4, 60MHz); δ = 1.05(s,3H); 1.80(t,2H); 2.25(s,3H); .3.65(s,4H); 3.95(masked t,2H); 7.30(d of d, 4H).
The problem with this route was the rapid decomposition of the tosylate. Complete decomposition occurred in a few hours, at -4°C, even when wet with ether. Since 3,3-dimethoxy butyl tosylate(discussed earlier) was more stable, the 3-dioxolane-n-butyl tosylate was not used in the next step.

4.2.4 Synthesis of 5-Hexene-2-one-1-^{13}C

The preparation of 5-hexene-2-one-1-^{13}C has never been reported. The strategy involved in designing a synthetic procedure was to introduce the ^{13}C label in the last step. This is advantageous because loss of labelled intermediates due to multistep synthesis, would not occur. The novel synthesis of 5-hexene-2-one-1-^{13}C is reported here.

Synthetic Scheme

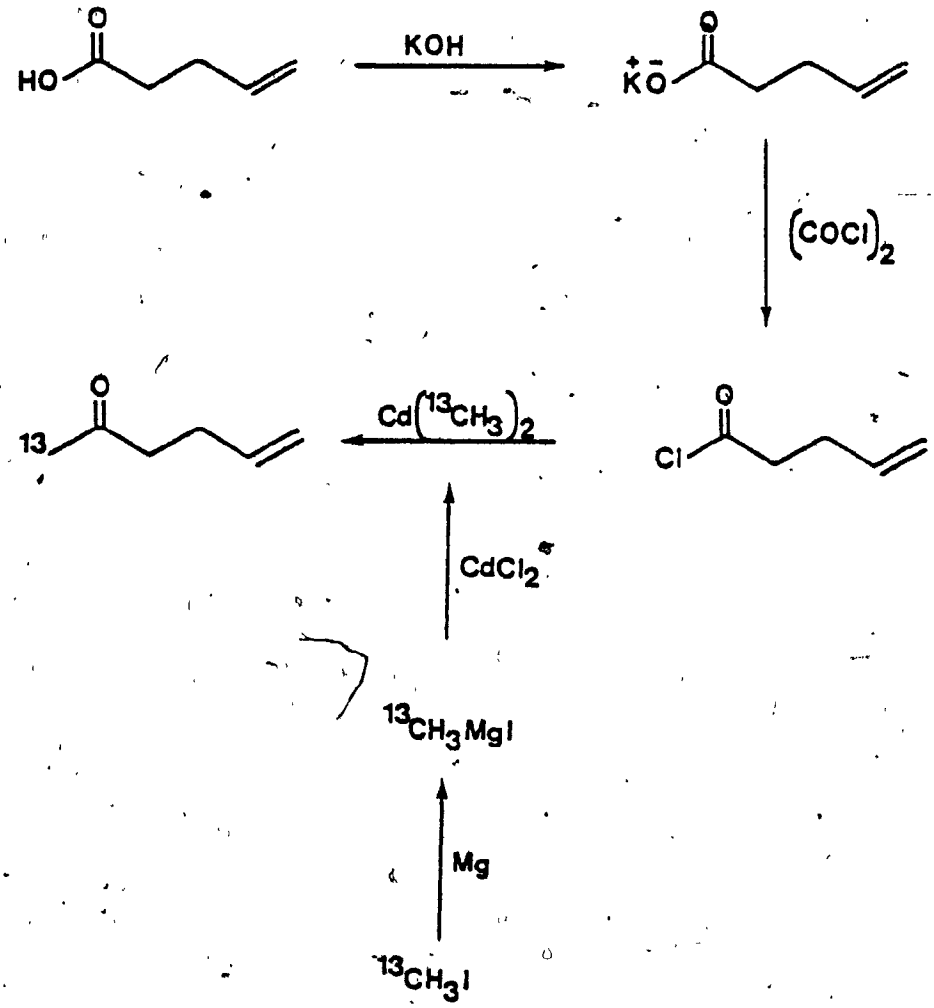

Procedure

The potassium salt of 4-pentenoic acid was prepared in a 50 ml round bottom flask by adding dropwise a 10 N KOH aqueous solution to a well stirred, ice cooled, solution containing 9.0 g of the acid, 1.5 ml of water and two drops of 0.1% phenolphthalein solution. The addition was stopped at the end point. The flask was then attached to a vacuum line (24 mmHg) and most of the water was removed. Drying of the salt was continued at 50°C for 12 hours and then the product was stored in a vacuum desiccator containing only silica gel.

Using a modification of Pichat's[37] procedure, a solution containing 6.5 ml of oxalyl chloride in 50 ml of ether was added under nitrogen to a stirred suspension of 9.0 g dry pentenoic acid potassium salt in 35 ml of ether. The mixture was allowed to stand under a nitrogen atmosphere for 20 hours at room temperature. An apparent slow evolution of gas (CO_2, CO)[37] indicated the progress of the reaction. After filtration of the solution and removal of ether under vacuum, distillation of the residue under reduced pressure afforded 4-pentenoyl chloride in 77% yield. ^{1}H-NMR(Pure, 60MHz); δ = 1.95(q,2H); 2.55(t,2H); 4.53(d, 1H); 4.77(d,1H); 5.20(m;1H).

Using a modification of known organocadium synthetic

methods,[38,39,40] 5-hexene-2-one-1-^{13}C was obtained in the following way. A solution of 1 g ^{13}C labelled methyl iodide (99 atom %) in 5 ml ether was added to 0.18 g of Mg in 5 ml ether with stirring. After the Grignard reaction was complete, 0.6875 g of dry $CdCl_2$ was added slowly at 0°C. The mixture was stirred and refluxed for one hour; the ether was distilled off to near dryness, and 10 ml of benzene was added. Distillation was continued until a head temperature of 70°C was reached. Care was taken to keep foaming to a minimum. More benzene (5 ml) was added to compensate for any losses and the solution was cooled to 5°C. At this point, 0.9 g of 4-pentenoyl chloride in 3 ml of benzene was added to the organocadmium complex. The mixture was stirred for 4 hours at room temperature, then excess ice and 1 ml of 10% H_2SO_4 were added consecutively. The benzene layer was separated and combined with three, 3 ml, benzene extracts of the aqueous layer. Washings with water, 5% sodium bicarbonate and then water were done on the combined organic layers. After drying over anhydrous $MgSO_4$ overnight, the benzene solution was concentrated down to a 4% 5-hexene-2-one-1-^{13}C solution. The product was identified by NMR spectroscopy and GC-MS. Samples of the labelled enone were isolated by preparative gas chromatography. The yield was not determined but a satisfactory amount of product was recovered. Yields based on two

previous trials using unlabelled methyl iodide, ranged from 60% to 65% from 4-pentenoyl chloride.

^{1}H-NMR(Benzene, 60MHz); δ = 1.45(d,3H, $J_{^{13}C-H}$ = 127 Hz); 1.95(m,4H); 4.69(m,2H); 5.40(m,1H).

GC-MS: m/z (%RA) = 27(34.8); 29(28.3); 39(34.2); 41(5.4); 44(47.8); 53(10.9); 55(100.0); 83(29.2); 84(7.5); 99(37.0); 100(21.0).

4.2.5 Synthesis of 5-Hexene-2-one-1,1,1-d_3

The synthetic method employed for this compound was similar to the one used for 5-hexene-2-one-1-^{13}C. Instead of the ^{13}C labelled reagent, deuterium labelled methyl iodide (CD_3I) was used to prepare the organocadmium complex. Deuterium oxide (99.8 atom %) was used in the workup at the last step and caused partial deuterium exchange at C-3 to give a mixture of labelled analogs. The composition of this mixture was determined by mass spectrometry to be: 47.7%, 5-hexene-2-one-1,1,1-d_3; 29.5%, 5-hexene-2-one,1,1,1,3-d_4; 5.6%, 5-hexene-2-one-1,1,1,3,3-d_5. This mixture was useful for obtaining mass spectroscopic data on 5-hexene-2-one-1,1,1-d_3 and 5-hexene-2-one-1,1,1,3-d_4.

^{1}H-NMR(Benzene, 60-MHz); δ = 2.2(m,3.5H); 4.95(m,2H); 5.75(m,1H).

GC-MS, m/z (% RA): 26(6.9); 27(34.7); 30(13.6); 38(5.0); 39(37.6); 41(21.3); 42(5.6); 43(6.7); 44(10.8); 45(93.3); 46(100.0); 47(8.4); 53(9.4); 54(7.3); 55(50.6); 56(37.0); 57(10.1); 83(10.2); 84(7.7); 101(14.4); 102(8.9).

In an attempt to upgrade the isotopic purity of 5-hexene-2-one-1,1,1-d_3, the synthetic procedure was repeated but this time distilled water was used in the workup. The ketone was obtained as a 5% solution in benzene.

^{1}H-NMR(Benzene, 60MHz); δ = 1.90(m,4H); 4.85(m,1H); 5.65(m,1H).

Two samples were isolated by preparative gas chromatography. Due to instrumental problems, two months passed before doing any mass spectroscopic work with the ZAB 2-F. The samples became black after this time period; presence of molecular iodine was suspected. Mass spectrometry gave very peculiar results. First, the conventional mass spectrum indicated a very small presence of d_3 labelled 5-hexene-2-one (5.6%). Since the band corresponding to C-1 in the NMR spectrum was absent the mass spectrum was contradictory. An abundant m/z 98 peak was observed and indicated that the unlabelled compound was present in 48.7% isotopic purity. Although deuterium exchange is a possible explanation it is unlikely. Care was maintained during the purification sequence to exclude any contact with water, base or acid.

The MIKE spectrum of m/z 101 showed an abundant m/z 82 metastable peak (21.3%). This would correspond to loss of HDO from the molecular ion. Loss of water from 5-hexene-2-one$^{7+\cdot}$ never exceeded 1.9% and therefore the above results can not be attributed to 5-hexene-2-one-1,1,1-$d_3^{7+\cdot}$. Chemical degradation of the product during the waiting time period was highly possible. Thus, mass spectroscopic results obtained from the second batch were disregarded.

4.2.6 Synthesis of 5-Hexene-2-one-6,6-d_2 and 5-Hexene-2-one-1,1,1,3,3,6,6-d_7

Synthesis of 5-hexene-2-one-6,6-d_2 was carried out by following Srinivasan's procedure[2,9] with minor modifications. Via deuterium exchange of the 6,6-d_2 labelled ketone, 5-hexene-2-one-1,1,1,3,3,6,6-d_7 was obtained. This compound was prepared because of poor yields obtained in the 5-hexene-2-one-4,4-d_2 synthesis. Essentially, the d_7 analog can be considered as a specifically hydrogen labelled compound at carbons 4 and 5.

Synthetic Scheme

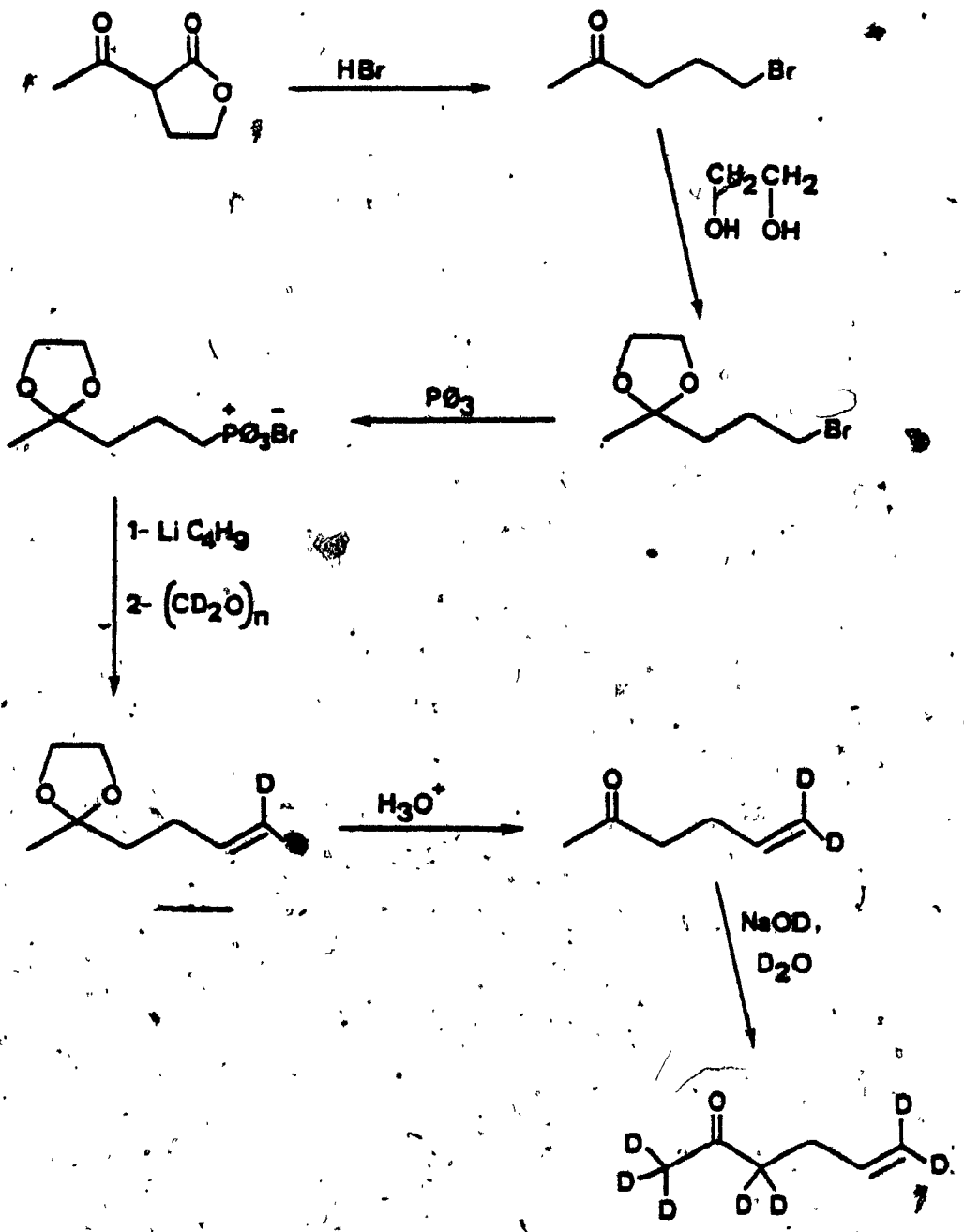

PROCEDURE:

5-Hexene-2-one-6,6-d_2

Following Bachetti's procedure,[41] to a 600 ml triple necked round bottom flask, equipped with two addition funnels and a condenser, was added a solution containing 300 ml of 48% HBr and 133.5 ml of H_2O. The acidic solution was brought to a vigorous boil and 117.2 ml of α-acetylbutyrolactone was added dropwise at a rate of one drop every four seconds. It was found important to maintain a slow addition rate otherwise yields decreased drastically (22% at one drop per second). During the course of the reaction, ten boiling chips (boileezers) were added every half hour. When this was omitted, an explosion occurred after about 1.5 hours.

The product was continuously steam distilled into a separatory funnel. After 75 ml of distillate was collected, the two layers were separated and the top layer was added dropwise to the reaction vessel. Once the addition of lactone was completed, steam distillation was continued for half an hour. The yellow organic liquid was distilled under vacuum to yield 5-bromo-2-pentanone in 79% yield. (B.P. = 88°C at 22 torr; lit[41] B.P. = 78-79°C at 20 torr). ^{1}H-NMR(Pure, 60MHz); δ = 2.20(q,2H); 2.25(s,3H); 2.85(t, 2H); 3.75(t,2H).

In accordance with Obol'nikova's procedure,[42] to a 500 ml round bottom flask, equipped with a Dean-Stark water separator and a condenser, was added 250 ml of benzene containing 0.117 g of p-toluenesulfonic acid and 22.34 g of ethylene glycol. With stirring, 50.0 g of 5-bromo-2-pentanone was added and the mixture was refluxed for two hours; 6.8 ml of water was collected. After cooling and neutralizing with 0.5 g of sodium methoxide, the benzene solution was washed twice with 50 ml portions of deionized water and dried over $MgSO_4$. Following removal of benzene under reduced pressure, the yellow residue was distilled under vacuo to afford 95% pure 5-bromo-2-pentanone dioxolane in 80% yield. (B.P. = 99°C at 16 torr; lit[42] B.P. = 83-84°C at 10 torr).

^{1}H-NMR(Pure, 60MHz); δ = 1.50(s,3H); 2.05-2.45(m,4H); 3.95(t,2H); 4.45(s,4H).

Lit[43]: ^{1}H-NMR(60MHz); δ = 1.26(s,3H); 1.63-2.22(m, 4H); 3.42(t,2H); 3.9(s,4H).

By combining procedures from Obol'nikova and Crombie,[42,43] 3-(2-methyl-1,3-dioxolan-2-yl) propyltriphenylphosphonium bromide was prepared in the following way. To a solution of 41.9 g of the bromo ketal in 57.6 ml of anhydrous benzene was added 52.5 g of triphenylphosphine. The solution was stirred and refluxed until a constant boiling point was reached (30 hrs). The precipitate was

filtered, washed with cold benzene and recrystallized from anhydrous ethanol. The phosphonium bromide was then dried under vacuum for 3 hours at 75°C. The product was found to be about 80% pure (81% yield); the unprotected analog was the major impurity. (M.P. = 210-214°C; lit[43] M.P. = 220-221°C).

^{1}H-NMR($CDCl_3$, 60MHz); δ = 1.4(s,3H); 1.8-2.5(m,4H); 3.9-4.40(m,2H); 4.25(s,4H); 8.50(m,15H).

Lit[15]: ^{1}H-NMR($CDCl_3$, 60MHz); δ = 1.2(s,3H); 1.4-2.16(m,4H); 3.84(s,4H); 3.62-4.07(m,2H); 7.75(m, 15H).

Following Srinivasan's procedure,[29] under a nitrogen atmosphere, 15.7 ml of a 2.6M n-butyl lithium in hexane solution was added slowly to a mixture containing 13.7 g of the phosphonium bromide in 80 ml of anhydrous ether. The orange mixture was stirred for two hours at room temperature. Then, 1.8 g of deuterium labelled paraformaldehyde was added to the mixture and stirring was continued under a nitrogen atmosphere for 24 hours at room temperature. The creamy slightly yellow mixture was filtered through celite, the filter cake was washed several times with ether and the solvent was removed from the filtrate to yield a yellowish oil containing 5-hexene-2-one-6,6-d_2 dioxolane.

The oil was redissolved in 9 ml of ether, combined with 10 ml of 2N HCl and the two phase system was vigorously

stirred for 3 hours at room temperature. The organic layer was then separated and the aqueous phase was extracted five times with 8 ml portions of ether. The combined ethereal layers were washed with 5 ml portions of saturated sodium bicarbonate, water and saturated brine. After drying, the solution was concentrated to a 70% 5-hexene-2-one-6,6-d_2 solution (43% yield based on the phosphonium bromide).

^{1}H-NMR(Pure, 60MHz); δ = 1.85(s,3H); 2.25(m,4H); 5.95(broad singlet, 1H).

GC-MS: m/z(%RA) = 27(11.9); 29(9.0); 30(7.0); 31(5.6); 39(8.6); 40(10.3); 41(8.3); 43(100.0); 55(4.7); 57(32.9); 85(3.9); 100(6.5).

5-Hexene-2-one-1,1,1,3,3,6,6-d_7

Analogous to the procedure in section 4.2.1, an ethereal solution containing 0.1 g (40% W/W) of 5-hexene-2-one-6,6-d_2 was added to 5 ml of 2N NaOD in D_2O(99.8 atom %). The two phase system was stirred for 36 hours at 4°C and then extracted five times with 5 ml portions of ether. After washing the organic layer twice with D_2O, the product solution was concentrated by distilling off most of the ether. A 40% 5-hexene-2-one-1,1,1,3,3,6,6-d_7 solution was obtained in good yield. The isotopic purity was found to be greater than 90%.

^{1}H-NMR(product solution, 60MHz); δ=2.10(d,2H); 6.00(broad singlet, 1H).

4.2.7 Attempted Synthesis of Trans-2-hexenal-5,5-d_2

The synthesis of trans-2-hexenal-5,5-d_2 was attempted by first preparing hexanal-5,5-d_2 followed by an elimination sequence. This approach was taken because synthetic routes for labelled hexenals were not previously reported. In contrast, procedures for labelled analogs of hexanal are well documented.(44,45)

The synthetic sequence was tried twice for the unlabelled trans-2-hexenal and gave unsatisfactory results. The problem seemed to reside in the elimination sequence. No yield of trans-2-hexenal was detected by employing either routes (E through G) or (H through K). In view of this and because of time limitation, the preparation of trans-2-hexenal-5,5-d_2 was not pursued. This section contains a detailed account of the procedures employed in the synthetic scheme.

Synthetic Scheme

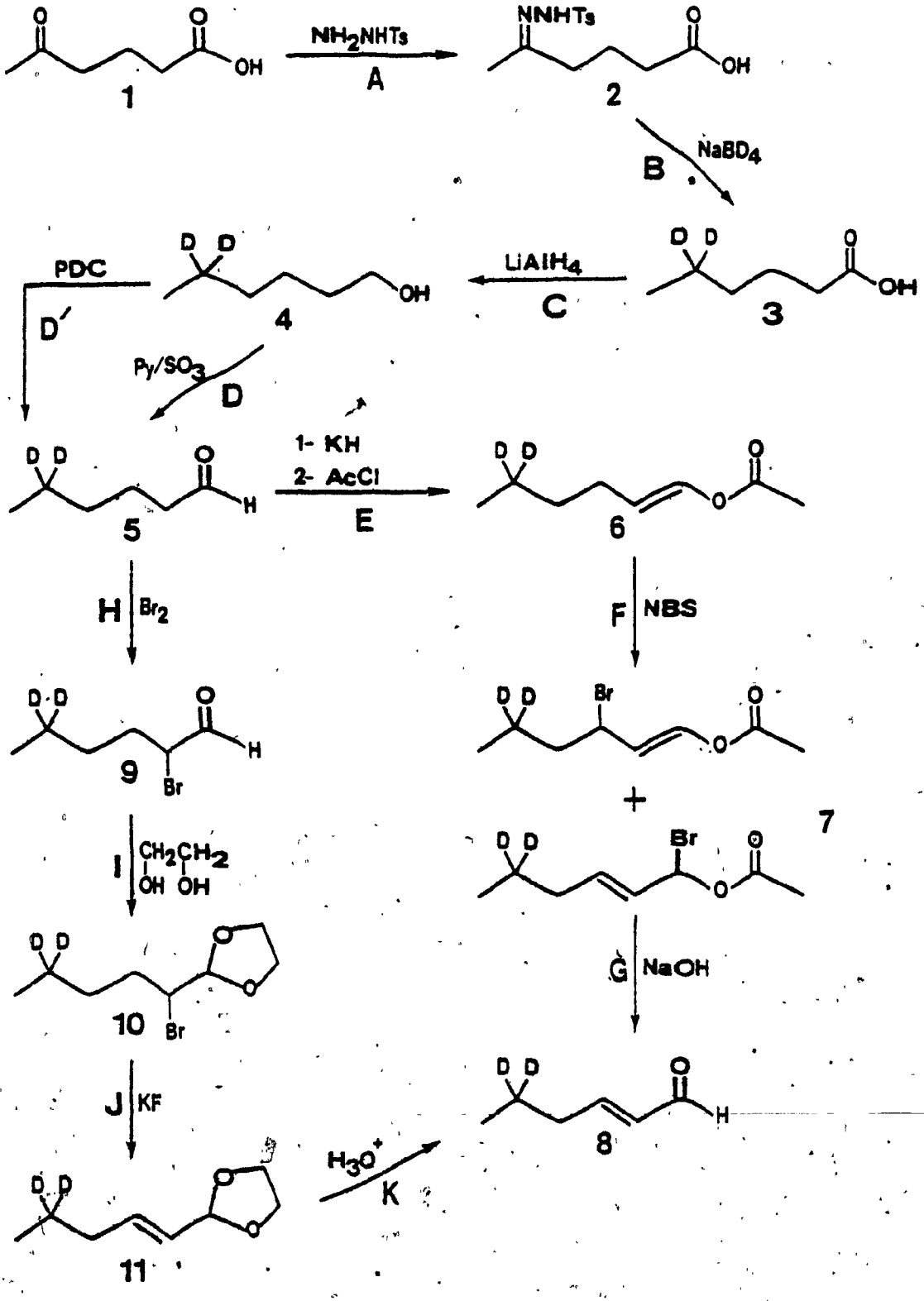

PROCEDURE:

(A) Tosylhydrazone (2):

The synthesis of intermediate(2) was done by employing a modification of the procedure used by Caglioti.[46] Acidified methanol was prepared by adding 2.0 ml of concentrated sulfuric acid to 100 ml of methanol. This was the solvent used in the reaction. A solution of 5.0 g of 5-ketohexanoic acid in 25 ml of acidified methanol was combined with a second solution containing 7.2 g of p-toluenesulfinic acid hydrazide in 50 ml of acidified methanol. The resulting mixture was allowed to stand 8 hours at room temperature. The formation of white crystals was observed during the last two hours. The precipitate was filtered, washed several times with water, ice cold methanol and air dried. A 76% yield of pure product (M.P. 97-98°C) was obtained. The product was identified using infrared spectroscopy.

IR-KBr pellet; $\bar{\nu}$, cm^{-1} = 3210 (sharp, N-H); 1704 (sharp, C=O); 1590 (medium, Ar); 1330 (sharp, C-N).

(B) Hexanoic acid (3):

This compound was prepared from a model procedure developed according to previous methods.[46,47,48] To a

stirred solution of 10 g tosylhydrazone (2) in 125 ml of dry dioxane was added slowly 3.0 g of sodium borohydride in a 500 ml round bottom flask. The resulting solution was stirred for one hour and then refluxed for 4 hours. After cooling, the excess sodium borohydride was cautiously destroyed with 10% HCl. The solution was made alkaline with 50% NaOH and extracted five times with 25 ml portions of 10% NaOH. The aqueous extract was then cooled in an ice bath and acidified by slowly adding 12N HCl. At this point an organic phase appeared. The acidic mixture was extracted six times with 30 ml portions of ether. The ethereal layers were combined and dried over anhydrous $MgSO_4$ for 2 hours. Following removal of ether under reduced pressure, vacuum distillation of the residue yielded 2.74 g (74%) of hexanoic acid. Infrared spectroscopy gave positive identification of the product. IR-Pure; $\bar{\nu}$, cm^{-1} = 2900-3500 (broad, carboxylic); 1765 (sharp and strong, C=O).

NOTE: Special note should be taken that in previous trials, when methanol was used as solvent in this reaction, about 10% yields of product were obtained.

(C) Hexanol (4):

Hexanoic acid was reduced to hexanol in the following manner. To a three necked 500 ml round bottom flask was attached an addition funnel, a distilling column equipped with a calcium chloride drying tube and a nitrogen line. The apparatus was flame dried and once cooled, 125 ml of ether was introduced. With stirring, 0.62 g of lithium aluminum hydride (0.75 molar equivalent) was added. A positive nitrogen flow was set and a solution containing 2.5 g of hexanoic acid in 50 ml of ether was added dropwise. The nitrogen line was replaced by a ground glass stopper and the mixture was refluxed for 1.5 hours. After cooling, the excess hydride was destroyed by first cautiously adding 2 ml of water followed with 2 ml of dilute HCl (5%). The white precipitate was filtered and washed with ether. Removal of traces of acid was done by washing the ethereal layer with 10% sodium bicarbonate and then saturated sodium chloride. The ether solution was dried over anhydrous magnesium sulfate for 2 hours. Filtration of the solution, followed by removal of ether under reduced pressure, afforded a residue containing 1-hexanol. Absence of a carbonyl band in the infrared spectrum indicated a positive reaction. Distillation of the residue afforded 1.5 g of product (69% Yield).

(D) Hexanal (5):

Following the procedure (step D') described by Corey and Schmidt[49] the oxidizing reagent, pyridinium dichromate (PDC) was prepared by introducing 40.3 ml of pyridine into an ice cooled solution containing 50 g of CrO_3 in 50 ml of water. The resulting reaction mixture was then diluted with 200 ml of acetone and cooled for 3 hours at -20°C. This resulted in the precipitation of orange crystals which were filtered, washed with ice cold acetone and dried in vacuo. A 64.5% yield of product was obtained.

To a stirred solution containing 11.05 g of PDC in 28 ml of dichloromethane was added 2.0 g of hexanol. Stirring was continued for 24 hours at room temperature. The solution was then diluted with ether, the precipitated solid was filtered out, and traces of chromium species were removed by refiltering the ethereal solution through 2.0 g of anhydrous $MgSO_4$. The solvent was evaporated using a roto- evaporator and the residue distilled. The product was identified by NMR spectroscopy to be hexanal.

^{1}H-NMR (CCl_4, 60MHz); δ = 0.75(t,3H); 1.30(m,6H); 2.25(t,3H); 9.50(unresolved t,1H).

A second procedure[50] (step D) for the oxidation of hexanol to hexanal was tried but gave no aldehyde. In this case, to a stirred solution of 7.2 g pyridine/SO_3 complex in 75 ml of dimethyl sulfoxide (DMSO) was added a solution

containing 1.5 g of hexanol and 11.1 g of triethylamine in 80 ml of DMSO. The mixture was stirred for 20 minutes, acidified with 10% H_2SO_4 and then extracted three times with 30 ml portions of ether. The ethereal extract was dried over anhydrous $MgSO_4$ overnight. After removal of ether under reduced pressure, an infrared spectrum of the residue showed no carbonyl absorption implying the absence of hexanal.

(E) 1-acetoxy-1-hexene (6):

The first step in the preparation of the enol acetate[51] required careful isolation of solid potassium hydride (KH) from a 25% KH/mineral oil suspension. This was done in the following way.[52] In order to maintain a homogeneous mixture, the suspension was shaken for one hour. The hydride was then placed in a glove bag equipped with a nitrogen line; the bag was purged twice and then filled with prepurified nitrogen. A 2.0 g sample of hydride was weighed and stored in a teflon capped vial. Potassium hydride residues, on the glassware used in the transfer, were destroyed with isopropyl alcohol. The glove bag was opened and unnecessary equipment for the next step were removed.

The glove bag was resealed with an atmosphere of nitrogen and the mineral oil was removed from the hydride by washing three times with dry ether. This was done by first adding about 5 ml of ether to the vial, mixing the mixture

for a few minutes and allowing the hydride to settle at the bottom. The solvent was carefully decanted. To the hydride was then added 5 ml of 1,2-dimethoxyethane, the mixture was transferred to a 25 ml round bottom flask. A solution containing 1.0 g of hexanal in 1.0 ml 1,2-dimethoxyethane was added dropwise to the stirred KH suspension. Vigorous bubbling indicated a positive reaction. After stirring for 15 minutes, the mixture was transferred to a stirred solution combining 7.57 g acetyl chloride, 0.06 g 4-dimethylamino-pyridine and 3 ml of 1,2-dimethoxy ethane. The resulting mixture was stirred for 15 minutes. It was then slurried in an ice/water-pentane mixture. The two phase system was removed from the bag, the pentane layer was separated and the aqueous layer was extracted twice with 25 ml aliquots of pentane. The combined organic layers were then washed twice with saturated sodium carbonate followed by two washings with water. After evaporation of the pentane and distillation of the residue, 0.76 g (66% yield) of 1-acetoxy-1-hexene was obtained (collected between 24°C to 60°C at 17 mmHg). An NMR spectrum was run on the product, showing a mixture of cis and trans isomers.

Cis isomer: ^{1}H-NMR(Pure, 60MHz); δ = 0.90(t,3H); 1.30(m, 4H); 1.95(masked t,2H); 3.40(s,3H); 4.70(q,1H); 6.90(unresolved d,1H).

Trans isomer: ^{1}H-NMR(Pure, 60MHz); δ = 0.90(t,3H); 1.30(m,4H); 2.00(masked t,2H); 3.20(s,3H); 5.30(m,1H); 7.00(d,1H).

Lit(23): ^{1}H-NMR(CCl_4, 60 MHz); δ = 4.75(1H, vinylic-cis); 7.00(1H, vinylic-cis); 5.30(1H, vinylic-trans); 7.05(1H, vinylic-trans).

NOTE: The cis and trans isomers were formed in the reaction in a ratio of 38:62. This is in agreement with the ratio of 40:60 obtained by Riehl.(51)

(F+G) Trans-2-hexenal (8):

According to Riehl's procedure,(53) steps F and G were done consecutively in the following way. To 8 ml of dry carbon tetrachloride was added 1.10 g of enol acetate, 0.964 g of N-bromosuccinimide and 0.16 g of azoisobutyro- nitrile. The mixture was stirred and warmed to 55°C. At this point, an exothermic reaction occurred which caused the solvent to reflux. After the reaction subsided, a solid white material (succinimide) floating on the solution's surface was observed. This gave an indication that bromination had taken place.(53) The mixture was cooled, filtered and the filtrate was kept for the following step.

The filtrate was added dropwise at room temperature to a stirred solution of 20% NaOH (3.2 ml) containing 0.64 ml of methanol and 0.136 g of tetrabutylammonium hydrogen sulfate.

After 40 minutes, the organic phase was isolated, washed with water, and dried over anhydrous magnesium sulfate. The solvent was removed and the residue was distilled. The NMR spectrum of the distillate did not match the one for trans-2-hexenal. A second trial was done employing the same procedure, except that a 2 hour reaction time at the elimination step was used. The NMR spectrum of the resulting product was also different. The products from both trials were analyzed by gas chromatography. A comparison of their chromatograms (Table 4.1) with the one obtained from a standard trans-2-hexenal/ether solution (~1:3) indicated the absence of the peak corresponding to trans-2- hexenal.

From Table 4.1, it is observed that with a longer reaction time, a greater amount of high molecular weight material was produced. This may be attributed to polymerization during the elimination step. However, this can not be taken as the only explanation for the absence of trans-2-hexenal because the products were not fully characterized.

The bromination step was checked by subjecting toluene through the same procedure as described earlier. Benzyl bromide was the resulting product ^{1}H-NMR(CCl_4, 60MHz); δ = 4.35(s,2H); 7.15(s,5H).

Thus, the reagents used for the bromination step were good. This result and that bromination of the enol acetate was indicated from the presence of succinimide, strongly suggests that the bromination step works. Thus, the problem should occur at the elimination step. Four more trials of the bromination/elimination sequence were done by varying the relative amounts of the constituents used during elimination (Table 4.2). The conditions for bromination were kept the same as described earlier. In all circumstances, no yield of trans-2-hexenal was observed. In view of this problem, a different procedure (H to K) for the conversion of hexanal to trans-2-hexenal was tried.

TABLE 4.1

Results from GC analysis of products obtained from bromination/elimination steps (F and G).

Trans-2-hexenal/ether		Unknown product/ether of last step			
		40 min		2 hrs	
Retention time(min)	Area (arb.units)	Retention time(min)	Area (arb.units)	Retention time(min)	Area (arb.units)
0.65	676.90	0.65	673.51	0.62	504.59
0.98	0.10	1.36	4.67	1.28	0.62
1.49	0.24	2.31	0.29	2.24	0.46
3.00	260.08	3.48	1.86	3.36	4.49
6.70	6.82	5.50	0.19	5.45	4.49
		11.11	8.79	10.62	5.86
		18.95	4.59	18.26	28.19

TABLE 4.2

Relative amounts used in step G.

Trial	Initial am't enol acetate (g)	20% NaOH (ml)	Methanol (ml)	Tetrabutyl-ammonium hydrogen sulfate (g)
3	2.3	7.0	5.0	0.312
4	0.6	8.0	0.64	0.013
5	0.6	7.0	1.0	0.312
6	0.335	7.0	0.62	0.312

(H) α-bromo hexanal (9):

Following Chamberlin's procedure,(54) in a 250 ml round bottom flask was added 6.5 ml of hexanal, 3.10 g of p-toluenesulphonic acid and 25 ml of dimethyl formamide (DMF). The resulting mixture was stirred and to it was added dropwise 15 ml of a 4M bromine solution in DMF. During the addition, the temperature was maintained below 20°C. The mixture was then stirred for 10 hours at room temperature. The initial dark orange coloured solution turned light yellow after the reaction's time period. Fifty ml of water was added to the solution, which was stirred for 15 minutes and extracted three times with 45 ml portions of ether. The ether layer was washed twice with water and dried over anhydrous calcium chloride. After removal of ether under reduced pressure, the residue was fractionated at 18 mmHg. The fraction boiling between 44°C and 60°C was found to be α-bromo hexanal (32% yield).

^{1}H-NMR(Pure, 60MHz); δ = 0.75(unresolved t,3H); 1.25(m, 4H); 2.1(q,2H); 4.15(t,1H); 9.15(d,1H).

A second fraction was collected during fractionation between 60°C and 90°C. The product was identified as 2,2-dibromo hexanal (33% yield). This indicated that the bromination reaction went too far; therefore a low yield of α-bromo hexanal was obtained.

^{1}H-NMR(Pure, 60MHz); δ = 0.75(t,3H); 1.20(m,4H); 2.10(q, 2H); 7.05(s,1H).

(I) α-bromo hexanal dioxolane (10):

In accordance with Salmi's procedure[55], in a 100 ml round bottom flask, equipped with a Dean-Stark trap and a condenser, was introduced 25 ml of benzene, 1.33 ml of ethylene glycol, 3.10 g of α-bromo hexanal and 0.10 g of p-toluenesulphonic acid. The mixture was stirred and refluxed for 26 hours. The benzene layer was then separated and the solvent was removed under vacuum. Vacuum distillation (17 mmHg) of the residue was done by collecting two fractions: one from 46°C to 70°C and a second one between 104°C and 113°C. The second fraction was composed of α-bromo hexanal dioxolane (65% yield).

^{1}H-NMR(Pure, 60 MHz); δ = 1.55(t,3H); 2.00(m,4H); 4.00(s, 4H); 4.25(m,4H).

(J+K) Trans-2-hexenal (8):

In a first trial, steps J and K were done consecutively using a modification of Elkik's procedure.[56] In a 50 ml round bottom flask were combined 0.025 moles of α-bromo dioxolane, 10 g of ethylene glycol and 4.5 g of potassium fluoride. The mixture was refluxed for 12 hours then cooled, and added to a solution containing 2.0 g of sodium bicarbonate in 25 ml of water. The resulting solution was extracted three times with 15 ml portions of ether. The ethereal phase was then washed twice with 5% potassium

carbonate and dried over anhydrous potassium carbonate. After removal of ether, the residue was used for the next step without further purification.

The residue was dissolved in an acetone/water mixture (10 ml/10 ml), 0.55 g of oxalic acid was then added and the resulting solution was refluxed for 2 hours. After cooling, the mixture was extracted four times with 10 ml portions of ether. The ether layers were combined, washed twice with water and dried over anhydrous magnesium sulfate for 0.5 hours. The solvent was removed under reduced pressure and the residue was fractionated into three fractions. The NMR spectrum of the first fraction (B.P. 34°C; 20 mmHg) indicated the presence of water and acetone. Since trans-2-hexenal has a boiling point of 63°C at 40 mmHg, a second fraction was collected from 63°C to 78°C at 40 mmHg. Its NMR spectrum did not match that for trans-2-hexenal.

^{1}H-NMR(Fraction 2, pure, 60MHz); δ = 0.75(unresolved t); 1.25 (multiplet); 2.15 (multiplet); 3.15(singlet); 3.45 (multiplet); 4.00 (multiplet); 5.00(s, water); 9.10 (singlet).

A third fraction was collected between 90°C and 110°C at 5 mmHg. Its NMR spectrum was also different from that of trans-2-hexenal.

^{1}H-NMR(Pure, 60MHz); δ = 1.50(unresolved t); 2.05(multiplet); 3.95(singlet); 4.25(multiplet).

Trans-2-Hexenal (Aldrich Chemical Co.):

^{1}H-NMR(pure, 60 MHz); δ = 0.85(t,3H); 1.30(sextet,2H); 2.05(quartet,2H); 5.90(m,1H); 6.55(m,1H); 9.25(d,1H).

Fractions two and three have NMR spectra very similar to that for the α-bromo dioxolane (10) intermediate. It can be speculated that elimination (step J) did not occur. As a result, the removal of the dioxolane group was difficult because the formation of the stable α,β-unsaturated system was not possible.

In a second trial of steps H through K, the product of the elimination reaction(J) was examinated by NMR spectroscopy. No vinylic protons were detected and the NMR spectrum of the product essentially matched the one for α-bromo hexanal dioxolane. This evidence supported our previous observation that elimination did not occur. In view of this difficulty and previous problems, the preparation of trans-2-hexenal-5,5-d_2 was abandoned.

^{1}H-NMR(Product from step J, 60MHz); δ = 1.55(unresolved t, 3H); 2.05(m,4H); 3.95(s,4H); 4.25(m,4H); 4.70(s, water).

4.2.8 Attempted Synthesis of Trans-2-hexenal-4,4-d_2

The approach employed for the synthesis of trans-2-hexenal-4,4-d_2 was similar as for the 5,5-d_2 labelled analog (4.2.7). Thus the preparation of hexanal-4,4-d_2 followed by an elimination sequence appeared to be a convenient route. Since the synthetic route from 1-hexanol to trans-2-hexenal was identical to the one for trans-2-hexenal-5,5-d_2 the same problems discussed in section 4.2.7 would have occurred. Hence, the preparation of trans-2-hexenal-4,4-d_2 was abandoned. Only the first two steps in the synthetic scheme were tried. They are reported in this section.

Synthetic Scheme

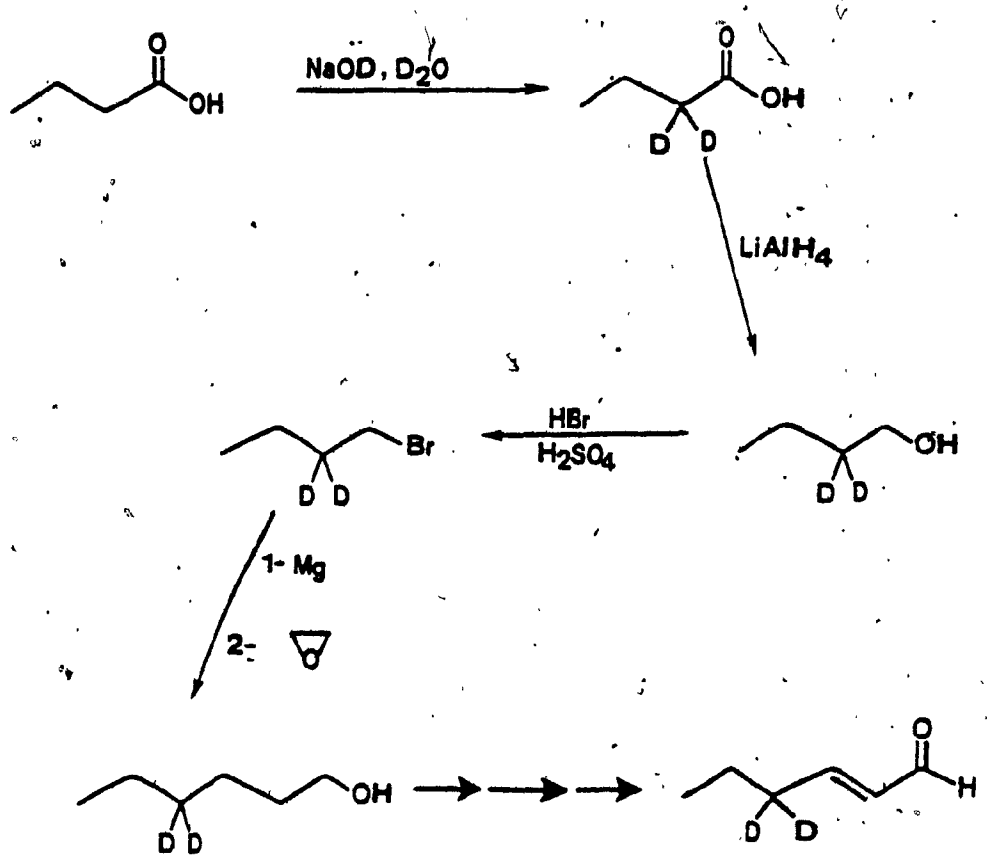

Procedure:

(A) Butyric acid-2,2-d_2[57]

To 40 ml of ice cold D_2O was added 2.55 g of freshly cut sodium metal (0.11 mole); next was added 8.80 g of butyric acid. The mixture was then placed in a steel bomb (Perkin-Elmer high pressure reaction vessel) and warmed to 180° C in a silicone oil bath. After 36 hours, the mixture was cooled to room temperature. The spent D_2O was removed under reduced pressure, fresh deuterium oxide was added to the residue and the exchange was repeated as described above. Three deuterium exchange were done. The acid was recovered by acidifying the reaction mixture with concentrated H_2SO_4 and steam distilling the product. The acid was extracted from the distillate using four 25 ml portions of ether. After drying the ethereal solution with anhydrous magnesium sulfate, the solvent was removed under reduced pressure. The residue was found to be > 95% isotopically pure butyric acid-2,2-d_2 (80 % yield).

^{1}H-NMR(D_2O, 60MHz); δ = 0.90(t,3H); 1.50(q,2H); 4.95(s, H_2O due to acid/water exchange).

From the authentic butyric acid sample:

^{1}H-NMR(D_2O, 60MHz); δ = 0.70(t,3H); 1.35(sextet,2H); 2.10(t,2H); 4.65(s, H_2O due to acid/water exchange).

(B) n-Butanol-2,2-d_2

This compound was prepared using the same procedure as discussed in 4.2.7 (step C).

A 70% yield of n-butanol-2,2-d_2 was obtained.

^{1}H-NMR(Pure, 60MHz); δ = 0.85(t,3H); 1.10(q,2H); 3.30(s, 2H); 4.85(broad s,1H).

From an authentic n-butanol sample:

^{1}H-NMR(Pure, 60MHz); δ = 0.80(unresolved t, 3H); 1.20(m; 4H); 3.25(q,2H); 4.85(t,1H).

CHAPTER 5 RESULTS AND DISCUSSION

The fragmentation processes generating the $C_5H_7O^+$ and CH_3CO^+ ions from the molecular ion of 5-hexene-2-one were studied. The formation of these fragment ions in the source has been considered by Djerassi et al[15] and will only be discussed briefly here. A detailed discussion of the metastable decompositions leading to these daughter ions is given; although two different mass spectrometers were used in this study it should be noted that the discussion is applicable to both instruments because ion transit times to the second field-free region are comparable.

There are some discrepancies in the conventional spectra (Appendix A) of 5-hexene-2-one and its labelled analogues. Very dilute solutions were used to obtain the GC-MS, resulting in a higher than normal source pressure. As a result intramolecular charge transfer[2] may occur, and this is thought to be a possible explanation for the observed reversal of relative peak intensities for m/z 55 and m/z 44 in the spectrum of 5-hexene-2-one-1-^{13}C. In view of this discrepancy, a qualitative approach is taken to the discussion of source fragmentations.

The ionization potential of 5-hexene-2-one was found to be 9.22 eV. By comparison with the values reported[58] for 2-hexanone (9.3 eV) and 1-hexene (9.48 eV) it appears

likely that the threshold ionization of 5-hexene-2-one occurs at the carbonyl. Ionization at the vinylic site cannot be ruled out, but it is postulated that such an ionization process would be followed by charge transfer to the carbonyl functionality.

5.1 The Formation of CH_3CO^+ and $C_5H_7O^+$ in the Ion Source

Fragmentation of the molecular ion of 5-hexene-2-one to give the acetyl cation gave predominant peaks at m/z 43, m/z 46 and m/z 44 in the conventional mass spectra of the 6,6-d_2, d_5 and 1-^{13}C labelled analogues, respectively. Other peaks observed in this region of the mass spectra were very minor, and are thought to arise from partially labelled compounds and from natural isotopic abundances of ^2H and ^{13}C. For the 6,6-d_2,d_5 and 1-^{13}C labelled compounds the major methyl losses are CH_3, CD_3 and $^{13}CH_3$, respectively (Table 5.1). These results are consistent with the α-cleavage mechanism proposed by Djerassi et al[15], as shown in Scheme 1.

TABLE 5.1

Methyl Loss Contributions (%) for Source Fragmentations

Labelled Compound	CH_3	CH_2D	CHD_2	CD_3	$^{13}CH_3$
6,6-d_2	74	13	13	-	-
1,1,1,3,3-d_5	7	7	13	73	-
1-^{13}C	20	-	-	-	80

Supporting evidence for the proposed $C_5H_7O^+$ structure (1) is provided by a comparison of the CA spectrum of source generated m/z 83 from 5-hexene-2-one and its ^{13}C labelled analogue with the CA spectrum of source generated m/z 83 from 4-pentenoic acid:

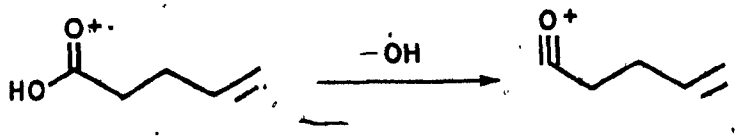

The method of Lehman and Bursey[59] (Appendix B) was used for the comparison. The criterion is that two ion structures are probably the same if the correlation coefficient, R, is greater than 0.95. This method must be used with caution because it makes one of the two CA spectra a standard. The correlation coefficient obtained from the comparisons was 0.98 in each case. The proposed structure (1, Scheme 1) for the $C_5H_7O^+$ ion generated via α-cleavage is therefore considered to be a good possibility.

Since loss of methyl involving other than C-1 is observed (Table 5.1), a second fragmentation pathway must be present. Although some contribution to these other methyl losses will result from incomplete labelling and natural isotopic abundances, loss of $^{12}CH_3$ from 5-hexene-2-one-1-^{13}C is too significant a process to be explained in those terms. A plausible explanation is that δ-cleavage

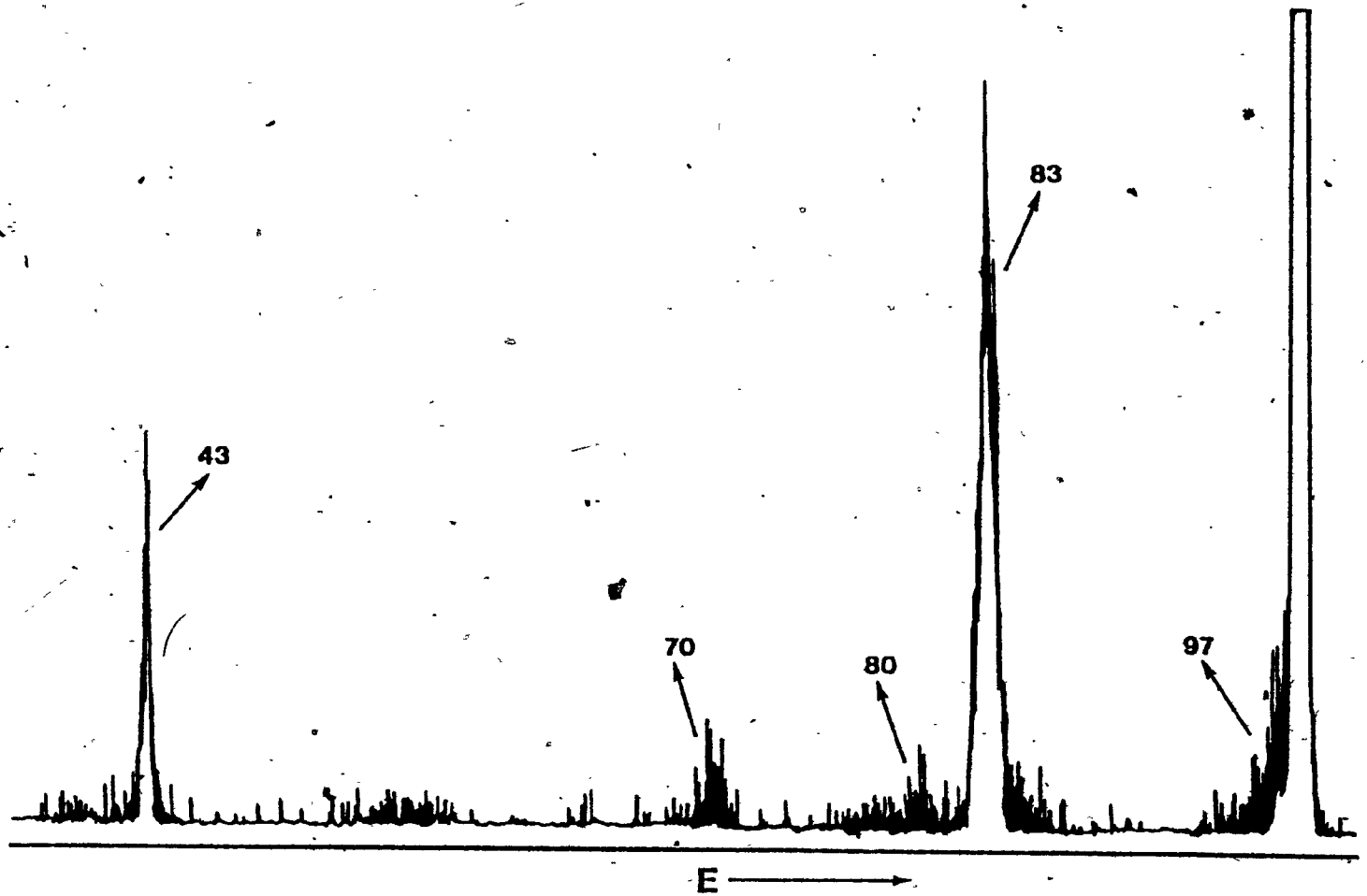

FIGURE 5.1 MIKE spectrum of 5-hexene-2-one$^{+\cdot}$

of the terminal carbon (C-6) may occur after a 1,3-hydrogen shift. This idea is supported by the results for the 6,6-d_2 labelled compound, in which loss of CH_2D and CHD_2 occur in a 1:1 ratio. Such a ratio would arise if the 1,3-hydrogen shift is reversible, causing the exchange of two deuteriums and two hydrogens. It is proposed, therefore, that loss of C-6 as methyl, following a 1,3-hydrogen shift, contributes to the minor methyl losses reported in Table 5.1 (mechanism shown in Scheme 4).

5.2 Metastable Fragmentations Leading to CH_3CO^+ and $C_5H_7O^+$ Ions

The MIKE spectrum of 5-hexene-2-one (Figure 5.1) shows that the major metastable transitions are:

$$M^{+\cdot} \rightarrow CH_3CO^+ + {}^{\cdot}C_4H_7$$
$$M^{+\cdot} \rightarrow C_5H_7O^+ + {}^{\cdot}CH_3$$

The formation of the acetyl ion is considered first in this section. Methyl loss in the metastable time frame is considerably more complex, and was therefore studied in greater detail.

5.2.1 Formation of the Acetyl Cation

The MIKE spectrum of 5-hexene-2-one-1-^{13}C shows the presence of daughter ions at m/z 43 and m/z 44 in a ratio of 7.5:92.5. Since m/z 44 corresponds to $^{13}CH_3CO^+$, its origin

SCHEME 1

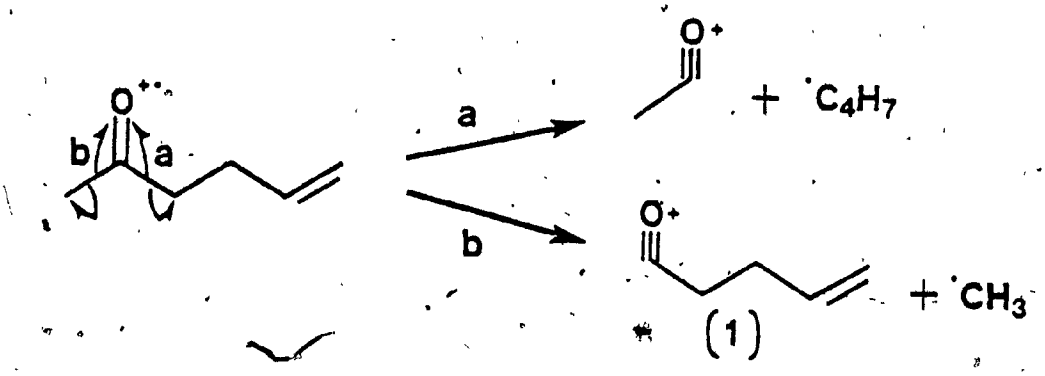

SCHEME 2

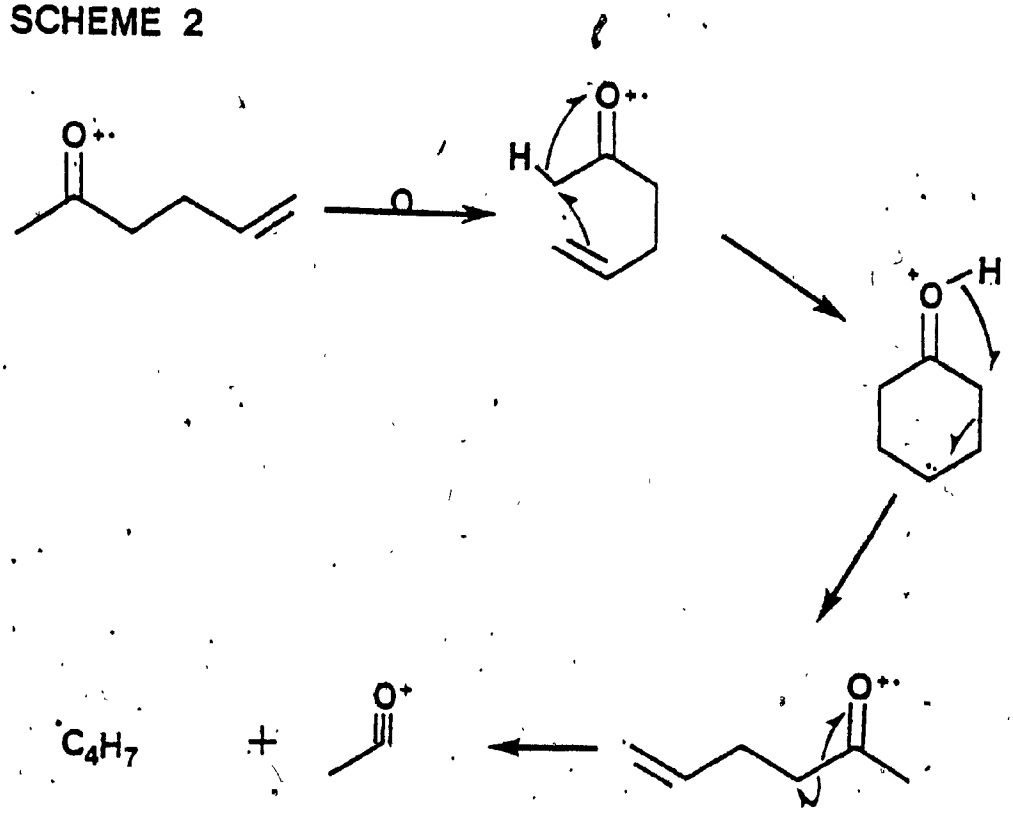

is taken as the α-cleavage fragmentation (Scheme 1). The metastable peak at m/z 48 cannot arise from unlabelled 5-hexene-2-one because the magnet was tuned to pass only ions with m/z 99. However molecular ions of unlabelled material containing a ^{13}C due to natural isotopic abundance would be transmitted by the magnetic sector and could make a contribution to the observed metastable peak at m/z 43. The isotopic purity of the 1-^{13}C labelled ketone was greater than 98%. Assuming that there was a maximum of 2% unlabelled compound, a 4.4% chance of ^{13}C incorporation in carbons C-3 to C-6 leads to 0.09% of the total sample having an unlabelled C-1 and a label in C-3 to C-6. If it is assumed that this 'mis-labelled' material fragments to lose acetyl in the same 7.5:92.5 ratio as 'correctly' labelled compound a negligible (ca. 1%) of the observed m/z 43 metastable peak can be accounted for.

The daughter ion at m/z 43 in the MIKE spectrum of the ^{13}C labelled analogue can be either $^{12}CH_3CO^+$ or $C_3H_7^+$. The latter possibility is excluded because in the MIKE spectrum of the 1,1,1,3,3,6,6 -d_7 compound no minor peaks were observed at m/z 47, 48, 49, or 50 (i.e. no $C_3H_3D_4^+$, $C_3H_2D_5^+$, $C_3HD_6^+$ or $C_3D_7^+$) but were recorded at m/z 45 and m/z 44, corresponding to CD_2HCO^+ and CDH_2CO^+, respectively. Thus in addition to formation of the acetyl cation by direct α-cleavage there is evidence for a second fragmentation pathway involving rearrangement of the

molecular ion prior to loss of acetyl. A plausible mechanism, involving fragmentation via a cyclic intermediate, is shown in Scheme 2.

5.2.2 Keto-Enol Tautomerism

Keto-enol tautomerism is a well established process in systems containing a keto group[2,16]. In the discussion which follows, the effects of keto-enol tautomerism on the acetyl cation elimination are examined.

The acetyl region of the MIKE spectra of a series of ^2H labelled 5-hexene-2-ones was examined. The relative per cent contributions of various deuterium labelled acetyls to the total acetyl formation was determined on the basis of the major peaks only, with minor peaks assumed to be due to the rearrangment process previously described. The experimental results are in good agreement (Table 5.2) with values calculated on the basis of total exchange of protons at C-1 and C-3. It is proposed that this exchange occurs via keto-enol tautomerism, as outlined in Scheme 3.

SCHEME 3*

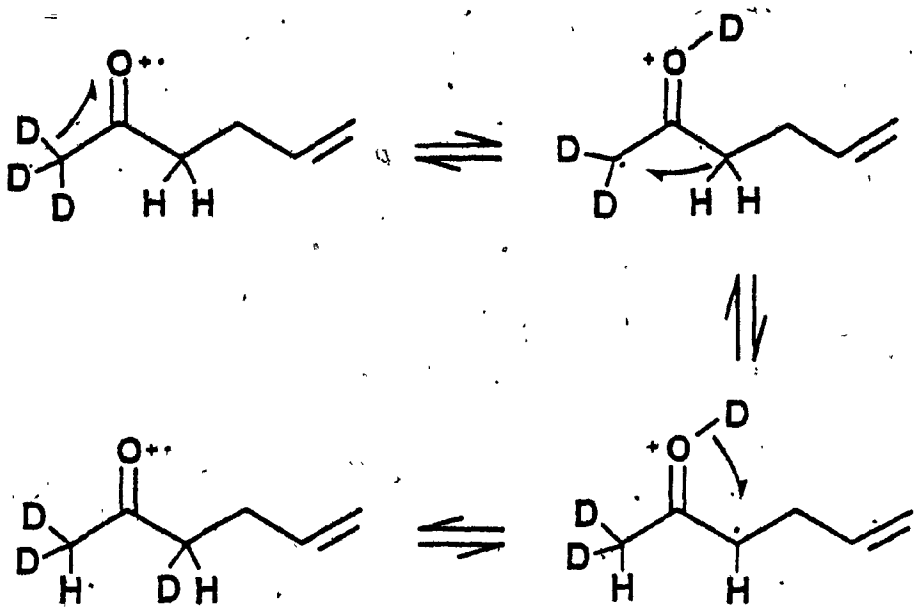

* Shown for 5-hexene-2-one-1,1,1-d_3 $^{7+\cdot}$

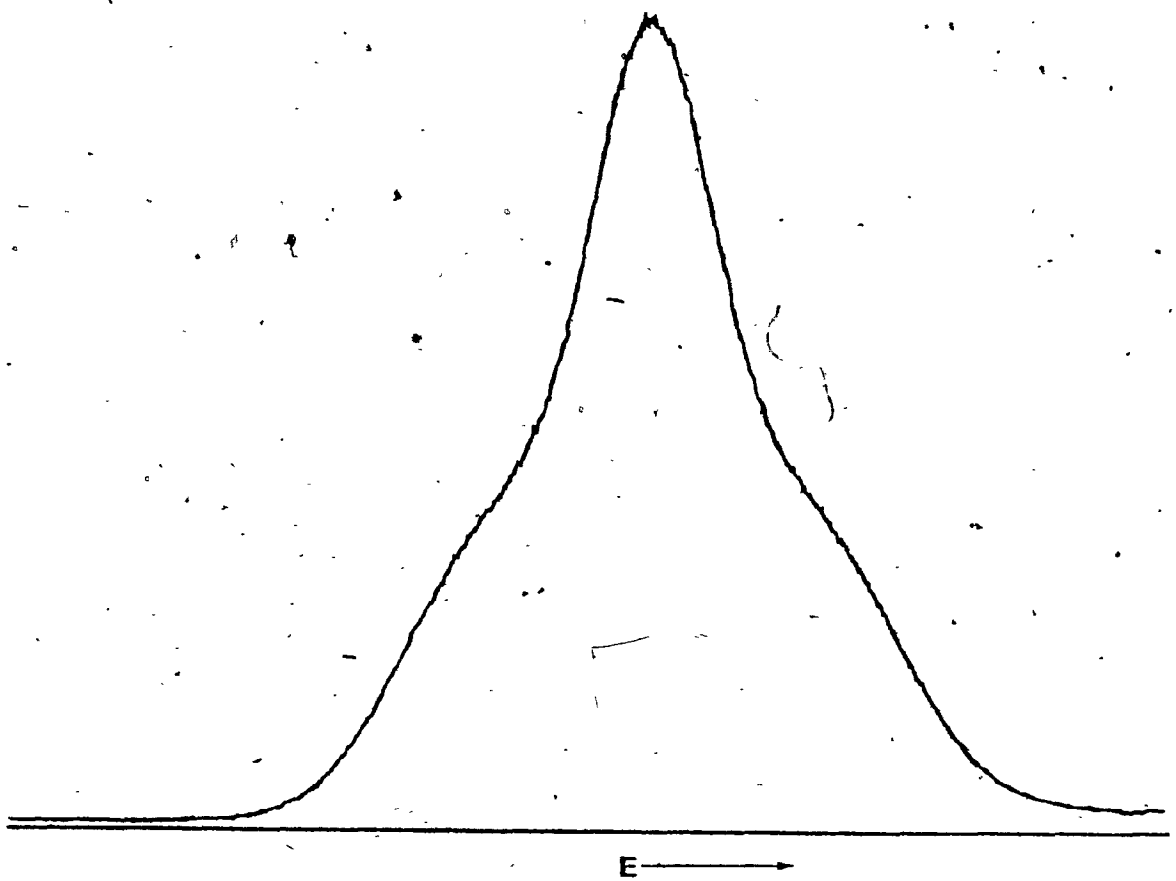

FIGURE 5.2 Metastable peak due to methyl loss from 5-hexene-2-one$^{+\cdot}$

TABLE 5.2

Relative % Contributions to Acetyl Formation

Labelled Compound	CD_3CO^+	CHD_2CO^+	CH_2DCO^+	CH_3CO^+
6,6-d_2	-	m	m[a]	100 (100)
1,1,1-d_3	10.6 (10)[b]	57.8 (60)	31.6 (30)	m
1,1,1,3-d_4	41.0 (40)	59.0 (60)	m	m
1,1,1,3,3-d_5	100 (100)	m	m	m
1,1,1,3,3,6,6-d_7	100 (100)	m -	m -	m -

a) m represents the minor components.

b) values in ( ) calculated on the basis of total exchange of protons at C-1 and C-3.

5.2.3 Metastable Fragmentations Leading to Loss of Methyl Radical

In agreement with the results of Lignac and Tabet[11], it was observed that the metastable peak for loss of methyl from the molecular ion of 5-hexene-2-one was clearly composite (Figure 5.2). The composite shape

indicates that at least two mechanisms for methyl loss are in operation. An attempt was made to eliminate one of the components of the metastable peak by lowering the energy of the ionizing electrons. The metastable peak remained composite even at 15 eV; below 15 eV the low signal-to-noise ratio made observations unreliable.

The methyl loss region of the MIKE spectrum of the 1,1,1,3,3-d_5 molecular ion shows an unexpectedly complex pattern (Figure 5.3). Loss of CH_3, CH_2D, CHD_2 and CD_3 is observed, but in each case the metastable peak is of composite shape. It is evidence that there is considerable loss of positional identity for H and D, but complete H/D randomization is ruled out by a comparison of experimental and calculated distributions (Table 5.3).

TABLE 5.3

Relative Metastable Peak Intensities for Methyl Loss

Labelled Compound	CH_3	CH_2D	CHD_2	CD_3
6,6-d_2	6.7 (7)[a]	2.6 (7)	1.0 (1)	0
1,1,1-d_3	4.4 (35)	7.3 (63)	4.9 (21)	1.0 (1)
1,1,1,3-d_4	1.2 (5)	2.1 (15)	2.3 (9)	1.0 (1)
1,1,1,3,3-d_5	1.0 (1)	2.3 (5)	1.6 (5)	3.5 (1)

a) Values in ( ) represent complete H/D randomization

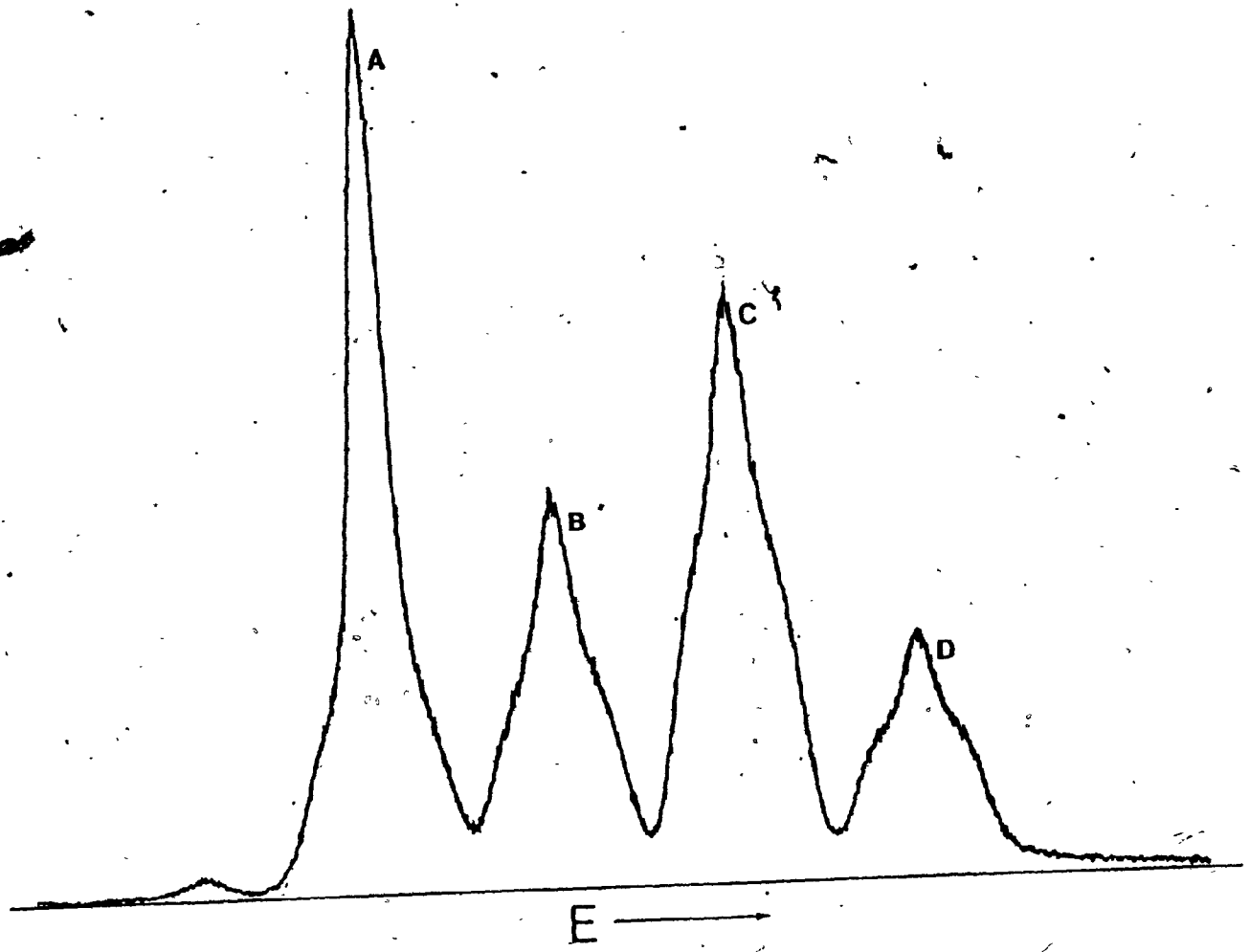

FIGURE 5.3 Partial MIKE spectrum of 5-hexene-2-one-1,1,1,3,3-d_5 $^{+\cdot}$ (A), $M^{+\cdot}-CD_3$; (B), $M^{+\cdot}-CD_2H$; (C), $M^{+\cdot}-CDH_2$; (D), $M^{+\cdot}-CH_3$

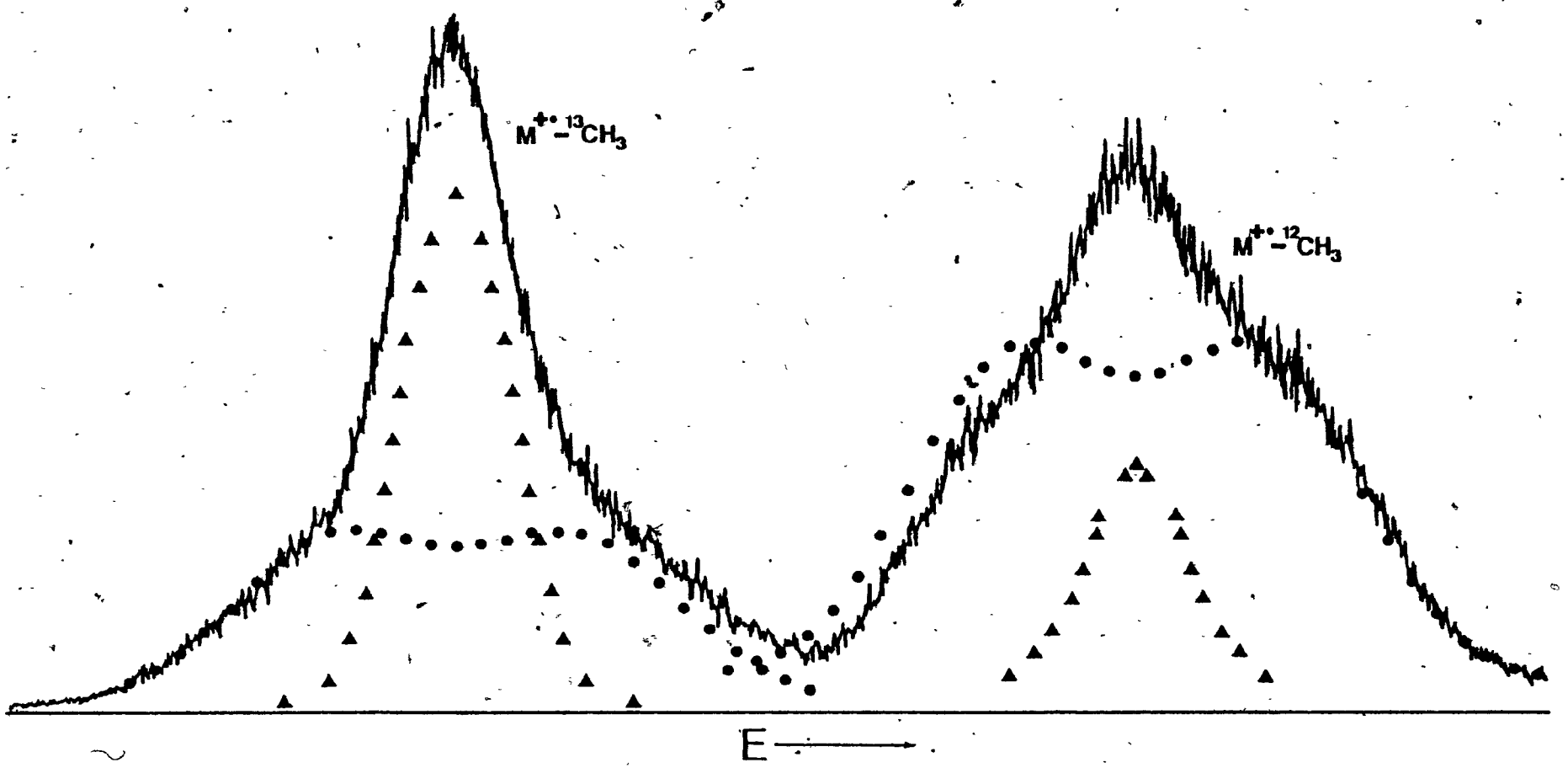

FIGURE 5.4 Metastable peaks for loss of CH_3 and $^{13}CH_3$ from 5-hexene-2-one-1-$^{13}C^{+\bullet}$. Deconvolution results shown as ▲, ●

The methyl loss region of the MIKE spectrum of the 1-^{13}C labelled ketone shows the presence of composite metastable peaks for loss of both $^{13}CH_3$ and $^{12}CH_3$, in a ratio of 1.2:1. Both peaks were deconvoluted by using the same shape controlling parameters for the broad component (Appendix C). The calculated curves fit very well with the undistorted sides of the broad components (Figure 5.4). After separating the sharp components, the corresponding $T_{0.5}$ were calculated; the results are shown in Table 5.4.

TABLE 5.4

$T_{0.5}$ Values (meV) for Methyl Loss from 5-Hexene-2-one-1-^{13}C

Fragment	Experimental Peak	Sharp Component	Broad Component
$^{13}CH_3$	23.1	13.2	186
$^{12}CH_3$	121	9.9	192

a) Values obtained after deconvolution analysis.

The deconvoluted sharp component due to loss of $^{13}CH_3$ gave a $T_{0.5}$ value of 13.2 meV, a value entirely consistent with a simple cleavage reaction[26]. Therefore α-cleavage

is a proposed metastable fragmentation pathway for loss of C-1, with a mechanism as shown in Scheme 1. Delocalization of the double bond in the proposed daughter ion structure is possible. A small $T_{0.5}$ value is also observed for loss of $^{12}CH_3$ from the ^{13}C analogue; a second simple cleavage mechanism is therefore porposed in Scheme 4. This mechanism, which involves loss of the terminal (C-6) carbon, parallels the pathway proposed for 2-hexanone by Cooks[60] to rationalize the predominant loss of CH_3 from 1,1,1,3,3-d_5 -hexan-2-one in the first field-free region. In the case of 5-hexene-2-one, α-cleavage is preferred over δ-cleavage on the grounds of kinetics. Prior to δ-cleavage, the double bond must move twice via 1,3-hydrogen shifts in order to obtain the proper reacting configuration. This gives ample time for α-cleavage to occur. For fragmentations in the source, δ-cleavage was previously considered as a minor possibility; the kinetic analogy could be an explanation of its low occurence.

Fragmentation of the exocyclic methyl group from the proposed daughter ion structure (2, Scheme 4) is a possibility, and was indeed observed in the CA spectrum of metastably generated m/z 84 from 5-hexene-2-one-1-^{13}C. Loss of $^{13}CH_3$ occurred in 10.4% relative abundance. This observation, while not directly supporting the proposed daughter ion structure, does not exclude it.

SCHEME 4

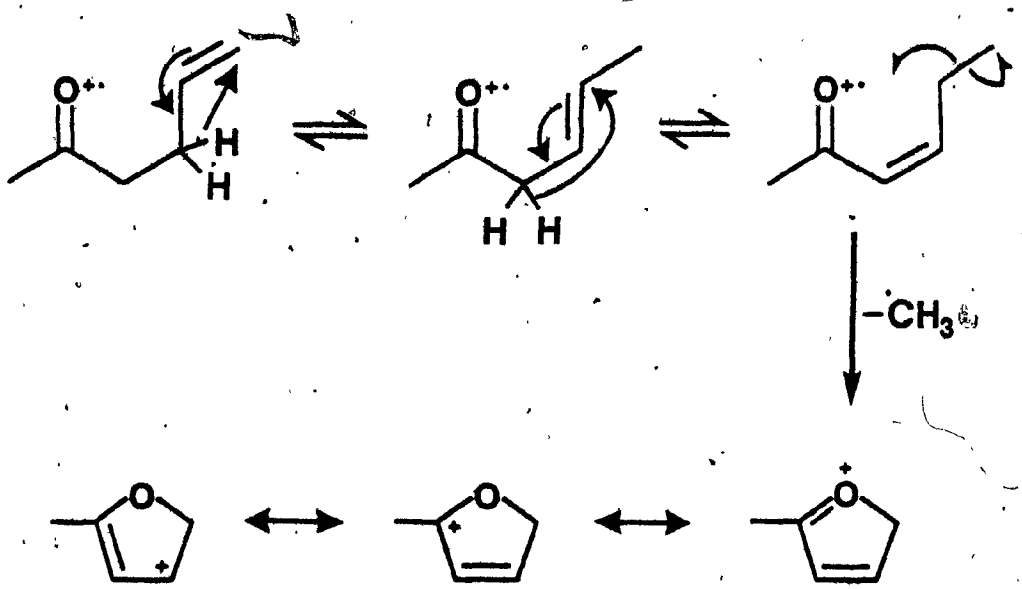

Equivalent To:

If the proposed simple cleavage reactions are considered, sharp components of the composite metastable peak would be expected for only certain methyl losses. For δ -cleavage, loss of CD_2H, CH_3 and CD_2H from the 6,6-d_2,1,1,1,3,3-d_5 and 1,1,1,3,3,6,6-d_7 would generate a sharp component, with a second sharp component observed for CH_3 and CD_3 losses occurring via the α-cleavage mechanism. However, the metastable peaks for all methyl losses were composite. Hence there is a strong possibility of there being a second H/D exchange process, independent of the 1,3-hydrogen shifts described above, involving the remote double bond. A possible exchange process was elucidated in the following way. For the 6,6-d_2, d_5 and d_7 labelled analogues, the chart height of the sharp component was measured from the horns to the tip, for each metastable peak due to methyl loss. The sum of the measured heights fort each compound were taken to represent the abundance of α- and δ-cleavage for that compound. The contributions due to α-cleavage were subtracted to yield the height values due to δ-cleavage. This was done by using the ratio of 0.649:0.351 for the chart components due to C-1 and C-6, respectively. The value of the ratio was obtained from the deconvolution analysis of the metastable peaks due to methyl loss from 5-hexene-2-one-1-^{13}C. Thus, for the 1,1,1,3,3-d_5 compound, the total height of the sharp component for methyl loss was found to be 22.8 cm. The contribution due to

α-cleavage is therefore 22.8 x 0.649 = 14.78 cm.

Loss of CD_3 from the d_5-ketone is assumed to occur via α-cleavage only. Some loss of CHD_2 can also arise via α-cleavage if 'leakage' of a hydrogen atom to C-1 takes place. Such 'leakage' is possible because C-3 is common to all the postulated H/D exchange processes. To allow for this effect, the following procedure was adopted: the peak height due to CD_3 loss was subtracted from the height assigned to α-cleavage (14.78 cm), leaving a residue of 1.95 cm attributible to loss of CHD_2 by α-cleavage. This residue was then subtracted from the total height for CHD_2 loss to give the true δ-cleavage contribution. The results of all the calcuations are given in Table 5.5.

The leakage effect is also observed in the acetyl cation region of the MIKE spectrum of the d_5 compound. In this case, the minor peaks represent 11% of the total acetyl ion formation. This is somewhat higher than the minor contributions observed for the 1-^{13}C analogue (7.5%). For the 6,6-d_2 and d_7 labelled compounds the minor contributions did not exceed 8%. It should be noted that the probability of observing the leakage effect is greatly reduced in the latter two compounds because there are more protons identical to the C-1 protons on the vinylic side of the molecule (eg. for the d_7 compound there are two deuteriums at C-3 and C-6). Because the leakage effect does not

interfere significantly in loss of acetyl by α-cleavage from the 6,6-d_2 and d_7 compounds, we assume that there will also be negligible interference with loss of methyl by α-cleavage. Therefore, the total calculated height due to α-cleavage was subtracted from the experimental heights corresponding to loss of C-1 as methyl, for these compounds. The resulting heights, representing methyl loss via δ-cleavage, are summarized in Table 5.5.

TABLE 5.5

Experimental Sharp Component Peak Heights (cm.) for Methyl Losses

Labelled Compound	CH_3	CH_2D	CHD_2	CD_3
6,6-d_2	9.6	2.6	1.0	-
	(1.0)[a]	(2.6)	(1.0)	-
1,1,1,3,3-d_5	1.8	4.9	3.5	12.6
	(1.8)	(4.9)	(1.6)	(0)
1,1,1,3,3,6,6,-d_7	-	1.0	3.1	9.6
	-	(1.0)	(3.1)	(0.9)

a) Values in ( ) are residuals heights after subtracting the estimated contribution due to α-cleavage.

SCHEME 5*

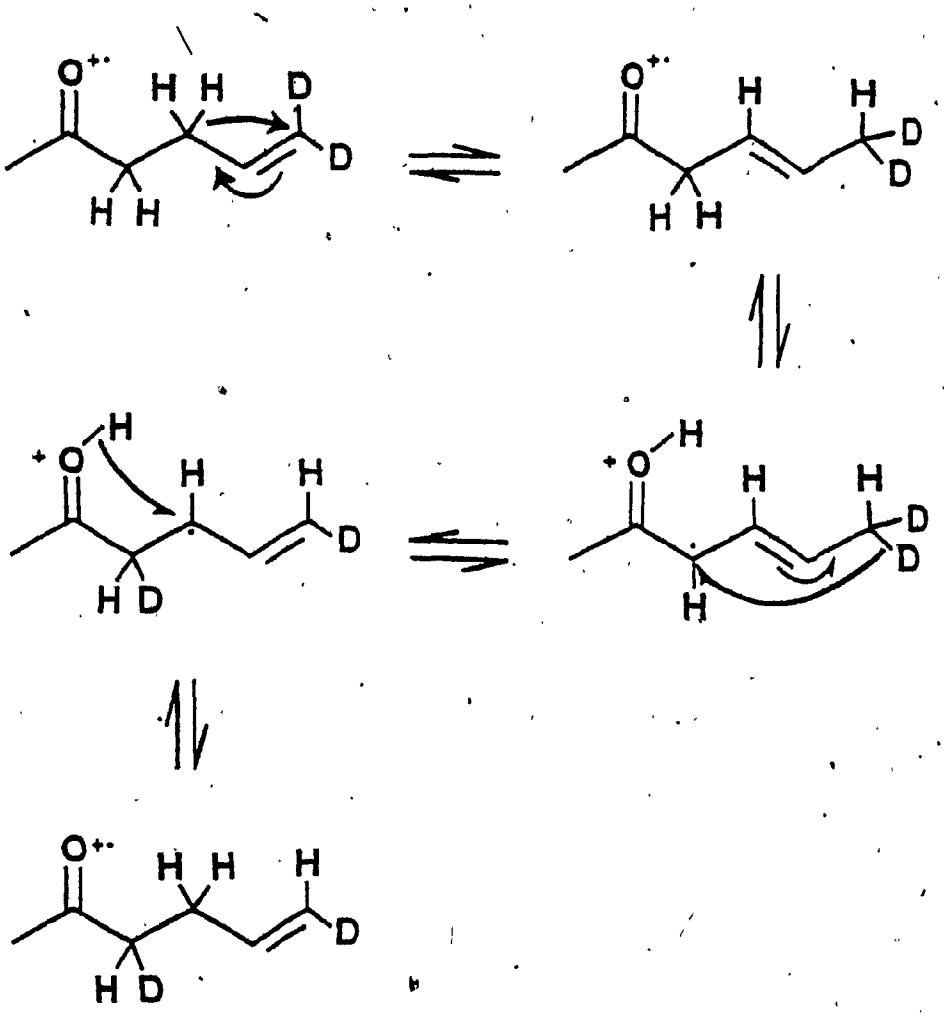

* Shown for 5-hexene-2-one-6,6-d_2 $]^{+\cdot}$

These values were then converted to percentage contributions, and compared with the calculated probabilities assuming 4 H atoms and 2 D atoms participate in a complete loss of positional identity. The results of this comparison are shown in Table 5.6; in view of the somewhat arbitrary measurements used the agreement between experimental and calculated values is excellent, and leads to the proposal of a second H/D exchange mechanism involving C-3, C-4 and C-6 as shown in Scheme 5.

TABLE 5.6

Experimental and Calculated Methyl Losses via δ-Cleavage

Radical	6,6-d_2	d_5	d_7	4H + 2D	4D + 2H
CH_3	22	22	-	20	-
CH_2D	56	59	20	60	20
CHD_2	22	19	62	20	60
CD_3	-	-	18	-	20

A third mechanism involving rearrangment is proposed to explain the broad component of the metastable peak for methyl loss from 5-hexene-2-one. As was previously seen, the same equation (appropriately scaled) fitted both broad components of the metastable peaks generated by methyl loss from

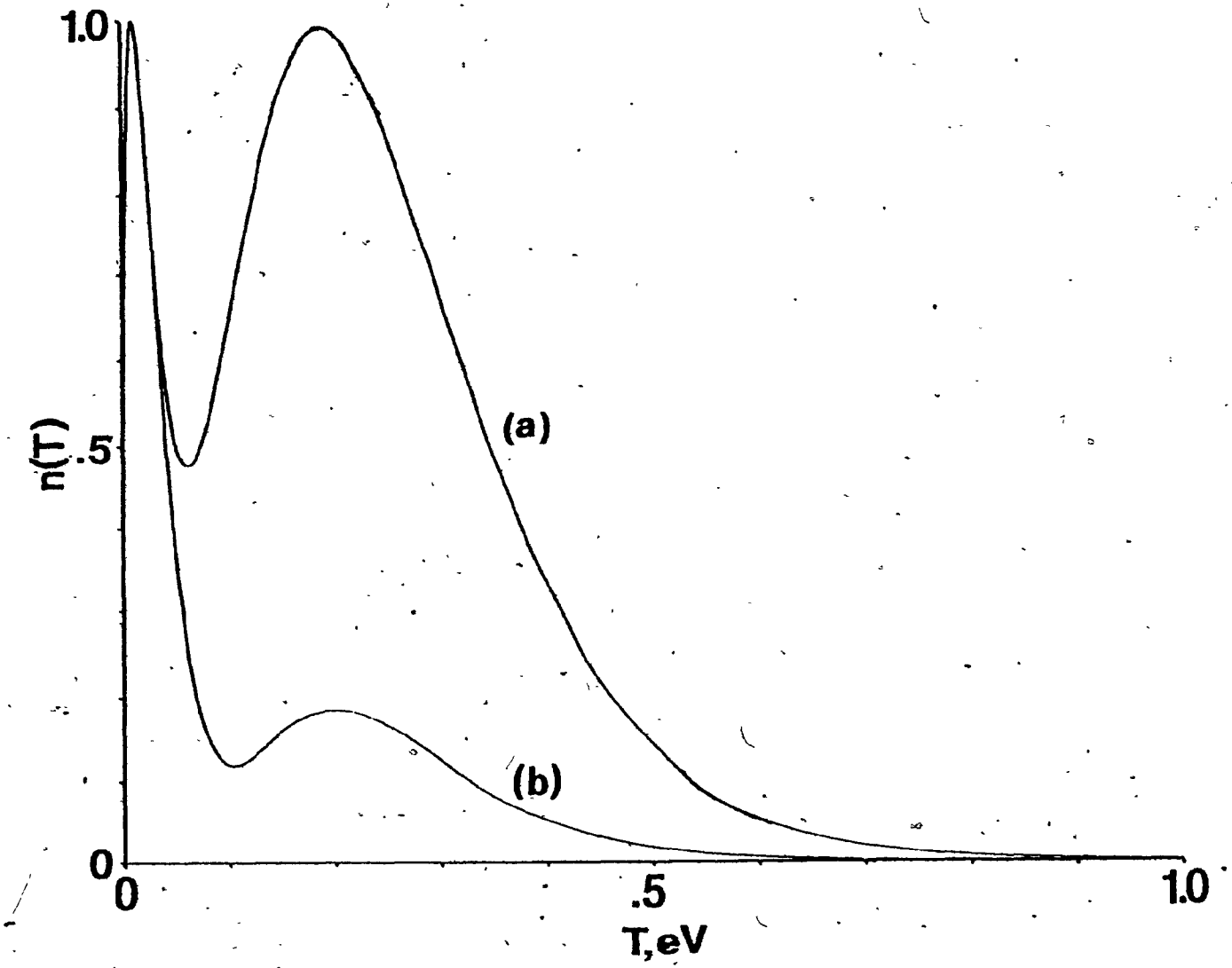

FIGURE 5.5 n(T) plots for (a) loss of $\dot{C}H_3$, (b) loss of $^{13}\dot{C}H_3$ from 5-hexene-2-one-1-$^{13}C^{+\cdot}$

5-hexene-2-one-1-^{13}C closely. The areas under the two broad components were estimated by graphical integration and gave a ratio of $^{13}CH_3$ loss to $^{12}CH_3$ loss of 1:2.5. Carbon atom scrambling is excluded because this ratio does not correspond to any calculated probability value. The $T_{0.5}$ values were calculated for the deconvoluted broad components; for loss of $^{12}CH_3$, $T_{0.5}$ = 192 meV, and for loss of $^{13}CH_3$, $T_{0.5}$ = 186 meV. These results suggest that a common mechanism is involved in loss of $^{12}CH_3$ and of $^{13}CH_3$. This idea is also supported by the n(T) distributions (Appendix B) calculated for the two metastable peaks (Figure 5.5). The marked similarity between the two broad curves is an indication that the loss of $^{12}CH_3$ and $^{13}CH_3$ involves, in each case, the same reaction channel. After considering a number of possibilities, a plausible mechanism was devised (Scheme 6) to rationalize the observed $^{12}CH_3$ and $^{13}CH_3$ losses from the 1-^{13}C labelled compound. It proposes that ring closure to give a symmetrical ion structure precedes loss of C-1 and C-6 as methyl radicals. Loss of C-6 would be favoured kinetically because the requisite ion structure is formed on ring closure. Loss of $^{13}CH_3$ (i.e. C-1) requires a considerable amount of H atom transfer in order to achieve the desired configuration, thus placing this fragmentation pathway at a disadvantage.

SCHEME 6

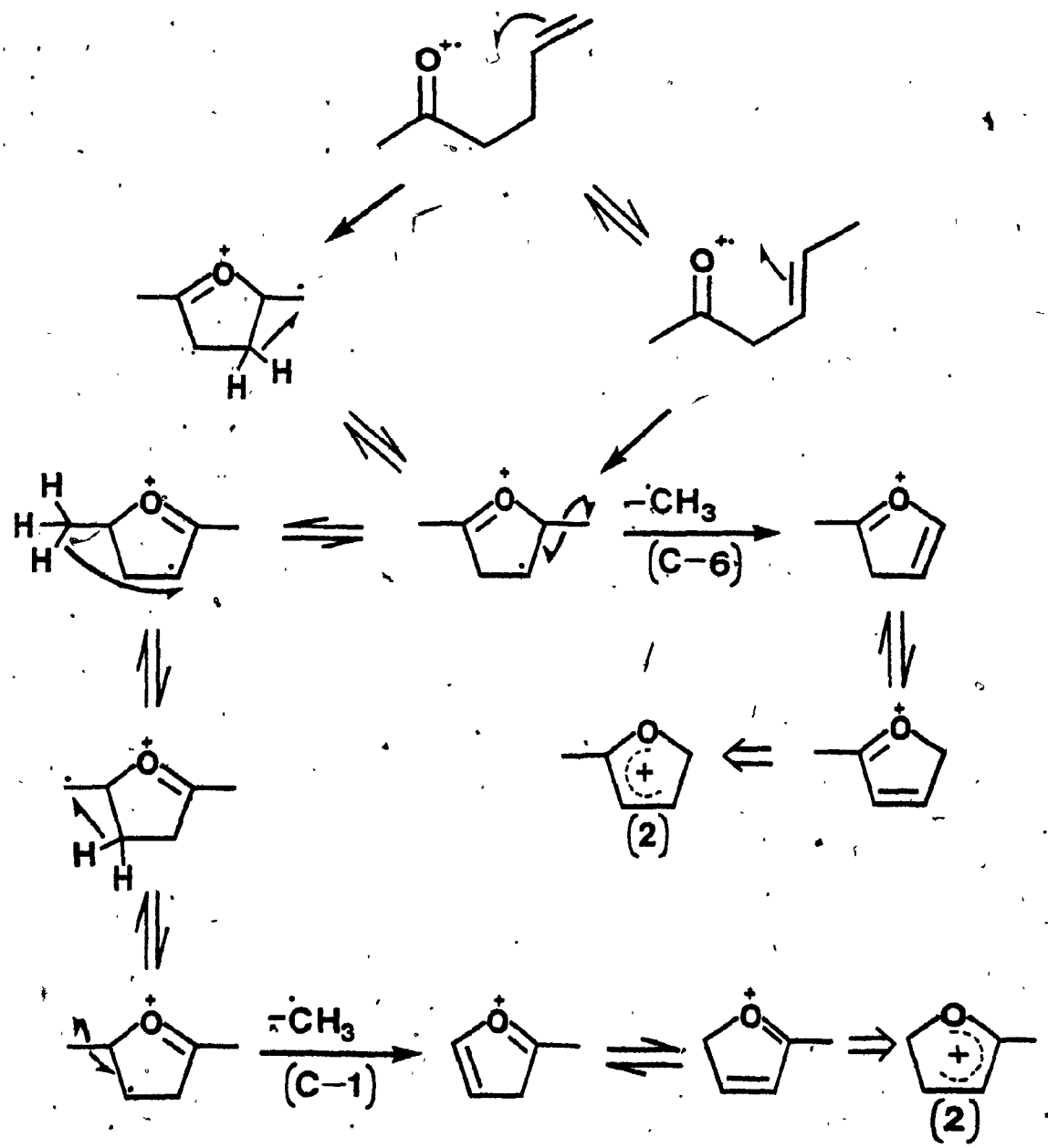

The daughter ion structure (2) is the same for the δ-cleavage (Scheme 4) and cyclization (Scheme 6) mechanisms, but different from the one resulting via α-cleavage (1, Scheme 1). Supporting evidence for more than one structure for $C_5H_7O^+$ is provided from CA spectrometry. The CA spectra of m/z 83 generated from 5-hexene-2-one-1-^{13}C in the source and in the first field-free region are significantly different (R = 0.27). This difference is also shown with the same comparison for the unlabelled analog (R = 0.32).

5.3 Conclusions

From the results obtained in this study we conclude that the formation of CH_3CO^+ from the molecular ion of 5-hexene-2-one proceeds exclusively via α-cleavage in the ion source, and is unaffected by the presence of the remote double bond. The predominant route to acetyl cation in the second field-free region is also α-cleavage, but there is evidence for the operation of a minor rearrangement pathway in this time frame.

Methyl loss from 5-hexene-2-one proceeds predominantly by α-cleavage in the ion source, but there is some evidence to indicate that a minor pathway, involving 1,3-hydrogen shifts and loss of C-6 via δ-cleavage, also contributes to the methyl loss observed in the conventional mass spectrum.

The presence of two independent H/D exchange processes

complicates the interpretation of methyl loss processes occurring in the metastable time frame. The participating exchange processes have been identified as a keto-enol tautomerism involving C-1 and C-3, and a randomization of hydrogen atoms on C-3, C-4 and C-6. The effect of coupling between these two independent exchange processes has been estimated.. It is assumed that both processes are complete prior to metastable fragmentation.

The complex pattern of methyl losses occurring in the metastable time frame can be rationalized in terms of three competing reaction pathways:

1. Loss of C-1 via α-cleavage.
2. Rearrangement involving 1,3 hydrogen shifts, followed by loss of C-6 via δ-cleavage.
3. Rearrangement to a cyclic reacting configuration, followed by competitive loss of C-1 and C-6.

We conclude that, for methyl loss occurring in the second field-free region, the presence of the remote double bond has a significant effect, facilitating cyclization of the molecular ion. The daughter ion generated from this cyclic reacting configuration by methyl loss can be stabilized by delocalization of the positive charge in the five-membered ring.

5.4 Suggestions for Further Studies

Many aspects of the work reported in this thesis require significant further study before definitive conclusions can be reached. Much additional evidence is required to prove the proposed structures of fragment ions. The comparison of methyl loss processes in 5-hexene-2-one with those in trans-2-hexenal cannot proceed until the difficulities encountered in the labelled hexenal syntheses have been resolved. Extension of the work to other isomers would lead to a better understanding of the mechanistic effects caused by the presence of dual functionalities in the fragmenting ion. In this section, some possible extensions of the present work are considered.

5.4.1 Acetyl Cation Formation from 5-Hexene-2-one

It was not our intention to pursue a detailed analysis of the metastable fragmentations leading to the acetyl cation, and our results are therefore somewhat qualitative. Further studies would involve a thorough examination of these fragmentations; site specific ^{13}C labelling in conjunction with these studies could lead to confirmation of the proposed cyclic intermediate (Scheme 2).

5.4.2 Methyl Loss from 5-Hexene-2-one

A prime objective of further work must be confirmation of the proposed δ-cleavage mechanism for methyl loss. This would involve, as a first step, synthesis of 5-hexene-2-one-6-^{13}C, for which synthetic procedures are available. Complete characterization of the daughter ion resulting from δ-cleavage will require, in addition to data for the ion generated from the 6-^{13}C ketone, generation of ions of the proposed structure from other precursors. Similar studies are required to confirm our conclusion that only one daughter ion structure results from the losses of C-1 and C-6 generating the broad component of the composite metastable peak.

Appendix A Mass Spectroscopic Data

A.1 5-Hexene-2-one

Conventional Mass Spectrum (ZAB 2-F)

m/z	%RA	m/z	%RA	m/z	%RA	m/z	%RA
26	4.8	41	14.3	52	2.2	71	2.3
27	23.0	42	6.7	53	8.0	79	2.3
28	5.5	43	100.0	54	3.9	83	11.9
29	17.4	44	6.0	55	48.9	84	1.0
39	3.7	45	1.7	56	4.1	97	1.0
39	24.4	50	4.6	57	1.5	98	15.0
40	2.5	51	4.8	58	2.2	99	1.3

MIKE Spectra

m/z 98 ↓	%RA		m/z 83 ↓	%RA	
	RMU-7	ZAB 2-F		RMU-7	ZAB 2-F
97	20.4	12.4	82	11.8	3.4
84	4.3	2.8	70	-	1.0
83	100.0	100.0	65	-	2.6
80	3.2	1.9	54	2.2	2.9
70	4.3	2.0	55	100.0	100.0
43	37.6	75.3	43	-	1.1

CA Spectra

m/z 98		m/z 83		m* 83[1]	
m/z of daughter ion	%RA	m/z of daughter ion	%RA	m/z of daughter ion	%RA
97	19.6	82	58.2	82	100.0
96	1.3	81	38.4	81	23.2
95	0.7	68	8.0	77	11.8
84	0.8	65	14.5	68	7.5
83	45.0	64	3.1	65	5.8
82	2.5	63	8.0	63	1.7
81	1.1	62	5.7	59	27.5
80	0.8	61	3.1	55	32.0
79	0.9	55	489.2	54	11.3
77	0.7	54	27.0	53	26.2
71	0.6	53	53.4	51	14.2
70	1.2	51	28.4	50	11.3
69	1.1	50	27.6	43	22.6
68	0.3	43	33.2	41	4.1
67	0.8	42	13.9	39	38.7
56	0.9	41	13.6	38	12.3
55	5.2	40	14.2	37	6.6
54	2.8	39	100.0	31	2.5
53	4.2	38	30.4	29	22.6
51	1.7	37	16.5	28	5.2
50	1.2	31	6.0	27	32.7
45	0.6	29	59.7	26	7.1
43	100.0	28	17.0	15	3.8
42	2.1	27	90.9	14	0.5
41	3.8	26	27.3		
39	6.2	25	5.7		
29	2.3	15	8.0		
28	1.2	14	3.4		
27	4.6				
26	1.1				
15	1.1				
14	0.3				

1 - m*83 originating in the 1st Field-Free region.

Metastable Peak Analysis Data

$98^{+\cdot} \rightarrow 83^{+} + {}^{\cdot}CH_3$ $\qquad$ $83^{+} \rightarrow 55^{+} + 28$

70 eV		18 eV			
Height (Norm.)	½ Width (Volts)	Height (Norm.)	½ Width (Volts)	Height (Norm.)	½ Width (Volts)
0.0725	36.76	0.0622	36.71	0.0602	59.83
0.1449	31.86	0.1243	32.41	0.1205	53.72
0.2174	28.01	0.1865	28.98	0.1807	49.45
0.2898	24.86	0.2486	25.66	0.2410	45.79
0.3623	20.31	0.3108	22.71	0.3012	42.43
0.4348	16.11	0.3729	19.34	0.3614	39.68
0.5072	12.95	0.4351	15.84	0.4217	36.63
0.5797	10.50	0.4972	13.63	0.4819	33.88
0.6522	8.75	0.5594	11.23	0.5422	31.14
0.7246	7.35	0.6215	10.01	0.6024	28.08
0.7971	5.95	0.6837	8.72	0.6627	25.03
0.8696	4.55	0.7458	7.55	0.7229	21.67
0.9420	2.80	0.8080	6.63	0.7831	17.09
1.0000	0	0.8701	5.22	0.8434	13.43
		0.9323	3.81	0.9036	9.77
		0.9633	2.58	0.9639	5.19
		1.0000	0	1.0000	0

A.2 5-Hexene-2-one-1,1,1,3,3-d_5

Conventional Mass Spectrum (RMU-7)

m/z	%RA	m/z	%RA	m/z	%RA	m/z	%RA
26	4.5	45	8.8	63	2.7	85	17.6
27	14.8	46	100.0	67	2.0	86	3.3
28	11.9	47	3.1	69	2.9	87	1.8
29	9.6	50	2.7	70	2.0	88	1.8
30	11.5	51	5.9	71	1.8	91	10.9
31	3.5	52	5.5	76	2.5	98	1.2
38	3.7	53	4.9	77	2.0	100	1.0
39	19.3	54	5.7	78	1.4	101	0.8
40	10.7	55	9.2	79	2.0	102	4.1
41	13.3	56	5.5	81	1.6	103	42.8
42	5.7	57	50.6	82	3.1	104	3.3
43	5.5	58	4.3	83	3.5		
44	11.5	59	1.6	84	2.9		

MIKE Spectra

m/z 103 ↓	%RA RMU-7	%RA ZAB 2-F
102	45.1	12.8
101	17.4	3.3
88	37.5	18.2
87	92.5	43.8
86	43.8	27.0
85	100.0	46.7
84	2.8	1.5
77	5.6	3.3
75	4.2	2.2
74	-	0.6
73	-	0.9
46	79.9	100.0
45	5.8	6.6
44	-	3.8
43	-	1.8

CA Spectra

m/z 103				m/z 85			
m/z of daughter ion	%RA	m/z of daughter ion	%RA	m/z of daughter ion	%RA	m/z of daughter ion	%RA
102	16.6	57	4.2	84	10.8	45	1.1
101	2.2	56	2.7	83	9.7	44	3.0
100	0.5	55	2.0	82	2.7	43	3.2
99	0.4	54	1.0	81	0.8	42	3.0
98	0.2	53	0.7	80	0.5	41	5.9
88	5.4	52	0.7	73	0.5	40	10.8
87	12.4	51	1.0	70	0.5	39	7.8
86	9.2	50	0.5	69	0.5	38	3.0
85	22.0	46	100.0	68	0.3	37	1.6
84	2.0	45	7.4	67	1.6	33	0.3
83	1.0	44	6.7	66	1.1	32	0.8
82	0.5	43	3.7	65	0.5	31	4.6
77	2.2	42	1.7	64	0.5	30	6.5
75	1.0	41	2.5	63	0.5	29	7.0
74	1.0	40	2.7	62	0.3	28	10.8
73	0.7	39	1.7	57	100.0	27	7.5
72	0.5	33	0.2	56	6.5	26	2.2
71	0.5	32	0.5	55	5.9	25	0.5
70	0.2	31	1.2	54	4.0	17	0.3
63	0.2	30	2.0	53	3.0	16	0.5
62	0.2	29	2.2	52	3.2	15	0.5
60	0.5	28	2.2	51	3.2	14	0.3
59	1.0	27	1.2	50	2.2		
58	1.2						

Metastable Peak Analysis Data (ZAB)

$103^{+\cdot} \rightarrow 85^{+} + {}^{\cdot}CD_3$

Height(norm)	½ Width(volts)	Height(norm)	½ Width(volts)
.0573	36.10	.5731	8.33
.1146	29.79	.6304	7.47
.1719	24.48	.6877	6.56
.2292	18.43	.7499	5.81
.2865	14.64	.8023	5.05
.3484	12.62	.8596	4.29
.4011	11.11	.9169	3.28
.4584	10.10	.9742	2.02
.5158	9.09	1.0000	0.00

A.3 5-Hexene-2-one-1-^{13}C

Conventional Mass Spectrum (GC-MS)

m/z	%RA	m/z	%RA	m/z	%RA	m/z	%RA
26	4.17	39	34.18	53	10.94	80	4.65
27	34.75	41	5.35	54	2.17	83	29.17
29	28.27	42	0.97	55	100.00	84	7.50
30	1.29	44	47.80	56	1.05	90	0.94
36	0.78	45	4.05	59	3.63	99	37.00
38	2.89	46	2.63	72	4.12	100	21.03

MIKE Spectra (ZAB 2-F)

m/z 99 ↓	%RA	m/z 83 ↓	%RA	m/z 84 ↓	%RA	m/z 84 ↓	%RA
98	15.8	82	62.9	83	100.0	68	2.5
84	93.8	81	2.4	82	5.7	67	1.1
83	100.0	80	1.5	81	5.7	66	5.4
81	3.8	79	3.0	80	7.9	60	11.6
71	3.4	65	2.1	78	3.7	59	1.4
70	2.4	59	0.7	77	1.7	56	100.0
57	1.7	55	100.0	73	16.1	55	19.8
44	73.9	43	0.7	72	1.4	48	2.5
43	6.0			71	3.1	44	2.8
				70	2.8	43	2.3
				69	30.3		

CA Spectra

m/z 83		m* 83[1]		m/z84		m* 84[1]	
m/z of daughter ion	%RA	m/z of daughter ion	%RA	m/z of daughter ion	%RA	m/z of daughter ion	%RA
82	163.7	82	173.0	83	175.8	83	100.0
81	34.9	81	173.0	82	175.8	82	24.7
68	7.4	71	64.0	72	24.7	72	44.1
65	12.6	70	26.4	71	11.3	71	10.4
63	5.1	69	39.5	70	6.1	70	2.4
55	611.6	68	15.9	69	91.8	68	10.4
54	32.6	66	18.0	68	24.7	66	16.1
53	46.5	65	14.9	67	6.1	63	7.1
51	23.3	64	6.4	66	18.6	60	100.0
50	22.8	62	12.7	65	4.8	56	26.6
43	18.6	61	15.9	64	6.1	54	23.4
42	14.9	60	22.3	60	61.5	52	15.6
41	18.6	59	100.0	59	6.1	46	35.0
39	100.0	58	43.5	56	432.9	40	27.3
38	27.9	57	11.7	55	128.1	39	26.6
37	14.0	55	62.6	54	81.4	38	14.3
31	4.7	53	49.9	53	35.9	30	10.4
29	60.5	52	18.0	52	46.3	29	19.5
28	18.6	51	27.6	51	43.7	28	18.8
27	94.0	50	21.2	48	136.4	27	25.3
26	27.0	43	23.4	44	93.1	26	7.1
15	5.6	42	10.6	43	36.8	16	5.8
14	4.2	41	12.7	42	33.8	15	2.6
		39	79.6	41	43.3		
		31	6.4	40	81.0		
		29	48.8	39	100.0		
		28	14.9	38	36.8		
		27	71.1	37	18.6		
		25	4.8	36	48.9		
		15	7.6	31	6.1		
		14	2.1	30	31.6		
				29	68.0		
				28	68.4		
				27	81.4		
				26	24.7		
				24	6.1		

1-m*83 and m*84 originating in the 1st field-free region.

Metastable Peak Analysis Data

$99^{+\cdot} \rightarrow 83^{+} + {}^{13}\dot{C}H_3$ $99^{+\cdot} \rightarrow 84^{+} + {}^{12}\dot{C}H_3$ $83^{+} \rightarrow 55^{+} + 28$

Height (norm.)	½ Width (volts)	Height (norm.)	½ Width (volts)	Height (norm.)	½ Width (volts)
0.0717	34.20	0.147	34.22	0.0677	57.88
0.1434	27.10	0.183	32.88	0.1353	51.95
0.2151	20.78	0.239	31.61	0.2030	47.16
0.2867	15.36	0.275	30.41	0.2706	42.55
0.3584	12.65	0.330	28.84	0.3383	39.74
0.4301	11.02	0.367	27.22	0.4065	36.45
0.5018	9.88	0.422	25.17	0.4736	33.81
0.5735	8.43	0.459	23.49	0.5414	30.51
0.6452	7.53	0.514	21.98	0.6089	27.21
0.7168	6.62	0.550	19.39	0.6766	23.91
0.7885	5.72	0.606	18.07	0.7442	21.93
0.8602	3.91	0.642	15.24	0.8119	16.82
0.9319	3.01	0.697	12.16	0.8796	11.54
1.0000	0	0.734	10.12	0.9472	7.92
		0.789	7.83	1.0000	0
		0.826	6.38		
		0.881	5.00		
		0.917	4.64		
		0.972	1.20		
		1.000	0		

A.4 5-Hexene-2-one-1,1,1-d_3

Conventional Mass Spectrum (GC-MS)

m/z	%RA	m/z	%RA	m/z	%RA	m/z	%RA
26	6.8	43	6.7	54	7.3	82	1.8
27	34.6	44	10.8	55	50.6	83	10.2
29	4.5	45	93.2	56	37.0	84	7.7
30	13.5	46	100.0	57	10.1	85	3.0
31	2.4	47	8.4	58	2.4	86	3.0
37	2.5	48	2.9	61	2.1	87	1.1
38	4.9	49	1.0	62	1.3	100	4.6
39	37.5	50	4.6	72	1.5	101	14.4
40	1.1	51	6.3	73	1.1	102	8.9
41	21.2	52	4.4	74	2.5	103	1.7
42	5.5	53	9.4	81	1.4		

MIKE Spectra (ZAB 2-F)

m/z 101 ↓	%RA	m/z 102 ↓	%RA
100	21.3	101	20.5
99	1.1	100	1.4
86	59.4	87	50.9
85	100.0	86	90.9
84	66.8	85	100.0
83	13.8	84	43.8
82	6.7	83	4.3
81	1.1	82	1.1
73	7.6	73	5.6
72	1.9	72	1.9
71	1.9	71	2.0
70	1.0	70	1.3
46	12.4	46	52.3
45	67.9	45	74.1
44	37.0	44	9.2
43	5.1	43	3.5

A.5 5-Hexene-2-one-6,6-d_2

Conventional Mass Spectrum (GC-MS)

m/z	%RA	m/z	%RA	m/z	%RA	m/z	%RA
26	2.4	40	10.3	52	2.4	79	0.5
27	11.9	41	8.3	53	2.3	81	0.7
29	9.0	42	5.3	54	2.9	83	0.7
30	7.0	43	100.0	55	4.7	84	0.7
31	5.6	44	3.0	56	2.9	85	3.9
37	0.6	45	1.2	57	32.9	100	6.5
38	1.5	50	1.1	58	2.4	101	0.7
39	8.6	51	2.5	71	1.0		

MIKE Spectra (ZAB 2-F)

	%RA	
m/z 100 ↓	RMU-7	ZAB 2-F
99	24.8	7.8
85	100.0	100.0
84	42.5	42.9
83	20.9	16.3
82	4.5	2.0
81	-	0.7
75	-	0.7
74	-	0.5
72	7.8	3.2
71	4.6	3.8
70	12.4	9.1
58	3.9	0.7
57	4.6	0.8
56	5.2	2.1
45	13.1	1.1
44	5.2	1.6
43	64.1	29.9

A.6 5-Hexene-2-one-1,1,1,3,3,6,6-d7

MIKE Spectra

m/z 105 ↓	%RA RMU-7	ZAB 2-F
104	17.0	8.6
103	10.7	5.3
90	-	2.2
89	24.3	23.0
88	74.7	76.5
87	100.0	100.0
86	2.7	1.7
85	-	0.7
79	9.3	4.1
78	-	0.7
77	4.3	2.7
75	-	0.7
74	-	0.8
73	-	0.6
46	61.0	41.9
45	8.0	3.0
44	4.0	0.7

A,7 4-Pentenoic Acid

Conventional Mass Spectrum (ZAB 2-F)

m/z	%RA	m/z	%RA	m/z	%RA	m/z	%RA
26	8.6	40	4.5	53	15.2	72	3.0
27	39.4	41	48.2	54	37.9	73	5.3
28	19.7	42	11.4	55	100.0	81	2.6
29	34.5	43	25.8	56	21.2	82	10.3
30	1.5	44	5.3	57	13.3	83	4.5
31	3.0	45	17.0	58	23.5	85	1.7
37	3.0	49	6.1	59	1.5	99	2.9
38	4.5	51	6.2	60	10.6	100	28.8
39	40.2	52	3.0	71	3.0	101	2.3

MIKE Spectra (ZAB 2-F)

m/z	83→ 82	81	80	68	65	56	55	54
%RA	32.0	1.1	0.6	24.0	0,8	3.6	100.0	4.0

CA Spectrum of m/z 83 (ZAB 2-F)

m/z of daughter ion	%RA	m/z of daughter ion	%RA	m/z of daughter ion	%RA	m/z of daughter ion	%RA
82	11.1	54	9.0	41	3.2	28	4.0
81	2.6	53	4.6	40	3.0	27	12.5
68	3.8	51	3.3	39	12.8	26	3.6
65	0.6	50	2.9	38	3.6	15	0.6
56	2.2	43	1.1	37	1.5	14	0.5
55	100.0	42	2.8	29	5.3		

A.8 Trans-2-Hexanal

Conventional Mass Spectrum (RMU-7)

m/z	%RA	m/z	%RA	m/z	%RA	m/z	%RA
26	8.4	41	100.0	54	12.4	70	16.7
27	54.0	42	62.5	55	72.4	79	6.5
28	29.5	43	34.2	56	12.8	80	6.7
29	41.3	44	24.8	57	43.1	83	45.1
38	9.0	50	5.8	67	5.3	97	9.5
39	69.1	51	8.0	68	6.4	98	34.5
40	13.4	53	13.5	69	52.4		

MIKE Spectra

m/z 98 ↓	%RA RMU-7	%RA ZAB 2-F
97	100.0	100.0
83	46.6	74.5
80	54.3	96.9
70	37.6	54.7
69	56.1	75.9
56	35.3	50.3
43	29.6	43.2

CA Spectrum of m/z 83

m/z of daughter ion	%RA	m/z of daughter ion	%RA	m/z of daughter ion	%RA	m/z of daughter ion	%RA
82	47.3	62	8.9	41	8.9	26	21.1
81	59.3	61	4.7	39	100.0	25	4.4
79	2.2	55	322.2	38	28.9	15	7.8
68	3.8	53	58.4	37	15.6	14	3.3
66	2.2	51	30.7	31	13.8	13	1.8
65	24.4	50	26.7	29	58.9		
64	5.1	43	41.1	28	12.2		
63	13.3	42	14.4	27	82.2		

Metastable Peak Analysis Data

$98^{+\cdot} \rightarrow 83^{+} + \cdot CH_3$

Height(norm.)	½ Width(volts)	Height(norm.)	½ Width(volts)
0.0673	41.29	0.6061	14.78
0.1347	36.52	0.6734	12.49
0.2020	32.90	0.7407	10.49
0.2694	29.75	0.8081	8.49
0.3367	26.70	0.8754	6.77
0.4040	23.31	0.9428	4.58
0.4714	20.31	1.0000	0.00
0.5387	17.45		

Appendix B. Mathematical Treatment of Mass Spectroscopic Data.

B.1 Purity of Isotopically Labelled Compounds.

The relative isotopic purity was obtained from the conventional mass spectrum by dividing the peak height corresponding to the labelled compound, M, by the sum of peak heights from other labelled analogs. Since the M + H and M - H processes were not accounted for % isotopic purities, reported in this paper, represent a minimum.

B.2 MIKE Spectra.

For MIKE spectra, the mass of the daughter ion associated with a particular metastable peak was determined from the following relationship:

$$M_2 = \frac{E_2 M_1}{E_1} \quad (Z = 1) \quad \ldots\ldots\ldots\ldots\ldots\ldots (B.1)$$

In equation (B.1), M_1 and M_2 are the masses of the parent and daughter ions, E_1 and E_2 are the corresponding ESA voltages. The voltage, E_2, was either read from a digital voltmeter or evaluated from a calibration ratio obtained by dividing the difference between the initial and final voltages of a scan by the chart distance between them. For the MIKE spectrum of 5-hexene-2-one^{+}, the calibration ratio was 9.25 ESA V./cm. Since the parent ion peak occurred at 265.1 ESA V. and the major metastable peak was 4.39 cm away from the

main beam, for the major process:

$$E_2 = 265.1 - 9.25 \times 4.39 = 224.5 \text{ V.} \quad (B.2)$$

Therefore, from equation (B.1):

$$M_2 = \frac{(224.5)(98)}{(265.1)} = 82.99 \text{ or } 83$$

The masses of daughter ions corresponding to other metastable peaks were computed in the same way.

The methyl loss regions of MIKE spectra, obtained by using an expanded scan, were employed in two ways. The contribution of an individual methyl loss process from a labelled compound was computed by dividing its peak height by the sum of all peak heights for methyl loss.

From metastable peaks obtained under conditions of good energy resolution, kinetic energy release distributions, n(T) vs T curves, were evaluated by using the method of Holmes and Osborne.[61] In general, the experimental peak widths, W, and the corresponding normalised peak heights, H(W), were fitted to an equation of the form:

$$H(W) = (C_1 + C_2W + C_3W^2 + C_4W^3)\text{Exp}(-C_5W^2)) \quad (B.3)$$

by employing a non-linear least squares parameter estimation

routine. An n(T) vs T curve was then constructed from the five coefficients, T, and γ, where the variable T was found from:

$$T = \gamma \left(\frac{W}{2}\right)^2 \quad \text{.....(B.4)}$$

and:

$$\gamma = \frac{M_1^2}{4M_2M_3V} \quad \text{.....(B.5)}$$

where V is the accelerating voltage for the main beam and M_3 is the mass of the neutral fragment. In the analysis, all values of W were corrected for the width of the main beam by using the following equation:(26)

$$W_C = (W_M^2 - W_B^2)^{\frac{1}{2}} \quad \text{.....(B.6)}$$

where W_M is the experimental width at a certain normalised height and W_B is the main beam width at the same height. The average kinetic energy release, was determined by using n(T) from:

$$T(av) = \frac{\int_0^\infty n(T)TdT}{\int_0^\infty n(T)dT} \quad \text{.....(B.7)}$$

The kinetic energy release at half height, $T_{.5}$, was found from equation (B.4) using the corrected width at half height.

B.3 CA Spectra:

The same method as described earlier was used to compute the daughter ion mass corresponding to a particular peak.

CA spectra were compared by using the linear least square method described by Bursey.[59] When two CA spectra were compared, the intensities of one spectrum were plotted in the X axis while those from the second spectrum represented the Y axis. The correlation coefficient, R, was evaluated via linear regression.

Appendix C. Deconvolution of Composite Metastable Peaks

A great deal of information can be obtained by separating the broad and sharp components from a composite metastable peak. This exercise involves a deconvolution procedure. In order to consider a mathematical technique, an understanding of some instrumental factors contributing to the peak shape is necessary.

Some years ago, Beynon[2] demonstrated that for fragmentations occurring in a field-free region, the daughter ion will acquire velocity components in the X, Y, and Z directions. This means that deflection from the initial flight line may occur. The angle of deflection will depend on the newly acquired velocity components which, in turn, are directly related to the kinetic energy release. Consider a fragment ion being formed in the second field-free region of a reversed geometry mass spectrometer. If this ion acquires a large Z-axial velocity component, a large deflection angle will occur. Depending on the distance between the site of fragmentation and the ESA entrance slit, Z-axial discrimination may occur because the entrance slit is of finite length. Daughter ions deflecting at large angles will need to be very close to the entrance slit for passage through the sector. This being the case, a large number of daughter ions will not be recorded and consequently a depression close

to the center of the metastable peak will result. Hence, a "dish topped" peak will be recorded.(2)

In the case of 5-hexene-2-one, the metastable peak due to methyl loss from the molecular ion was clearly composite. Since the bottom portion of the peak was quite broad (i.e. large kinetic energy release) the assumption was made that this metastable peak is the combination of a sharp, Gaussian type, component and a "dish topped" component. Deconvolution would be possible by defining a function related to the "dish" and then subtracting it from the original metastable peak to get the sharp component. This requires a knowledge of the instrumental effects on the degree of depth in the center of the "dish topped" component. Since this information was not available, a semi-empirical deconvolution procedure was developed.

It is apparent that the metastable peak is symmetrical about the center. Therefore, the "dish" shaped broad component could be defined as the sum of two reflected exponential functions. A suitable equation relating peak height with peak width was found to be the following:

$$F(X) = \frac{A}{\sqrt{2\pi}\sigma}\left[\text{Exp}\ \frac{-(x-u)^2}{2\sigma^2} + \text{Exp}\ \frac{-(x+u)^2}{2\sigma^2}\right] \cdots\cdots (C.1)$$

In this relation, the values u and r are highly characteristic of shape and represent the position of the "horns"(62) and the peak broadness(63), respectively. Factor A is simply a

multiplier denoting the height of the broad component. Variable X is the transformed ½ width (volts) at a particular normalised peak height. The constant u can be found by an intercept technique while A and σ can be estimated via 'manual graphical bisection', a method analogous to the bisection algorithm[64]. The data necessary for deconvolution analysis are the same as that used for the n(T) vs T curves.

The deconvolution procedure is demonstrated for the metastable peak due to methyl loss from 5-hexene-2-one$^{+\cdot}$. The ½ width data were transformed via multiplication by 0.05 (Table C.1). This was a requirement for convergence of equation (C.1) towards the broad component. The normalised heights were plotted vs X on both sides of X = 0 (fig. C.1) and two straight lines, for data points originating at the inflection, were found by linear regression. For the side of the sharp component, data points 5 to 9 were used; points 9 to 13 yielded the line for the side of the broad component. The value for u was then obtained from the intersection of both lines. The following two straight line equations were determined for the sharp and broad components:

$$N(X) = -0.649\ X + 0.941 \qquad \text{(C.2)}$$

$$M(X) = -0.369\ X + 0.737 \qquad \text{(C.3)}$$

After plotting these equations, the intersection gave a value of 0.73 for u. The next step involved estimating A and σ

simultaneously. Clearly, with respect to the X interval, will not exceed one[63]. This means that the value for must lie between 0 and 1. It could be obtained through bisection in the following way.

Table C.1

Transformed data points for the metastable peak due to methyl loss from 5-Hexene-2-one$^{+\cdot}$

Data Point No.	Height, H(X) (Norm.)	½ Width[1] (Volts)	X
1	1.0000	0	0
2	0.9420	2.80	0.140
3	0.8696	4.55	0.228
4	0.7971	5.95	0.298
5	0.7246	7.35	0.368
6	0.6522	8.75	0.438
7	0.5797	10.50	0.525
8	0.5072	12.95	0.648
9	0.4348	16.11	0.806
10	0.3623	20.31	1.016
11	0.2898	24.86	1.243
12	0.2174	28.01	1.401
13	0.1449	31.86	1.593
14	0.0725	36.76	1.838

1- Only positive values are shown.

Table C.2

Values of A obtained from the iteration procedure for the deconvolution of the metastable peak for:

5-hexene-2-one$^{+\cdot}$ $\longrightarrow$ 83^{+} + $\cdot CH_3$

X	σ				
	0.500	0.750	0.625	0.563	0.594
1.243	0.614	0.662	0.630	0.617	0.623
1.401	0.670	0.594	0.603	0.623	0.611
1.593	0.805	0.520	0.587	0.662	0.619
1.838	1.059	0.402	0.546	0.709	0.615

The requirement for a good fit is that the experimental height, H(X), equals F(X):

$$H(X) = F(X) = \frac{A}{\sqrt{2\pi}\sigma}\left[\text{Exp}\ \frac{-(x-0.73)^2}{2\sigma^2} + \text{Exp}\ \frac{-(x+0.73)^2}{2\sigma^2}\right] \quad \ldots(C.4)$$

This is rearranged to the following:

$$\frac{\sqrt{2\pi}\ \sigma\ H(x)}{\left[\text{Exp}\ \frac{-(x-0.73)^2}{2\sigma^2} + \text{Exp}\ \frac{-(x+0.73)^2}{2\sigma^2}\right]} = A \quad \ldots(C.5)$$

Ideally, A should be single valued for a perfect fit. Through an iterative procedure, a constant value for A could be obtained by converging to the right σ value. Data points 11 to 14, from Table C.1, were used for the iterations because, in that interval, no contribution to the experimental height

exists from the sharp component. The iteration procedure was started by choosing σ to be the midpoint in the interval (0-1); this value then became a new limit for the next interval. After computing the corresponding A values, one examined the trend. If A increased with X, the σ value became the lower limit in the next interval while the higher limit was taken to be the one from the old interval. When A decreased and X increased, the contrary was done. This procedure was continued until no more trend was observed for A. Table C.2 demonstrates that after five iterations the values of A were essentially constant. Therefore, in this case, σ equalled 0.594 and A averaged to 0.617.

For the example, equation (C.1) may now be written as follows:

$$F(X) = \frac{0.617}{\sqrt{2\pi}\,(0.594)}\left[\text{Exp}\ \frac{-(x-0.73)^2}{2(0.594)^2} + \text{Exp}\ \frac{-(x+0.73)^2}{2(0.594)^2}\right] \quad \text{.....(C.6)}$$

or simply as:

$$F(X) = 0.414\ [EXP(-1.417(X-0.73)^2) + EXP(-1.417(X + 0.73^2)] \quad \text{...(C.7)}$$

Equation (C.7) was then evaluated at several X points and plotted over the normalised metastable peak (Fig. C.2). The sharp component was then found by subtracting the dish shaped function from the experimental peak. Since X equalled the ½ width (volts) divided by 100, the original experimental peak could be deconvoluted using equation (C.7).

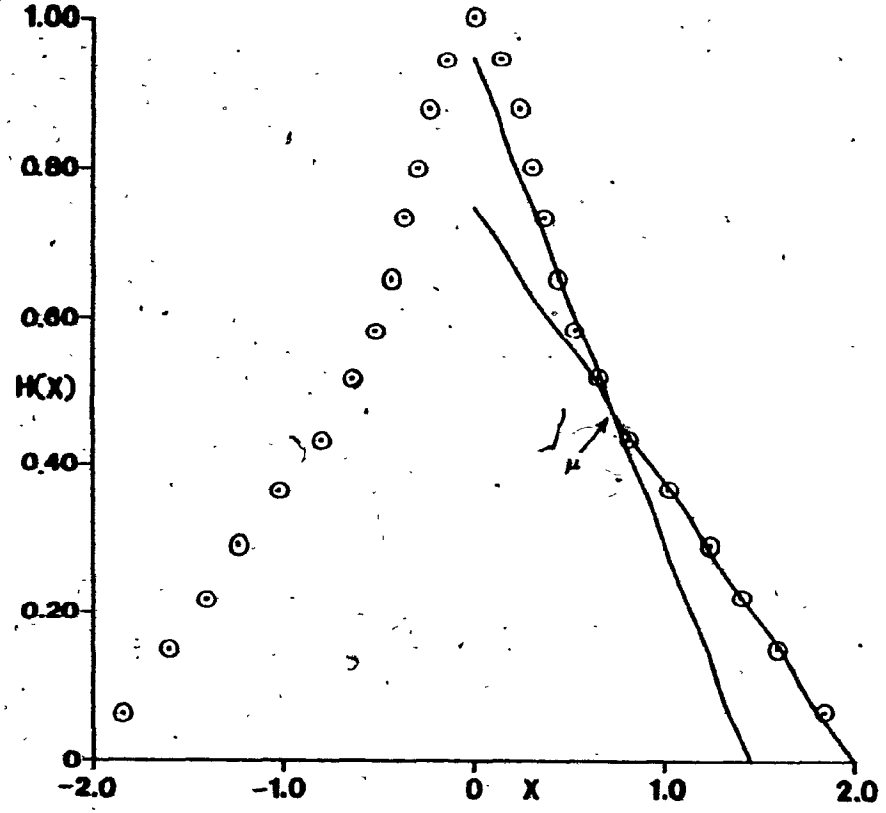

Figure C.1. Normalised metastable peak for methyl loss from 5-hexene-2-one$^{+\cdot}$.

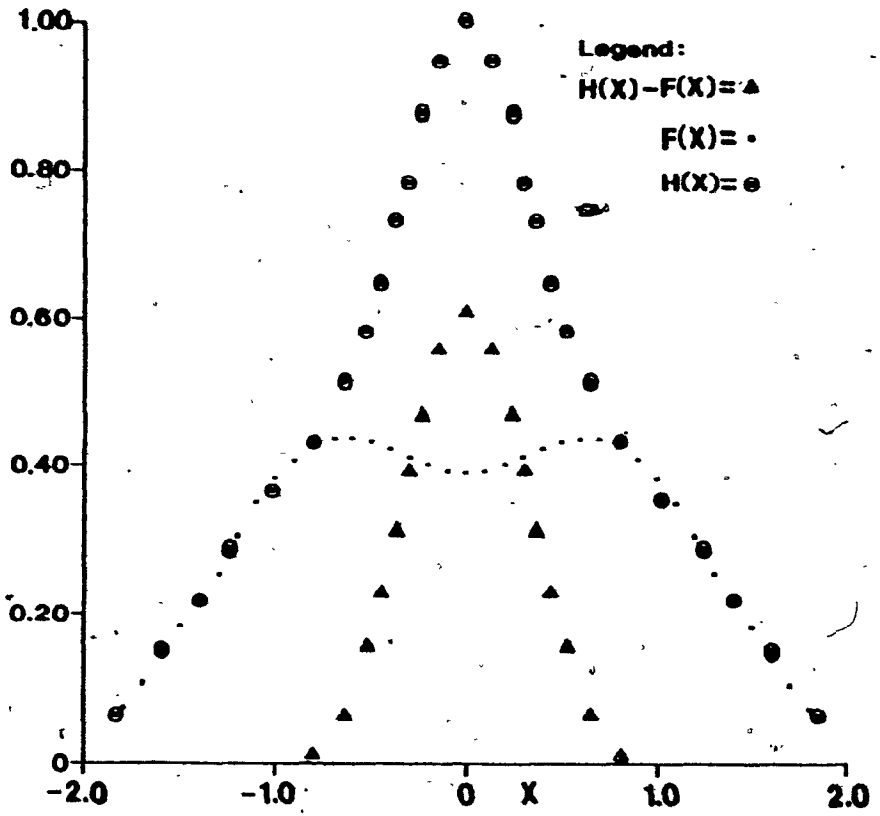

Figure C.2 Normalised metastable peak after deconvolution analysis

Appendix D. ^{1}H-NMR Spectra of Synthetic Isotopically Labelled Analogs of 5-Hexene-2-one.

This appendix compiles ^{1}H-NMR spectra of synthetic compounds used for mass spectroscopic studies. They are presented on the PPM (δ) scale. Except where indicated all spectra were obtained with external TMS standard. The ^{1}H-NMR spectrum of 5-hexene-2-one is shown for comparative purpose.

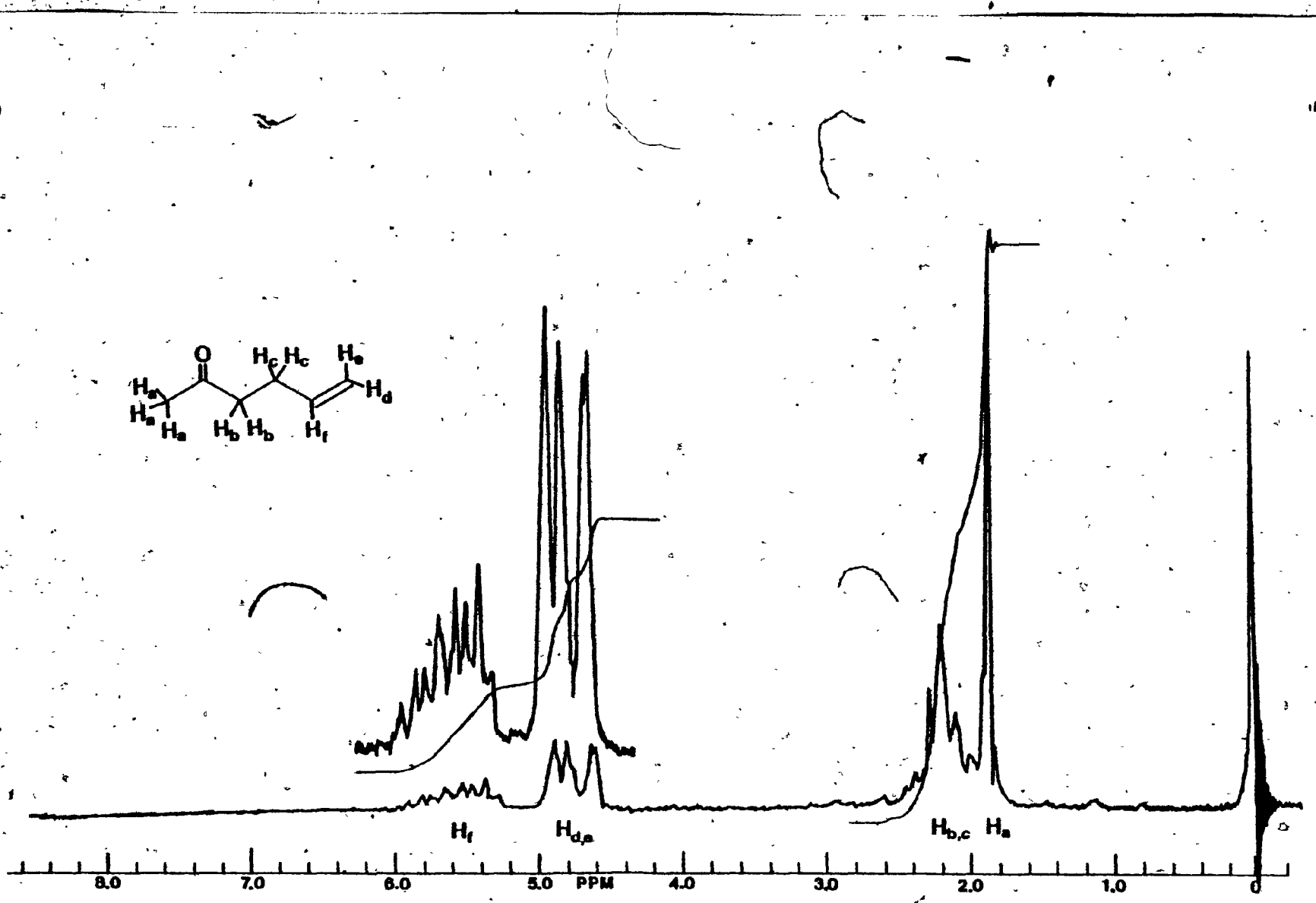

Figure D.1 - ^{1}H-NMR spectrum of 5-hexene-2-one in CCl_4 with internal TMS

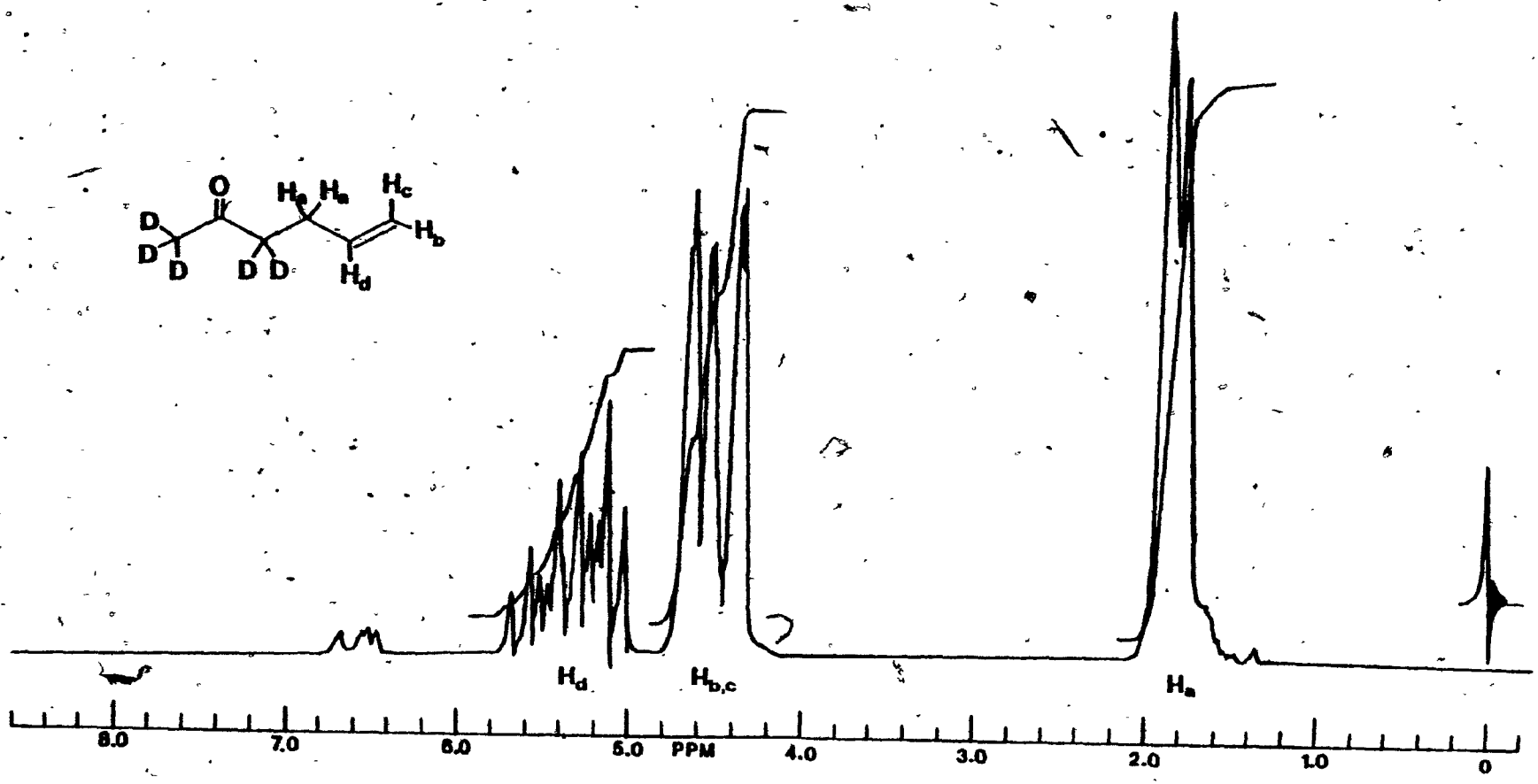

Figure D.2 ^{1}H-NMR spectrum of 5-hexene-2-one-1,1,1,3,3-d_5 in CCl_4

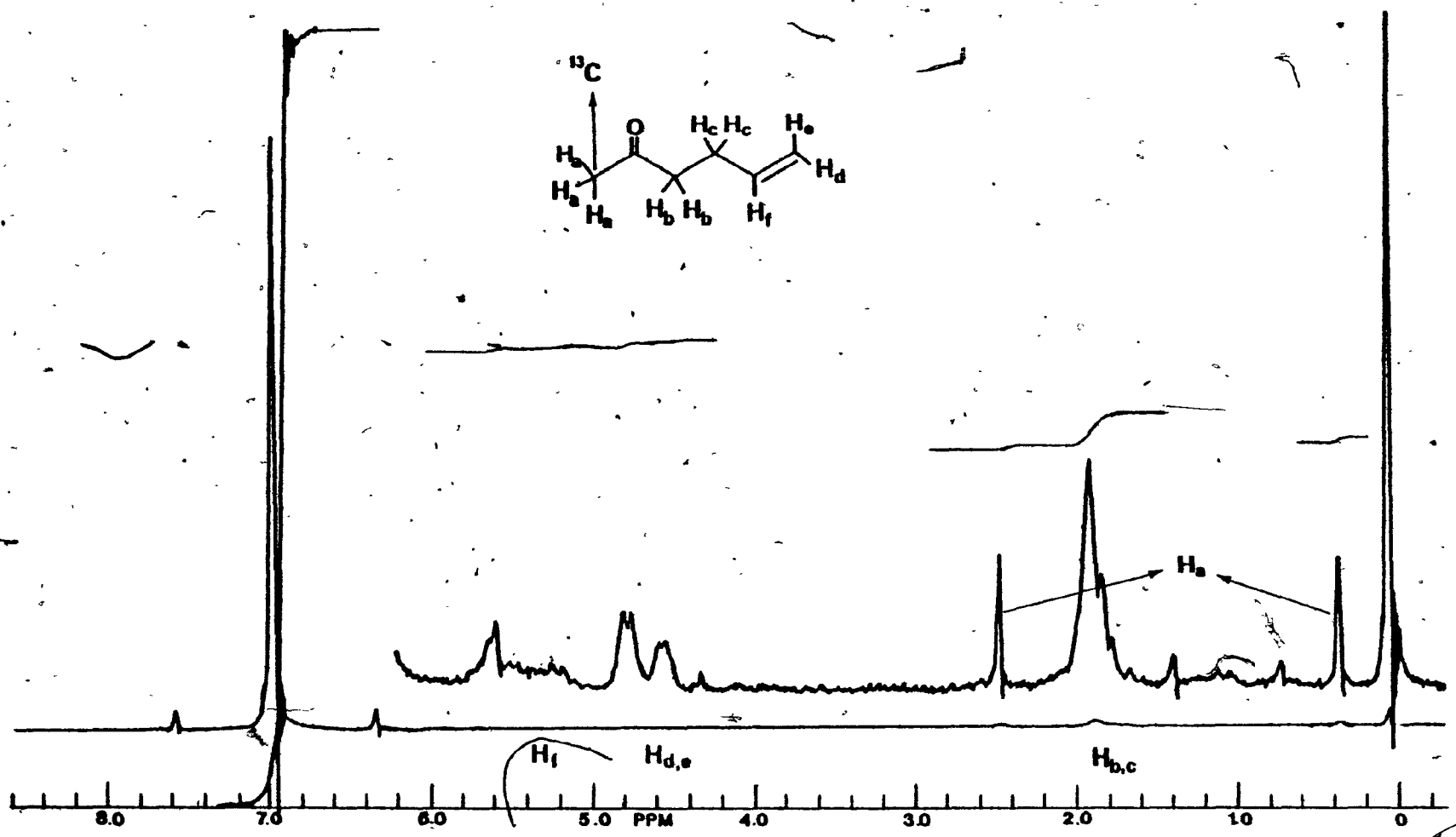

Figure D.3 ^{1}H-NMR spectrum of 5-hexene-2-one-1-^{13}C in benzene (4% W/W)

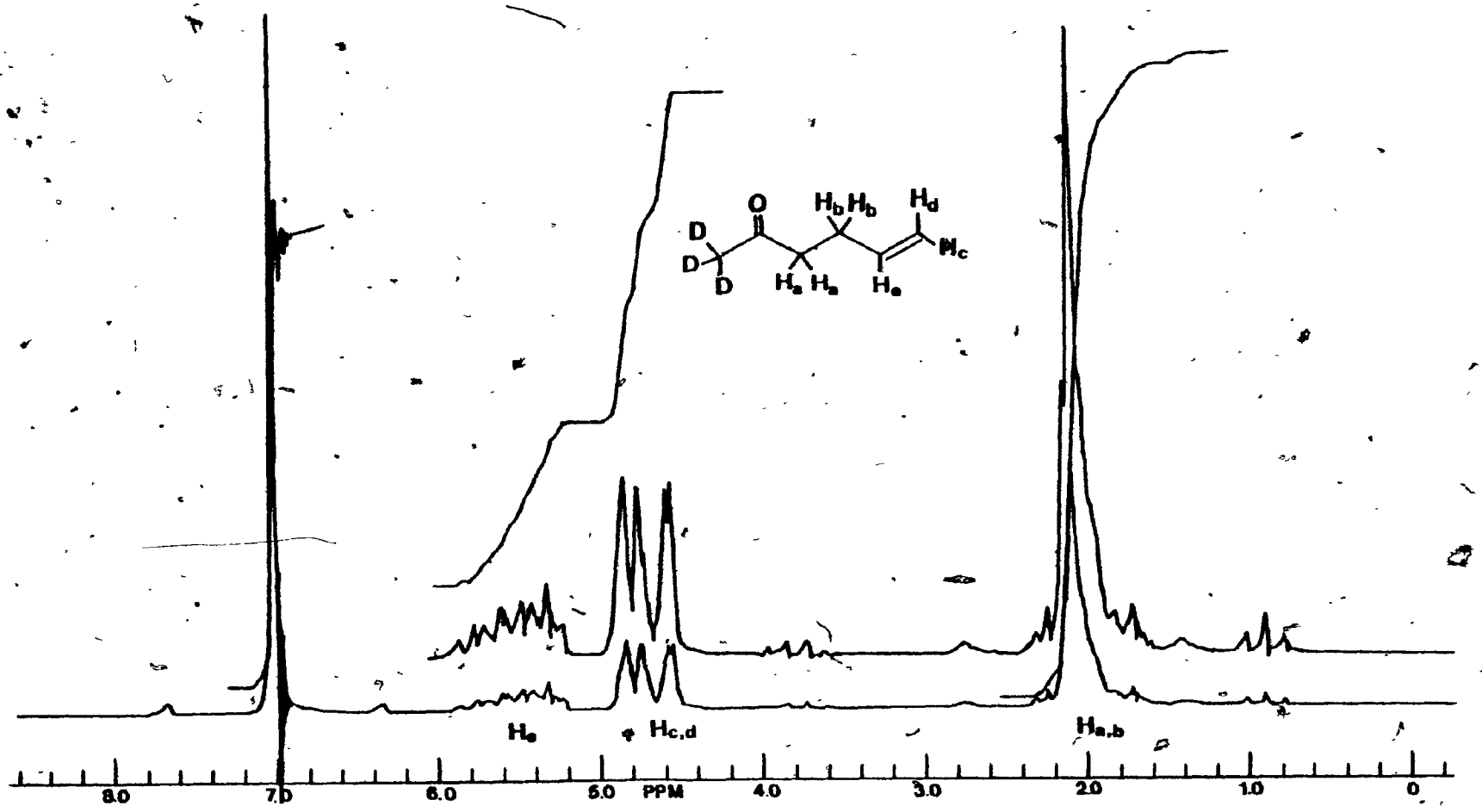

Figure D.4 ^{1}H-NMR spectrum of 5-hexene=2-one-1,1,1-d_3 in benzene (70% W/W)

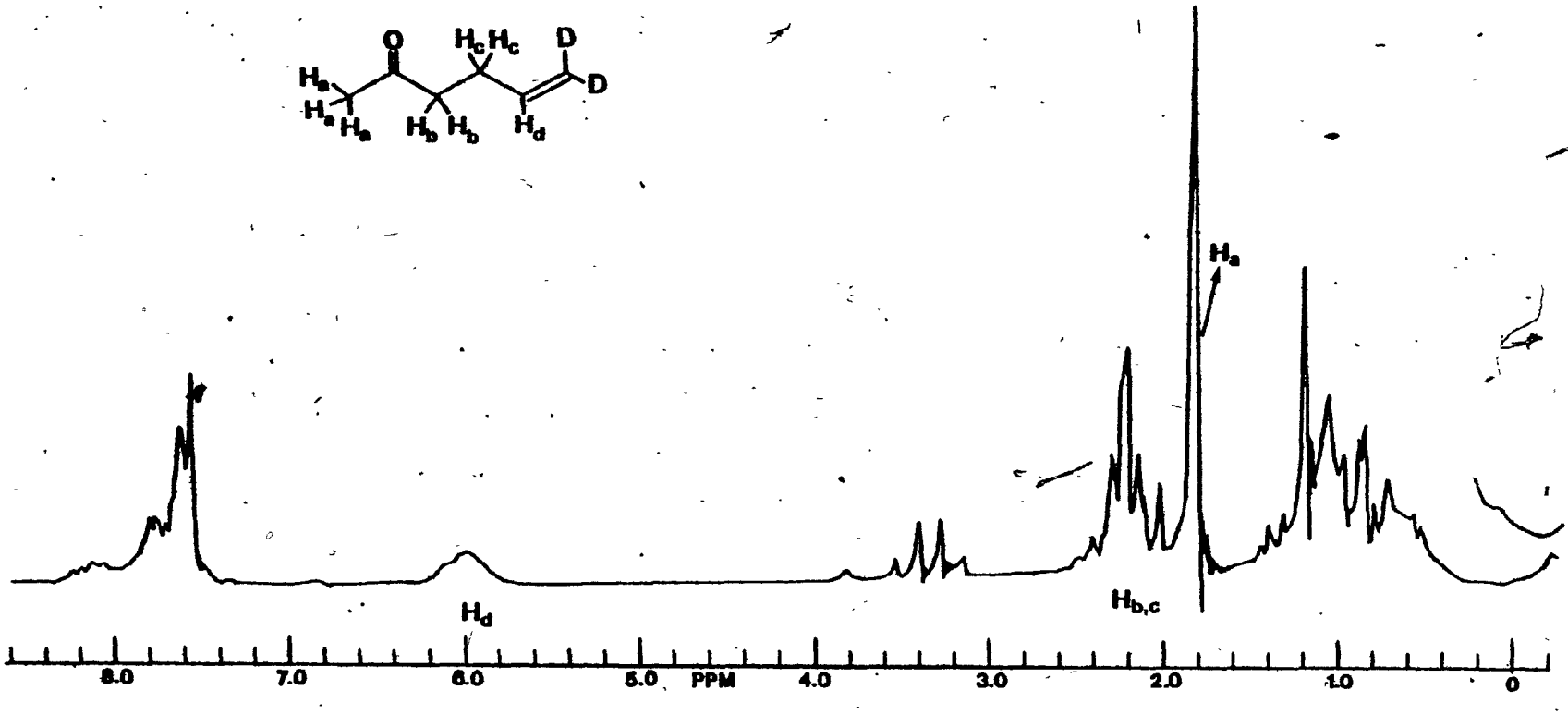

Figure D.5 ^{1}H-NMR spectrum of 5-hexene-2-one-6,6-d_2 in concentrated product mixture (70% W/W)

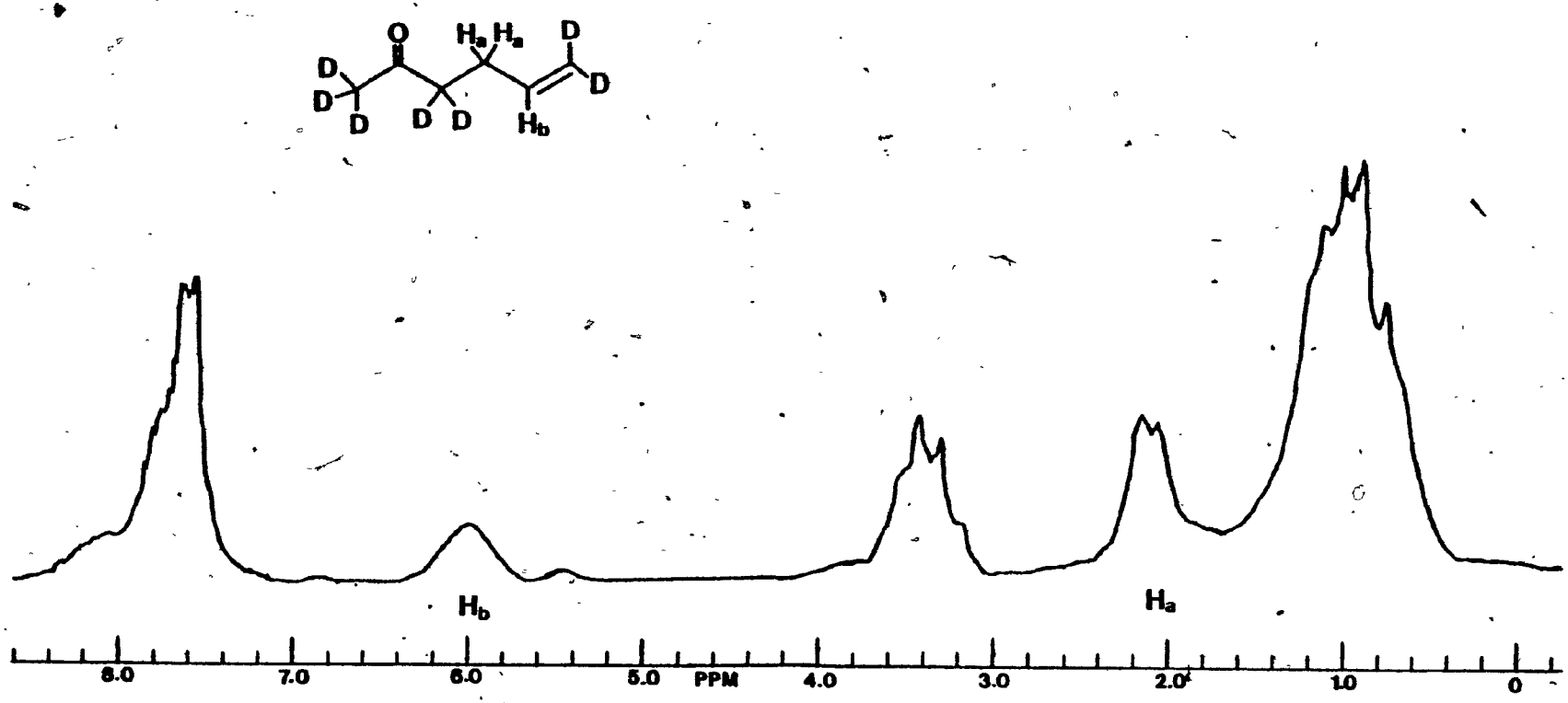

Figure D.6 ^{1}H-NMR spectrum of 5-hexene-2-one-1,1,1,3,3,6,6-d_7 in concentrated product mixture (40% W/W)

References

1. C.J. Porter, J.H. Beynon and T. Ast, Org. Mass Spectrom., 16, 101 (1981).
2. R.G. Cooks, J.H. Beynon, R.M. Caprioli and G.R. Lester, "Metastable Ions", Elsevier Scientific Publishing Company, Amsterdam, The Netherlands, 1973.
3. F.W. McLafferty, P.F. Bente, R. Kornfeld, S.C. Tsai and I. Howe, J. Amer. Chem. Soc., 95, 2120 (1973).
4. C.E. Hudson and D.J. McAdoo, Org. Mass. Spectrom., 17, 366 (1982), and references cited therein.
5. J.K. Terlow, W. Heerman and J.L. Holmes, Org. Mass Spectrom, 16, 306 (1981) and references cited therein.
6. C.C. van de Sande, C. de Meyer and A. Masquetiau, Bull. Soc. Chim. Belge, 85, 79 (1976).
7. F.W. McLafferty, "Mass Spectrometry of Organic Ions", Academic Press, New York, N.Y., 1963.
8. S. Meyerson, Int. J. Mass Spectrom. Ion Phys., 1, 309 (1968).
9. T.J. Adley, C. Matteo and R.T.B. Rye, Org. Mass Spectrom., 14, 562 (1979)

10. D. Braem, F.O. Gulacar, U. Burger and A. Bucks, Org. Mass Spectrom., 14, 602 (1979).

11. C. Lignac and J.C. Tabet, Int. J. Mass Spectrom. Ion Phys., 47, 375 (1983).

12. D. Braem, S. Siles, F.O. Gulacar and A. Bucks, Org. Mass Spectrom., 17, 102 (1982).

13. J.P. Morizur, J. Mercier and M. Sarraf, Org. Mass Spectrom., 17, 327 (1982).

14. N.S. Vul'fson, G.M. Zolotareva, V.N. Bockkerev, B.V. Unkovskii, V.B. Mochalin, Z.I. Smolina and A.N. Vol'fson, Izv. Akad. Nauk. SSSR, Ser. Khim., 1125 (1970).

15. J.R. Dias, Y.M. Sheikeh and C. Djerassi, J. Am. Chem. Soc., 94, 473 (1972).

16. K. Levsen, "Fundamental Aspects of Organic Mass Spectrometry", V.4, Verlag Chemie, New York, New York, 1978.

17. H.H. Bauer, C.D. Christian and J.E. O'Reilly, "Instrumental Analysis", Allyn and Bacon, Boston, Massachusetts, 1978.

18. D.H. Williams and I. Howe, "Principles of Organic Mass Spectrometry", McGraw Hill, London, England, 1972.

19. A.H. Struck and H.W. Major, ASTM E-14, Dallas, Texas, 1969.

20. J.L. Holmes, D. Yuan, R.T.B. Rye, Org. Mass Spectrom., 12, 254 (1977).

21. K. Levsen and H. Schwartz, J. Chem. Soc. Perkin Trans. II, 1231 (1976).

22. J.L. Occolowitz, J. Am. Chem. Soc., 91, 5202 (1969).

23. A.N.H. Yeo and D.H. Williams, J. Am. Chem. Soc., 93, 395 (1971).

24. C.W. Tsang and A.C. Harrison, Org. Mass Spectrom., 7, 1377 (1973).

25. A.M. Fallick and A.L. Burlingame, J. Am. Chem. Soc., 97, 1525 (1975).

26. J.L. Holmes and J.K. Terlow, Org. Mass Spectrom., 15, 383 (1980).

27. B. Van de Graaf, P.P. Dymerski and F.W. McLafferty, J. Chem. Soc. Chem. Commun., 978 (1975).

28. L. Simeral and G.E. Marciel, J. Phys. Chem., 77, 1590 (1973).

29. W.J. Leigh and R. Srinivasan, J. Am. Chem. Soc., 104, 4428 (1982).

30. T. Wach, P.F. Bente and F.W. McLafferty, Int. J. Mass Spectrom. Ion Phys., 9, 333 (1972).

31. W.C. Agosta, D.V. Bowen, L. Brodsky, M.E. Rennekamp and F.H. Field, J. Org. Chem., 41, 136 (1976).

32. V.M. Micovic and M.L.J. Mihailovic, J. Org. Chem., 18, 1190 (1953).

33. J. Hooz and R.B. Layton, Can. J. Chem., 48, 1626 (1970).

34. G.B. Kauffman and L.A. Teter, Inorg. Synthesis, 7, 9 (1963).

35. C.R. Johnson and G.A. Dutra, J. Am. Chem. Soc., 95, 7777 (1973).

36. G.B. Kauffman and R.P. Pinell, Inorg. Synthesis, 6, 3 (1960).

37. L. Pichat, J. Loheac and M. Herbert, Bull. Soc. Chim. Fr., 3268 (1966).

38. L.F. Cason, J. Am. Chem. Soc., 68, 2078 (1946).

39. K.W. Sherk, M.V. Augur, M.D. Soffer, J. Am. Chem. Soc., 67, 2239 (1945).

40. W.R. Biggerstoff and A.L. Wilds, J. Am. Chem. Soc., 71, 2136 (1949).

41. T. Bacchetti and A. Fiecchi, Gazz. Chim. Ital., 83, 1037 (1953).

42. E.A. Obol'nikova and G.I. Somokhvalov, Zhur, Obshchei. Khim., 33, 1860 (1963).

43. L. Crombie, P. Hemesley and G. Pattenden, J. Chem. Soc., 1016 (1969).

44. R.J. Liedtke and C. Djerassi, J. Am. Chem. Soc., 91, 6814 (1969).

45. P.J. Derrick, A.M. Falick, S. Lervis and A.L. Burlingame, J. Phys. Chem., 83, 1567 (1979).

46. L. Caglioti and P. Grasselli, Chim. Ind., 46, 799 (1964).

47. L. Caglioti and P. Grasselli, Chem. Ind., 153 (1964).

48. L. Caglioti, Tetrahedron, 22, 487 (1966).

49. E.J. Corey and G. Schmidt, Tetrahedron Letters, 399 (1979).

50. J.R. Parikh and W. von E. Doering, J. Am. Chem. Soc., 89, 5505 (1967).

51. D. Ladjama and J.J. Riehl, Synthesis, 504 (1979).

52. C.A. Brown, J. Org. Chem., 39, 3913 (1974).

53. F. Jung, D. Ladjama, J.J. Riehl, Synthesis, 504 (1979).

54. E.M. Chamberlin, E. Tristram, T. Utne and J.M. Chemerda, J. Am. Chem. Soc., 79, 456 (1957).

55. E.J. Salmi, Ber., 71, 1803 (1938).

56. E. Elkik, Bull. Soc. Chim. Fr., 283 (1968).

57. J.G. Atkinson, J.J. Csakvary, G.T. Herbert and R.S. Stuart, J. Am. Chem. Soc., 90, 498 (1968).

58. J.L. Holmes, M. Fingras and F.P. Lossing, Can. J. Chem., 59, 80 (1981).

59. T.A. Lehman, M.M. Bursey and J.R. Hass, Org. Mass Spectrom., 18 (9), 373 (1983).

60. R.G. Cooks, A.N.H. Yeo and D.H. Williams, Org. Mass Spectrom., 2, 985 (1969).

61. J.L. Holmes and A.D. Osborne Int. J. Mass Spectrom. Ion Phys., 23, 189 (1977).

62. J.L. Holmes, A.D. Osborne and G.M. Weese, Int. J. Mass Spectrom. Ion Phys., 19, 207 (1976).

63. H.J. Larson, "Introduction to Probability Theory and Statistical Inference", John Wiley and Sons, New York, New York, 1974.

64. R.L. Burden, J.D. Faires and A.C. Reynolds, "Numerical Analyses", Prindle, Weber and Schmidt, Boston, Massachusetts, 1978.